THERMODYNAMICS OF AQUEOUS AMINO ACID SOLUTIONS

A thesis presented in partial fulfilment
of the requirements for the degree of
Doctor of Philosophy in Chemistry
at Massey University

Rex Stuart Humphrey

1977

ABSTRACT

1. The vapour pressures of L-serine-water solutions have been measured at 288.15K and 298.15K using a differential static method. From these the activity coefficients for L-serine as a function of concentration at each temperature have been calculated.

2. The integral enthalpies of finite dilution of aqueous solutions of L-alanine, L-arginine, L-cysteine, glycine, L-serine and L-valine have been measured at 298.15K using an LKB 10700-1 flow microcalorimeter. These have been used to calculate the relative apparent molal enthalpies and the relative partial molal enthalpies of the particular solutes as a function of concentration.

3. The relative partial molal entropies of water in aqueous solutions of the amino acids L-alanine, glycine, L-serine and L-valine have been calculated from activity data and from enthalpy of dilution data.

4. The results have been discussed qualitatively in terms of the proposals of Frank and Evans for water-solute interactions.

ACKNOWLEDGEMENTS

I would like to thank Professor G.N. Malcolm and Dr I.D. Watson for their supervision of this thesis.

For many helpful suggestions I would like to thank Dr G.R. Hedwig. Also I would especially thank Dr I.R. McKinnon for his timely encouragement and many useful discussions.

I would like to express my appreciation to the technical staff for their assistance and in particular, Messrs H. Grant, S. Coates, N. Foot and M. Milne whose cheerful assistance was invaluable in development and construction of the vapour pressure apparatus.

For financial assistance I acknowledge the awards of a Postgraduate Scholarship and a Shirtcliffe Fellowship from the University Grants Committee and also a Departmental Demonstratorship from Massey University.

Finally, I would like to thank my wife, Anne, for her patient support and encouragement during this thesis.

TABLE OF CONTENTS

LIST OF FIGURES

CHAPTER I
INTRODUCTION

I.A. INTRODUCTION

Much interest has been stimulated in recent years over the study of the thermodynamic properties of aqueous solutions of simple organic compounds, since their behaviour can be considered to reflect on that of more complex biochemical systems. The focus of these studies has been the role and nature of water-solute interactions.

In particular, Kauzmann[1] proposed that for proteins in aqueous solution the interaction between non-polar amino acid side chains and water played a major role in maintaining their tertiary structure. He introduced the expression 'hydrophobic bonding' to describe the manner in which non-polar groups were driven to associate because of their ordering effect on the local aqueous environment. The discussion was in terms of the concepts proposed by Frank and Evans[2] and later Frank and Wen[3] that the presence of a non-polar solute molecule caused an increase in the order of the water surrounding the solute. This region of increased order was labelled an 'iceberg' by these authors, with the caution that the word should not be taken too literally. The thermodynamic behaviour of aqueous amino acid solutions has been studied as a model for the more complex solution behaviour of proteins. The emphasis has been on the determination of the effect of the non-polar, hydrophobic groups on the solution behaviour of amino acids so that at some later stage some assessment might be made of the contribution of this hydrophobic interaction to the conformational stability of proteins. For example, measurements of the solubilities of amino acids and related substances, in water and in organic solvents, have been used to assess the contribution of protein side chains to the free energy of transfer from water to the organic solvent[4]. Direct measurements of the enthalpies of transfer of amino acids from water to water + urea solutions[5] and to water + ethanol solutions[6] have been made for similar reasons. The effect of the amino

acid side chains on their solution behaviour has also been considered from the measurement of partial molar heat capacities of amino acids in aqueous solution[7].

To further our understanding of the observed thermodynamic behaviour of amino acids in water from a molecular point of view a consideration of firstly the structure of water, and secondly the thermodynamic properties of other types of solutes, should prove helpful.

Water Structure

The structure of liquid water is exceedingly complex, and there is at present no one model which can be used to explain all of the observed properties of either pure water or of dilute aqueous solutions. All of the experimental information for pure water (thermodynamic properties, physical properties, spectroscopic properties, X-ray diffraction data) suggests that liquid water possesses some kind of partly broken down ice structure. The many theories which have been proposed to give explicit expression to this widely accepted but vague idea can be broadly classified as either continuum models or mixture models.

The main continuum model is associated with the names of Pople[8] and Bernal[9]. It is proposed in this model that when ice melts the flexibility of the hydrogen bonds becomes greatly increased so that the regular crystal lattice of ice is destroyed by the bending or distortion of the hydrogen bonds rather than by their rupture. It has not yet been possible to develop the model to any great extent on a quantitative basis and its use for the qualitative discussion of solute effects is not easy.

The mixture models take up the idea that liquid water contains molecules in two different structural situations, one in which the molecules are bound into a hydrogen-bonded network and the other in which the molecules are not hydrogen-bonded to their neighbours and are therefore able to pack more closely together. In the 'water-hydrate'

or clathrate model of Claussen[10], and Pauling and Marsh[11] the network is supposed to be similar to the solid water structures observed in the crystals of some non-metal hydrates, which contain much larger cavities than are present in the ice network. This more open network is presumed to extend throughout the volume of the liquid, and non-bonded water molecules are supposed to exist within the cavities of the network as interstitial or clathrate molecules. In this model solute molecules could be accommodated as interstitial molecules without disrupting the network.

The other main mixture model is that of Frank and Wen[3]. They proposed that the network structure is confined to aggregates or clusters of finite numbers of molecules, and that these aggregates are dispersed among non-hydrogen-bonded and more closely packed water molecules. The water molecules in a non-bonded region are imagined to be able to switch rapidly and cooperatively into a network cluster, which in turn may suddenly revert in a cooperative manner to the non-bonded state. This concept has led to the adoption of the picturesque title of 'the flickering cluster model' for this theory.

Solute effects can be discussed qualitatively in the flickering cluster model in terms of a shift in the balance of 'equilibrium' between the more dense non-bonded water and the less dense network or cluster water. This point will be taken up in the following sections.

Ionic Solutes

A useful group of solutes for comparison with the zwitterionic amino acids are the simple electrolytes whose behaviour provides information about ion-water interactions in aqueous solution. Solutions of ions are characterised by negative enthalpies and entropies of hydration as shown in Table I.1. Ionic solutions also exhibit negative partial molal heat capacities of the solute at infinite dilution, as shown in Table I.2 for the alkali metal halides. For a given anion the negative values of $C^{\circ}_{p,2}$

become larger as the size of the cation increases.

TABLE I.1

Thermodynamic Hydration Functions of Gaseous Ions at 298K[12]

($\Delta X_n^{\ominus}$ refers to the process:

M^+ (g, hypothetical 1atm.) $\longrightarrow$ M^+ (solution, hypothetical 1m))

Ion	$-\Delta H_h^{\ominus}$/J mol^{-1}	$-\Delta S_h^{\ominus}$/J mol^{-1} K^{-1}	Ion	$-\Delta H_h^{\ominus}$/J mol^{-1}	$-\Delta S_h^{\ominus}$/J mol^{-1} K^{-1}
H^+	1128.0	130.9	F^-	473.6	133.1
Na^+	443.6	109.6	Cl^-	339.8	76.1
K^+	359.9	74.0	I^-	267.9	37.6
Cs^+	314.3	58.9	OH^-	423.0	148.9
Be^{2+}	2560.7	425.1	$Na^+ + F^-$	917.1	242.7
Mg^{2+}	1996.4	310.8	$Cs^+ + I^-$	582.2	96.5
Ba^{2+}	1377.3	202.9	$K^+ + Cl^-$	699.7	150.1

TABLE I.2

Standard Partial Molal Heat Capacities of Alkali Metal Halides in Water at 298K[13]

Solute	$-C_{p,2}^{\ominus}$/J K^{-1} mol^{-1}	Solute	$-C_{p,2}^{\ominus}$/J K^{-1} mol^{-1}
NaF	73.2	LiBr	65.8
KF	102.6	NaBr	84.5
RbF	123.5	KBr	113.2
CsF	135.3	RbBr	133.1
LiCl	62.5	CsBr	148.5
NaCl	81.4	NaI	72.2
KCl	109.8	KI	102.9
RbCl	130.6	RbI	124.8
CsCl	142.8	CsI	137.5

Frank and Wen[3] suggested that structural changes in the water surrounding the ion in solution were responsible for the large negative heat capacities and the entropies of hydration of the ions. The ionic solution model they proposed envisages three distinct regions about the ion (Figure I.1).

FIGURE I.1 Frank and Wen Ionic Solution Model

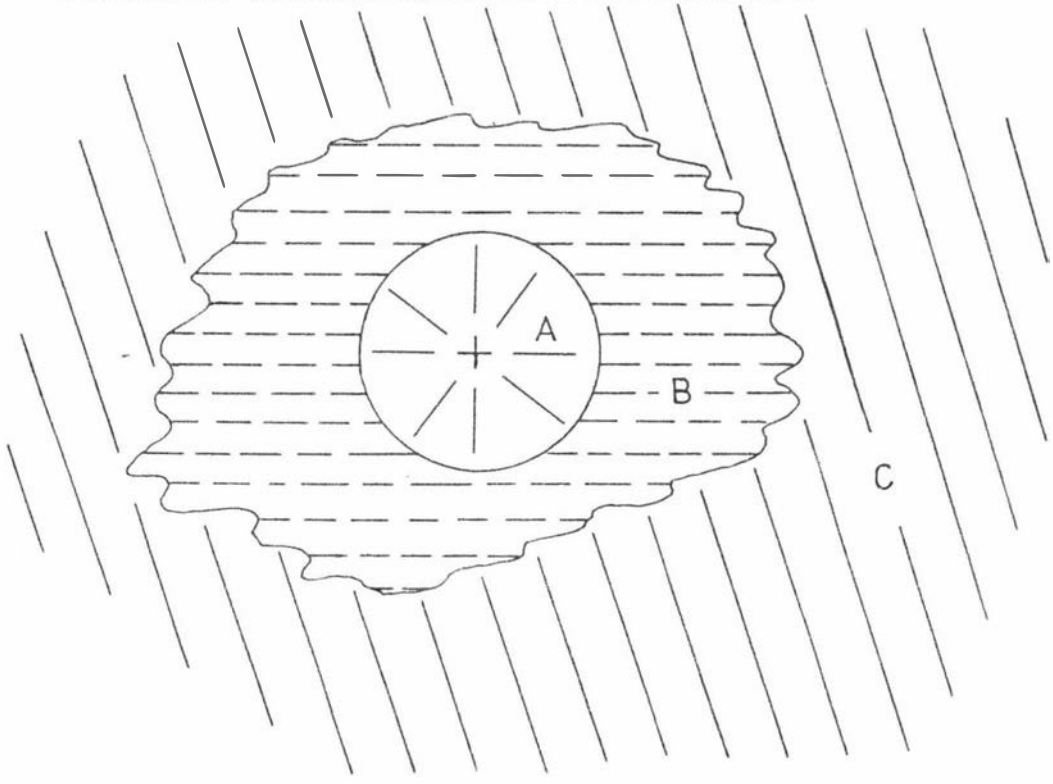

In region A in the immediate neighbourhood of the ion strong ion-dipole forces produce an oriented shell of water molecules; this is usually referred to as electrostrictive hydration. In region C far removed from the ion the normally tetrahedral structure of water is largely intact. However, there is also an intermediate region, B, in which the mutually incompatible effects of tetrahedral hydrogen-bonding and the radial coulombic field interact to produce a random orientation of water molecules. The authors called this a structure-broken region. According to this model the observed properties of ionic solutions should reflect the relative importance of electrostriction and randomisation. Frank and Wen suggested that the region of electrostrictive hydration always exists and that small ions and multiply-charged ions such as Li^+,

F^- and Mg^{2+} might induce additional structure of some sort beyond the first hydration layer. They remarked that the outward orientation of like poles in region A should always produce some degree of randomisation or disorder in region B, but that largely singly-charged ions such as I^- and Cs^+ seem also to have a net structure-breaking effect larger than would be expected from such disorder. Care, however, must be used in applying the terms structure-making and structure-breaking to characterise the effect of ions on the observed properties of water, for the stable electrostrictive hydration in the vicinity of a Li^+ ion (normally classed as a structure-maker) is quite different from a type of hydrogen-bonded structure which exists in unperturbed water.

Hydrocarbon Solutes

Hydrocarbon solutes are non-polar and differ markedly from ionic solutes in their solution behaviour. These compounds have very low solubilities and consequently their thermodynamic properties in aqueous solution have largely been derived from the temperature dependence of the solubility. In Table I.3 the thermodynamic properties of some aqueous hydrocarbon solutions are given. The quantities listed are the standard partial solution functions defined by the relation

$$\bar{X}^{\ominus}_{Soln} = \bar{X}_2^{\ominus} - X_2^{\circ}$$

where $\bar{X}_2^{\ominus}$ is the partial molar property of the solute in the standard state (the one molal solution with the intensive properties of the infinitely dilute solution), and X_2° is the molar property of the pure liquid solute.

The lower hydrocarbons show an interesting thermodynamic behaviour in that the positive standard free energy of solution is a consequence not of a positive standard enthalpy of solution but rather of a negative standard entropy of solution. If the solution process involved the breaking of hydrogen bonds in the solvent in order to accommodate the solute the enthalpy and the entropy of solution would be

TABLE I.3

Thermodynamic Properties of Aqueous Hydrocarbon Solutes at 298K[14]

Substance	$-\Delta\bar{G}^{\ominus}_{soln}$/J mol^{-1}	$-\Delta\bar{H}^{\ominus}_{soln}$/J mol^{-1}	$-\Delta\bar{S}^{\ominus}_{soln}$ J mol^{-1} K^{-1}	$\Delta\bar{C}^{\ominus}_{p,soln}$ J K^{-1} mol^{-1}
Methane	10,500 to 13,179	9414 to 11966	70.3 to 76.9	226.9
Ethane	13,891 to 16,150	5314 to 9916	70.3 to 81.6	250.9
n-Propane	20,502 to 20,543	6067 to 8745	89.1 to 98.3	294.8
n-Butane	24,351 to 25,104	3012 to 4017	91.6 to 95.0	303.3

expected to be positive, which is exactly the opposite of what is observed. To account for the observed thermodynamic behaviour in terms of the flickering cluster model for liquid water it is suggested that hydrocarbon molecules in aqueous solution cause an increase in the amount of network water at the expense of non-bonded water in the vicinity of the non-polar solute molecules. The formation of more of the network water from non-bonded water in the region surrounding the solute molecules would produce a negative enthalpy change and a negative entropy change on solution of the hydrocarbon. Moreover if the network or 'clustered' water is highly sensitive to temperature changes, an increase in the proportion of network water would increase the total heat capacity of the system, which would account for the observed large positive partial molal heat capacities of the solute in these solutions.

Alcohol Solutes

The low molecular weight alcohols provide an interesting series of solutes to consider in regard to their thermodynamic solution behaviour in water. They have a non-polar (hydrophobic) portion and a polar functional group capable of direct interaction with water molecules. This latter interaction is responsible for the high solubility of alcohol molecules in water.

From an inspection of Table I.4 it is evident that the dominating

influence on solution behaviour is the negative entropy of solution, $\Delta S^{\ominus}_{soln}$, which again suggests the production of some additional 'clustered' water in the region about the solute. It would appear that the non-polar portion of the alcohol molecule is affecting the water in a similar fashion to the hydrocarbons. The heat capacities of solution also show the effect of the non-polar group as they are large and positive.

TABLE I.4

Thermodynamic Properties of Alcohols at Infinite Dilution in Water at 298K[15]

Alcohol	$-\Delta H^{\ominus}_{soln}$/J mol^{-1}	$-\Delta S^{\ominus}_{soln}$/J mol^{-1} K^{-1}	$\Delta C^{\ominus}_{p,2}$/J K^{-1} mol^{-1}
Methanol	7251	27.6	75.3
Ethanol	10,104	44.8	141.8
n-Propanol	10,133	56.1	208.8
i-Propanol	12,979	60.7	205.8
n-Butanol	9,276	64.0	260.2
t-Butanol	17,309	78.7	264.8

Tetraalkylammonium Halide Solutes

Thermodynamic studies of aqueous solutions of tetraalkylammonium salts at infinite dilution clearly show the effect of the large, non-polar groups on the net solution behaviour of the ions. In particular, the heat capacities of solution are large and positive, which is typical of the effect of non-polar groups on water. The responsibility of the non-polar portions for the large positive heat capacities of solution of these ions, is indicated by the dependence of $\Delta C^{\ominus}_{p,2}$ on the nature and size of the substituent groups on the ion[16]. The Bu_4N^+ ion for instance has a more positive $\Delta C^{\ominus}_{p,2}$ than the Pr_4N^+ ion. Clearly, the non-polar portions govern the interactions of the ions with water and in place of electrostrictive structure-making and structure-breaking effects observed

for simple ions, the tetraalkylammonium ions exhibit non-polar solution behaviour. Further evidence for the importance of the non-polar groups is provided by a study of the entropies and enthalpies of dilution of these tetraalkylammonium halides in aqueous solution[17]. The enthalpies of dilution for a given halide are negative and decrease numerically in the order $Bu_4N^+ > Pr_4N^+ > Et_4N^+ > Me_4N^+$. The apparent molal excess entropies for Bu_4N^+ and Pr_4N^+ also suggest that these large ions have a greater structure-making than would be expected from a consideration of their ionic charge and size alone. Thus Cs^+ has a comparatively small structure-making effect but these ions have a much greater effect.

Amino Acid Solutes

The differential entropies of dilution, $\bar{S}_1 - \bar{S}_1^{\Theta}$, of aqueous solutions of some amino acids have been determined[16]. It was concluded that the values of $\bar{S}_1 - \bar{S}_1^{\Theta}$ were controlled largely by the size and structure of the hydrocarbon part of the amino acid, and only to a minor degree by its dipole moment. The positive values of $\bar{S}_1 - \bar{S}_1^{\Theta}$ for glycine solutions were interpreted as a structure-breaking effect on water, and the negative values for the other amino acids studied were interpreted as a structure-making effect which increased with the size of the hydrocarbon side chain.

The partial molar heat capacities at infinite dilution, $C_{p,2}^{\Theta}$, of several alkylamino acids have been determined directly and from the temperature dependence of enthalpies of solution[7], some of which are listed in Table I.5. The values are large and positive and increase with the size of the alkyl side chain. This result is again indicative of the domination of aqueous solution behaviour by the non-polar groups. The amino acid serine shows a decrease in $C_{p,2}^{\Theta}$ compared with alanine presumably because of the presence of a polar OH group in its side chain. (See Figure I.2 for some amino acid structures.)

Figure I.2 The structures of some amino acids

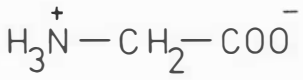

Glycine

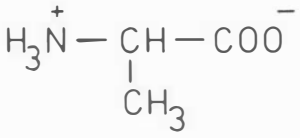

Alanine

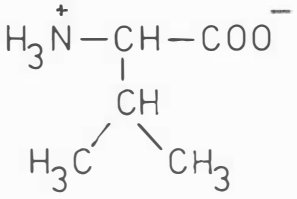

Valine

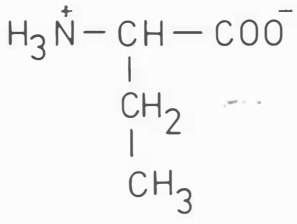

α-Aminobutyric acid

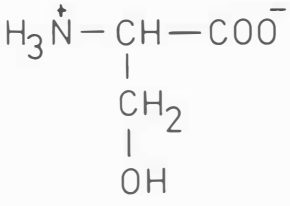

Serine

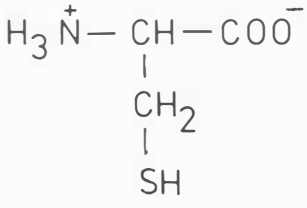

Cysteine

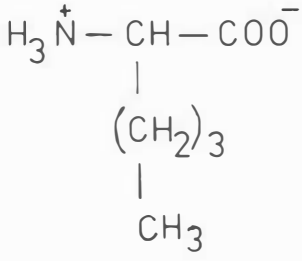

Norleucine

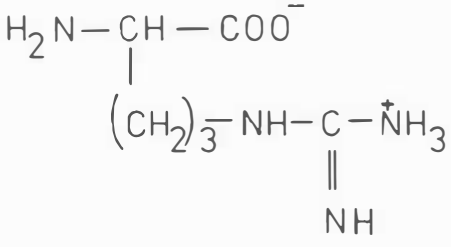

Arginine

TABLE I.5

Partial Molar Heat Capacities, $C^{\ominus}_{p,2}$, of Amino Acids in Aqueous Solution at 298K

Amino Acid	$C^{\ominus}_{p,2}$/J K^{-1} mol^{-1}
Glycine	44
Alanine	146
α-Aminobutyric Acid	226
Valine	307
Leucine	382
Serine	125

In view of the importance of amino acids to our attempts to understand the aqueous solution behaviour of proteins (and also water-solute interactions in general), it was decided to determine the activity coefficients and enthalpies of dilution for aqueous solutions of several amino acids to add to the pool of thermodynamic data available for these solutions.

I.B THERMODYNAMICS OF AMINO ACID SOLUTIONS

In this section the thermodynamic equations relating to the vapour pressure and enthalpy of dilution measurements are outlined, and some of the thermodynamic relationships used in later chapters are derived. Basic thermodynamic equations have not been derived but rather are given in Table I.6 along with terms and symbols used throughout this thesis. Denbigh[19], Lewis and Randall[20] and Glasstone[21] have been used as reference textbooks.

I.B1 Ideal Solutions

An ideal solution can be defined as one in which the chemical potential μ_i of each component i of the solution is given by the equation

$$\mu_i(T, p, x_i) = \mu_i^*(T, p) + RT \ln x_i \qquad (I.1)$$

where $\mu_i^*(T, p)$ is the chemical potential (molar Gibbs free energy) of pure liquid i at the temperature T and pressure p of the solution being studied.

The properties commonly attributed to ideal solutions are all deducible from this relationship.

I.B2 Real Solutions

Real solution behaviour is conveniently characterised by reference to corresponding ideal solution properties. One of the methods of comparison usually adopted is that of using activity coefficients as a measure of deviation from ideal behaviour.

In order to utilise the convenient form of Equation I.1 an activity coefficient of the component i, γ_i (which is a function of temperature, pressure and composition) is introduced such that the equation

$$\mu_i(T, p, x_i) = \mu_i^*(T, p) + RT \ln \gamma_i x_i \qquad (I.2)$$

is correct whatever the deviation from ideality.

TABLE I.6

Thermodynamic Properties and Relations

Property	Symbol	Definition
mass	m	
volume	V	
density	ρ	
pressure	p	
fugacity	f	
thermodynamic temperature	T	
amount (number of moles)	n	
mole fraction	x	
second virial coefficient	B	
enthalpy	H	
entropy	S	
Gibbs free energy	G	$H - TS$
chemical potential i	μ_i	$(\partial G/\partial n_i)_{T,p,n_j}$
apparent molal enthalpy	ϕ_H	
activity i	a_i	
activity coefficient i	γ_i	a_i/x_i

Gibbs-Duhem Relation

$$x_1(\partial \mu_1/\partial x_1)_{T,p,x_2} + x_2(\partial \mu_2/\partial x_1)_{T,p,x_1} = 0$$

For complete definition of the activity coefficient we must also specify the conditions under which it becomes unity. In the case of real solutions such as aqueous solutions of amino acids we adopt a convention that specifies the conditions when the activity coefficient becomes unity for both the solvent and the solute as follows:

$$\left.\begin{aligned} &\text{For the solvent: } \mu_1 = \mu_1^* + RT \ln \gamma_1 x_1 \text{ and } \gamma_1 \longrightarrow 1 \text{ as } x_1 \longrightarrow 1 \\ &\text{For the solute: } \mu_2 = \mu_2^* + RT \ln \gamma_2 x_2 \text{ and } \gamma_2 \longrightarrow 1 \text{ as } x_2 \longrightarrow 0 \end{aligned}\right\} \quad (I.3)$$

For the solvent under the limiting conditions the logarithm vanishes and so μ_1^* is equal to the Gibbs free energy per mole of the pure solvent at the same temperature and pressure as the solution. However, for the solute the activity coefficient tends to unity at infinite dilution, so that μ_2^* is the chemical potential of the pure solute (i.e. when $x_2 = 1$) in a hypothetical liquid state which has the properties of the infinitely dilute solution (i.e. $\gamma_2 = 1$).

I.B3 Activity Coefficients from Vapour Pressure Measurements

For a one component system the chemical potential of the vapour considered as a perfect gas is given by the expression

$$\mu(T, p) = \mu^{\ominus}(T, p^{\ominus}) + RT \ln (p/p^{\ominus}) \quad (I.4)$$

$\mu^{\ominus}(T, p^{\ominus})$ is a function of T only since the reference pressure $p^{\ominus}$ is fixed at the chosen value.

If the vapour does not behave like a perfect gas it is convenient to define a corrected pressure called the fugacity to which the chemical potential of the vapour is related by an equation of exactly the same form as Equation I.4. This equation is

$$\mu(T, p) = \mu^{\ominus}(T, p^{\ominus}) + RT \ln (f/f^{\ominus}) \quad (I.5)$$

Since it is known by observation that the real vapour approaches perfect gas behaviour as the pressure tends to zero the fugacity is also defined so that

$$f/p \longrightarrow 1 \text{ as } p \longrightarrow 0 \qquad (I.6)$$

For any single component gas

$$\left(\frac{\partial \mu}{\partial p}\right)_T = v \qquad (I.7)$$

where v is the molar volume. For the special case of a perfect gas Equation I.7 can be changed to

$$\left(\frac{\partial \mu}{\partial p}\right)_T = \frac{RT}{p} \qquad (I.8)$$

By subtracting Equation I.8 from Equation I.7, integrating the resulting equation, substituting equations I.4 and I.5 into the left hand side of the integrated equation, and finally making use of Equation I.6, it can be shown that

$$\ln(f/p) = \frac{1}{RT} \int_0^p (v - RT/p)\, dp \qquad (I.9)$$

Equation I.9 applies at constant temperature. For a vapour which deviates slightly from the perfect gas law the molar volume can be expressed by the empirical equation

$$pv = RT + Bp$$

where B is a constant which depends on T but not on p. By using this result in Equation I.9 it is found that

$$\ln f = \ln p + Bp/RT \quad \text{at constant T} \qquad (I.10)$$

For a two component non-ideal solution (with an involatile solute) in contact with its vapour (which we consider as imperfect) the equilibrium condition is given by:

$$\mu^l_1 (T, p) = \mu^v_1 (T, p) \qquad (I.11)$$

where μ^l_1 is the chemical potential of the solvent at the temperature T and pressure p of the solution and μ^v_1 is the chemical potential of the solvent vapour also at the temperature and pressure of the solution under consideration.

Now, from Equation I.2, we can write:

$$\mu_i^l (T, p) = \mu_i^* (T, p) + RT \ln \gamma_i x_i$$

If we define the product of the mole fraction, x_i, and the activity coefficient, γ_i, as the activity, a_i, of this component, the above equation becomes for the solvent:

$$\mu_1^l (T, p) = \mu_1^* (T, p) + RT \ln a_1 \qquad (I.12)$$

$$= \mu_1^* (T, p^o) + \int_{p^o}^{p} (\partial \mu_1^* / \partial p)_T dp + RT \ln a_1$$

where p^o is the saturated vapour pressure of the solvent at the temperature T of the solution. $(\partial \mu_1^* / \partial p)_T$ is equal to the molar volume of the pure solvent, V_1^*. Thus we have:

$$\mu_1^l (T, p) = \mu_1^* (T, p^o) + \int_{p^o}^{p} V_1^* dp + RT \ln a_1 \qquad (I.13)$$

For the imperfect vapour we can write the chemical potential μ_1^v (using Equation I.5 with $p^\ominus = 1$) as:

$$\mu_1^v (T, p) = \mu_1^\ominus (T, 1) + RT \ln \left[f(p)/f(1)\right] \qquad (I.14)$$

Now it is apparent that at the saturated vapour pressure of pure solvent, p^o, and at temperature T, the chemical potential of pure liquid solvent is equal to the chemical potential of its vapour i.e.

$$\mu_1^* (T, p^o) = \mu_1^v (T, p^o)$$

Thus:

$$\mu_1^* (T, p^o) = \mu_1^\ominus (T, 1) + RT \ln \left[f(p^o)/f(1)\right] \qquad (I.15)$$

Substituting for $\mu_1^* (T, p^o)$ in Equation I.13 we obtain:

$$\mu_1^l (T, p) = \mu_1^\ominus (T, 1) + RT \ln\left[f(p^o)/f(1)\right] + \int_{p^o}^{p} V_1^* dp + RT \ln a_1 \qquad (I.16)$$

Returning to the expression for equilibrium (Equation I.11) and expressing μ_1^l in terms of Equation I.16 and μ_1^v in terms of Equation I.14 we obtain:

$$\mu_1^\ominus(T, 1) + RT \ln\left[f(p^o)/f(1)\right] + \int_{p^o}^{p} V_1^* dp + RT \ln a_1 = \mu_1^\ominus(T, 1) + RT \ln \left[f(p)/f(1)\right]$$

which on simplification yields

$$RT \ln a_1 = RT \ln\left[f(p)/f(p^o)\right] - \int_{p^o}^{p} V_1^* dp$$

whence

$$\ln a_1 = \ln\left[f(p)/f(p^o)\right] - \int_{p^o}^{p} (V_1^*/RT)\, dp \qquad (I.17)$$

Utilising Equation I.10 we can express the fugacities at p and p^o in terms of p, p^o and B (the second virial coefficient of water vapour). On doing this we obtain:

$$\ln a_1 = \ln (p/p^o) + (B/RT)(p - p^o) - \int_{p^o}^{p} (V_1^*/RT)dp \qquad (I.18)$$

If we consider V_1^* to be constant over the range of integration then Equation I.18 becomes:

$$\underline{\ln a_1 = \ln(p/p^o) + \left[(B - V_1^*)/RT\right]\left[p - p^o\right]} \qquad (I.19)$$

Thus from a knowledge of B and V_1^* and the measurement of the vapour pressure of the solution, p, and the saturated vapour pressure of the pure solvent, p^o, both at temperature T, it is possible to directly determine the activity a_1 of the solvent.

A consideration of the magnitudes of the various components of the last term of Equation I.19 revealed that for the vapour pressure measurements made in this study this term made a negligible contribution. Thus for the vapour pressure measurements in this thesis we can write:

$$\ln a_1 = \ln(p/p^o)$$

$$\text{whence} \qquad \underline{a_1 = p/p^o} \qquad (I.20)$$

In this work, the saturated vapour pressure of the pure solvent, p^o, was measured at temperature T and the vapour pressure difference, $p^o - p = \Delta p$, was also measured at temperature T (see Section II.B). In terms of the quantities which were measured a_1 can be expressed as

$$a_1 = p/p^o = 1 - (\Delta p/p^o) \qquad (I.21)$$

Since the solute is involatile the Gibbs-Duhem equation relating

the activity of the solvent to that of the solute needs to be used to determine the activity coefficient of the solute.

I.B4 Activity Coefficient of the Solute from that of the Solvent

The Gibbs-Duhem equation for a two component system in which the mole fractions are x_1 and x_2 is:

$$x_1(\partial\mu_1/\partial x_1)_{T,\,p} + x_2(\partial\mu_2/\partial x_1)_{T,\,p} = 0 \qquad (I.22)$$

Using Equation I.2, performing the necessary differentiations and substituting in Equation I.22 above, we obtain the following alternative form of the Gibbs-Duhem equation:

$$x_1(\partial \ln \gamma_1/\partial x_1)_{T,\,p} + x_2(\partial \ln \gamma_2/\partial x_1)_{T,\,p} = 0$$

which can be written as:

$$x_1\, d\ln\gamma_1 + x_2\, d\ln\gamma_2 = 0 \qquad (I.23)$$

where it is understood that we are concerned with changes of composition at constant temperature and pressure.

If we regard component 1 as being the solvent whose activity coefficients have already been directly determined from vapour pressure measurements then upon integration of Equation I.23 we have:

$$\ln\gamma_2' = -\int_{x_2=0}^{x_2=x_2'} (x_1/x_2)\, d\ln\gamma_1 \qquad (I.24)$$

where γ_2' is the value of γ_2 at the particular mole fraction of the solute which is the upper limit of the integration. The value of γ_2 at the lower limit $x_2 = 0$ has been taken as unity in accordance with Equation I.3.

With values of γ_1 available down to dilute concentrations it is possible to evaluate the integral in Equation I.24 by a graphical method and so obtain γ_2'. A difficulty with the graphical method arises from the fact that x_1/x_2 in the integrand approaches infinity as $x_2 \longrightarrow 0$ thus making it difficult to determine the area under the curve of x_1/x_2 plotted against $\log\gamma_1$ with any accuracy. However the semi-empirical graphical

procedure devised by Lakhanpal and Conway[22] and used in this thesis (see Section IV.A1) enables this difficulty to be avoided, thus giving the activity coefficients of the solute with a reasonable precision.

I.B5 Enthalpies of Solutions

If the total enthalpy of a solution containing n_1 moles of solvent and n_2 moles of solute is represented by H, then the partial molal enthalpies are given by

$$\bar{H}_1 = (\partial H/\partial n_1)_{T,\ p,\ n_2} \text{ and } \bar{H}_2 = (\partial H/\partial n_2)_{T,\ p,\ n_1} \quad (I.25)$$

Since we cannot determine absolute values of enthalpies, it is necessary to express them in relation to some specified reference state. Thus the partial molal enthalpies of the solvent and solute are expressed relative to their values in the infinitely dilute solution, $\bar{H}_1^{\infty}$ and $\bar{H}_2^{\infty}$, giving the 'relative partial molal enthalpies', $\bar{L}$, as follows:

$$\bar{L}_1 = \bar{H}_1 - \bar{H}_1^{\infty} \text{ and } \bar{L}_2 = \bar{H}_2 - \bar{H}_2^{\infty} \quad (I.26)$$

It should be noted that for the solvent $\bar{H}_1^{\infty} = H_1^{o}$ where H_1^{o} is the molar enthalpy of the pure solvent.

The total enthalpy of the solution can be expressed in terms of the partial molal enthalpies as

$$H = n_1\bar{H}_1 + n_2\bar{H}_2 \quad (I.27)$$

By substituting for $\bar{H}_1$ and $\bar{H}_2$ from Equation I.26 we obtain

$$H - (n_1\bar{H}_1^{\infty} + n_2\bar{H}_2^{\infty}) = n_1\bar{L}_1 + n_2\bar{L}_2 \quad (I.28)$$

The quantity $n_1\bar{H}_1^{\infty} + n_2\bar{H}_2^{\infty}$ can be considered as the reference value for the total enthalpy of the solution, which we can represent as H^{∞}. H^{∞} is not the enthalpy of the infinitely dilute solution but rather the enthalpy of a hypothetical solution containing n_1 moles of solvent and n_2 moles of solute with the intensive properties $\bar{H}_1^{\infty}$ and $\bar{H}_2^{\infty}$ of the infinitely dilute solution.

From Equation I.28 we can define the relative enthalpy of the solution, L, as

$$L = H - H^{\infty} \tag{I.29}$$

$$= n_1\bar{L}_1 + n_2\bar{L}_2 \tag{I.30}$$

We note from Equation I.29 that

$$\left(\partial L/\partial n_1\right)_{T,\ p,\ n_2} = \left(\partial (H - H^{\infty})/\partial n_1\right)_{T,\ p,\ n_2}$$

$$= \bar{H}_1 - \bar{H}_1^{\infty}$$

$$= \bar{L}_1 \qquad \text{by Equation I.26}$$

Similarly $\left(\partial L/\partial n_2\right)_{T,\ p,\ n_1} = \bar{L}_2$. Thus the relative properties L, $\bar{L}_1$ and $\bar{L}_2$ are governed by relationships analogous to those which govern H, $\bar{H}_1$ and $\bar{H}_2$.

For dilute solutions there is particular interest in the values of $\bar{L}_2$. These can be readily calculated if L is known as a function of n_2 for a fixed value of n_1. The requirement of a fixed value of n_1 can be conveniently met if the solution composition is expressed as the molality, m, of the solute since n_1 is then fixed at 55.51 moles of water solvent. A method of obtaining L as a power series in m is set out below.

Consider the following dilution process which can easily be carried out experimentally.

Initial solution (n_1 moles solvent, n_2 moles solute) + Pure solvent ($n_1' - n_1$ moles) ⟶ Final solution (n_1' moles solvent, n_2 moles solute).

The heat change, q, for this process can be measured in a calorimeter. If the initial and final pressures in the experiment are the same we can write

$$q = q_p = \Delta H \text{ (dilution)}.$$

Now for the dilution process

ΔH (dilution) = H (final solution) - H (initial solution) - H (pure solvent).

If we replace H for each solution by $(L + n_1\bar{H}_1^{\infty} + n_2\bar{H}_2^{\infty})$ for that solution,

according to Equations I.28 and I.29, and if we recall that $\bar{H}_1^o = H_1^o$ so that "H (pure solvent)" for the process = $(n_1' - n_1)\,\bar{H}_1^o$, we find that

$$\Delta H \text{ (dilution)} = L \text{ (final solution)} - L \text{ (initial solution)}$$
$$= L_f - L_i \qquad \text{(I.31)}$$

The values of ΔH (dilution) for various experiments can be brought on to a common basis if we express them as the values per mole of solute, i.e. ΔH (dilution)$/n_2$. This latter quantity may be called the integral enthalpy of finite dilution per mole of solute, i.e. ΔH_{ID}. Introducing ΔH_{ID} into Equation I.31 we obtain

$$\underline{\Delta H_{ID} = (L_f/n_2) - (L_i/n_2)} \qquad \text{(I.32)}$$

The quantity (L/n_2) is a well-defined property of each solution which will be a function of the solution composition variables n_1 and n_2. If the composition is expressed as the molality of the solute, m, rather than as n_1 and n_2, we can write in general terms

$$(L/n_2) = (L/m) = A_1 m + A_2 m^2 + A_3 m^3 + \ldots\ldots \qquad \text{(I.33)}$$

The power series in Equation I.33 has been written without a term independent of m, since the limit of L/m as $m \longrightarrow 0$ is zero. By substituting Equation I.33 into I.32 we obtain

$$\underline{\Delta H_{ID} = A_1(m_f - m_i) + A_2(m_f^2 - m_i^2) + A_3(m_f^3 - m_i^3) + \ldots} \qquad \text{(I.34)}$$

From which the coefficients A_1, A_2, A_3, etc. can be determined by normal least-squares fitting procedures. Equation I.33 then gives L as a power series in m for a constant value of n_1 so that $\bar{L}_2$ is readily obtained by differentiation with respect to m. Finally, values of $\bar{L}_1$ can be calculated from the equation

$$\bar{L}_1 = (L - m\bar{L}_2)/55.51$$
$$= -(A_1 m^2 + 2A_2 m^3 + 3A_3 m^4 + \ldots)/55.51 \qquad \text{(I.35)}$$

As a final comment in this section it is worth pointing out that the quantity L/n_2 for a solution is identical with the "relative apparent

molal enthalpy" of the solution which has been used by many workers and is given the symbol ϕ_L. The identity of L/n_2 and ϕ_L can be shown as follows:

The apparent partial molal enthalpy, ϕ_H, is defined by

$$\phi_H = (H - n_1 H_1^{\circ})/n_2 \qquad (I.36)$$

where H_1° is the molar enthalpy of the pure solvent. Then the relative apparent partial molal enthalpy, ϕ_L is defined by

$$\phi_L = \phi_H - \phi_H^{\circ} \qquad (I.37)$$

where ϕ_H° is the value of ϕ_H for the infinitely dilute reference solution. If we substitute Equation I.36 into I.37 we obtain

$$\begin{aligned} \phi_L &= (H/n_2 - n_1 H_1^{\circ}/n_2) - (H^{\circ}/n_2 - n_1 H_1^{\circ}/n_2) \\ &= (H - H^{\circ})/n_2 \\ &= L/n_2 \qquad \text{(by Equation I.29)} \end{aligned} \qquad (I.38)$$

Equation I.38 can now be written as

$$\phi_L = A_1 m + A_2 m^2 + A_3 m^3 + \ldots\ldots \qquad (I.39)$$

I.B6 The Temperature Dependence of the Activity Coefficient

A rearrangement of Equation I.2 gives

$$\mu_i^*/T = \mu_i/T - R \ln \gamma_i - R \ln x_i$$

Since this is an identity it may be partially differentiated at constant pressure and composition to give

$$\partial(\mu_i^*/T)/\partial T = \partial(\mu_i/T)/\partial T - R\,\partial \ln \gamma_i/\partial T \qquad (I.40)$$

If we substitute for

$$\left[\partial(\mu_i/T)/\partial T\right]_{p,\, n_i,\, n_j} = -\bar{H}_i/T^2 \qquad (I.41)$$

in Equation I.40 above we obtain

$$\partial(\mu_i^*/T)/\partial T = -\bar{H}_i/T^2 - R\,\partial \ln \gamma_i/\partial T, \qquad (I.42)$$

where $\bar{H}_i$ is the partial molal enthalpy of the particular species in the

solution being considered.

If we now apply the limiting conditions of Equation I.3; to Equation I.42 above; where γ_i approaches unity as x_i approaches zero, we obtain

$$\partial(\mu_i^*/T)/\partial T = - \bar{H}_i^{\Phi}/T^2 \qquad (I.43)$$

where $\bar{H}_i^{\Phi}$ is the partial molal enthalpy of the component in the infinitely dilute solution.

Now μ_i^* is independent of composition and therefore $\partial(\mu_i/T)/\partial T$ has the same value whether we consider some particular solution or the solution in the limit where γ_i approaches 1. Thus by combining Equations I.42 and I.43 above we obtain the temperature dependence of the activity coefficient as

$$\begin{aligned} \partial \ln \gamma_i/\partial T &= - (\bar{H}_i - \bar{H}_i^{\Phi})/RT^2 \\ &= - \bar{L}_i/RT^2 \end{aligned} \qquad (I.44)$$

I.B7 Entropies of Dilution of Amino Acid Solutions

The relationship G = H - TS for the total properties of a solution applies in the same form to the partial molal properties so that we have

$$\bar{G}_1 = \bar{H}_1 - T\bar{S}_1 \qquad (I.45)$$

for the solvent of a binary solution.

Similarly, this equation applies also in the reference state so that

$$\bar{G}_1^{\circ} = \bar{H}_1^{\circ} - T\bar{S}_1^{\circ} \qquad (I.46)$$

Subtracting (I.46) from (I.45) we have

$$\begin{aligned} \bar{G}_1 - \bar{G}_1^{\circ} &= (\bar{H}_1 - \bar{H}_1^{\circ}) - T(\bar{S}_1 - \bar{S}_1^{\circ}) \\ &= \bar{L}_1 - T(\bar{S}_1 - \bar{S}_1^{\circ}) \end{aligned} \qquad (I.47)$$

Now $\bar{G}_1 - \bar{G}_1^{\circ} = RT \ln a_1$

Hence $(\bar{S}_1 - \bar{S}_1^{\circ}) = \bar{L}_1/T - R \ln a_1 \qquad (I.48)$

$\bar{S}_1 - \bar{S}_1^{\circ}$ is the entropy change for the transfer of one mole of water from a large amount of an infinitely dilute solution to a large amount of a solution of finite concentration.

This equation includes the entropy contribution arising solely from the mixing of the components. If this is subtracted from Equation (I.48) we have

$$(\bar{S}_1 - \bar{S}_1^{\circ}) - (-R \ln {}^{x_1}/_{x_1 o}) = \bar{L}_1/T - R \ln a_1 - (-R \ln {}^{x_1}/_{x_1^{\circ}})$$

$$\text{i.e.} \quad (\bar{S}_1 - \bar{S}_1^{\circ})^* = \bar{L}_1/T - R \ln {}^{a_1}/_{x_1} \qquad \text{(I.49)}$$

Since $x_1^{\circ} = 1$.

$$(\bar{S}_1 - \bar{S}_1^{\circ})^* = (\bar{S}_1 - \bar{S}_1^{\circ}) - (-R \ln x_1)$$

where the quantity $(\bar{S}_1 - \bar{S}^{\circ})^*$ may be called the relative partial molal entropy corrected for the entropy of mixing term.

CHAPTER II

EXPERIMENTAL

II.A DETERMINATION OF ACTIVITIES OF AMINO ACIDS IN WATER

II.A1 Methods of Determining Activities

II.A1(i) Isopiestic comparison method

This comparative method of determining vapour pressures of solutions was first introduced by Sinclair[23] following a suggestion by Bousfield and Bousfield[24]; and it has been widely applied to solutions of inorganic salts[25] and to aqueous solutions of amino acids[26-32].

The method is applicable to systems with only one volatile component and relies on the fact that when two solutions with different involatile solutes are contained within a constant temperature environment, distillation of the common solvent will occur until the vapour pressures of both the solutions are the same. Such solutions are termed 'isopiestic'. Determination of the vapour pressure and consequently the activity of the solvent requires accurate information about the vapour pressure of the reference solution as a function of its composition.

The technique has consisted of enclosing two or more shallow metal (usually silver) dishes of high thermal conductivity, each containing approximately 2cm^3 of solution, in a large, evacuated glass or metal container. Heat transfer between the solutions was facilitated by sinking the dishes into a large copper block, and in some cases thermal contact was further improved by a film of solution between each dish and the copper block. The entire assembly was placed in a thermostat and rocked slowly to gently agitate the solutions. The time required for equilibrium to be attained depended on the concentrations of the solutions, with the more dilute solutions often requiring up to a week. When equilibrium had been attained, the vacuum was broken and the dishes were removed and weighed to determine the concentration of the isopiestic solutions.

Several difficulties have been experienced with the method. In cases where thermal contact between the dishes and the block has been poor

and a film of solution has been placed between them, the dishes have needed to be washed before weighing. Splashing has resulted from degassing of the solutions during evacuation. Long diffusion paths in some forms of the apparatus have produced extremely long equilibration times. Often the apparatus to be rocked in a thermostat has been large and cumbersome. Finally, condensation sometimes occurs in the evacuated chamber when air is admitted at the completion of a run.

Hutchens, Figlio and Granito[31] have described an isopiestic method which has attempted to avoid some of these difficulties. The solutions to be compared were placed as droplets in shallow depressions close together in the same metal block, thus providing good thermal conduction and short diffusion paths. Resultant equilibrium times were shorter, shaking was not necessary and with a small apparatus several comparisons could be made separately in the one constant temperature bath. The isopiestic solution concentrations were determined using specific gravity gradient tubes. The improved thermal conduction and small gas space permitted reasonably short incubation periods without drastic evacuation thereby avoiding the possibility of splashing of the solutions. Despite the initial optimism concerning this method, the authors concluded their paper with the following words:

> "More precise values of isopiestic ratios could be obtained through a better knowledge of the molalities of standard solutions. This can readily be achieved through more precise weighing of solutes. That we did not do so reflects our early disenchantment with the method, from which we did not recover in time to improve our procedure."

Isopiestic measurements have been made on solutions from saturation down to concentrations of about 0.1 molal, although by taking extreme precautions, Gordon[33] has used the method down to 0.03 molal. He experienced difficulty with the extremely slow rate of attainment of equilibrium under the slight vapour pressure head present and with the need to shield the apparatus from temperature fluctuations or at any rate from

fluctuations that were not slow in comparison with the rate at which thermal equilibrium was established in the system.

It has been generally found that the ratio of the concentrations of the isopiestic solutions can be determined with an accuracy of 0.1 - 0.2% down to concentrations in the region of 0.1 molal, thus yielding values for the activity coefficient of the solute with an accuracy of about 2%.

II.A1(ii) Freezing point depression method

The freezing point depression method of determining the activity of the solvent is appropriate for very dilute solutions (0.1 - 0.001 molal). It depends on the measurement of the temperature at which a solution is in equilibrium with its pure solid solvent. In the 'equilibrium' method of measuring freezing points the problem is to maintain the solid solvent and the solution at equilibrium, and to determine the temperature and composition as accurately as possible.

To illustrate the method, the experimental apparatus and procedure developed and used by Scatchard, Jones and Prentiss[34] to determine the freezing point depressions of glycine-water solutions is described.

In their work, the temperature differences were measured between ice in equilibrium with pure water and ice in equilibrium with a solution, each being contained in a gold-plated silver vessel. These vessels were divided by vertical walls into three compartments, the two outer ones being smaller than the central one. Solution was pumped from the outer compartments through the ice contained in the central compartment. Silvered Dewar flasks were used to contain the vessels in order to secure as nearly as possible, adiabatic conditions; and a stream of nitrogen was passed through the solution to remove dissolved air (since nitrogen has only half the solubility of oxygen in water). The temperatures were measured with a multi-junction copper-constantan thermocouple and the concentration of the solution after coming to equilibrium with the ice

was determined by light absorption or specific conductivity measurements on an aliquot removed from the equilibrium mixture.

The authors concluded that the freezing point depressions could be measured to about 2×10^{-5}°C and that a concentration of 0.001 mol l^{-1} was about the lowest at which measurements could be profitably made. Thus at 1 mol l^{-1} an error of 2×10^{-5} in the temperature corresponds to an error of about 0.002 in log γ.

II.A1(iii) Osmotic pressure method

The osmotic pressure of a solution is related to the activity of the solvent in it and hence the measurement of the osmotic pressure should provide in principle a method for the determination of activities.

In fact, experimental difficulties have meant that the method has not had a widespread application. In particular there have been problems developing a truly semi-permeable membrane as well as obtaining accurate data for the variation of the partial molar volume of the solution with concentration and pressure.

II.A1(iv) Static vapour pressure method

In the static equilibrium methods of vapour pressure measurement the liquid is confined in an evacuated vessel and the pressure exerted by the vapour when the liquid is maintained at constant temperature, is measured. This technique is especially suitable for measurements on solutions in which only one component is volatile, for then the vapour consists of only one component and it is unnecessary to determine its composition.

The liquid must be thoroughly degassed. Also the vapour must be at the same or a higher temperature than the water bath, as otherwise condensation will occur giving spurious vapour pressure readings.

The static method may be used either in a direct manner in

TABLE II.1

Examples of Methods Used for the Determination of Activities

Method	System	Reference
Isopiestic	Glycine + water at 298.15K	Richards[28]
Isopiestic	Glycine + water at 298.15K	Smith and Smith[26]
	(Alanine, α-amino butyric acid, α-amino-n-valeric acid, α-amino-i-butyric acid, valine) + water at 298.15K	Smith and Smith[27]
	(β-Alanine, β-amino-n-butyric acid, β-amino-n-valeric acid, γ-amino-n-butyric acid, γ-amino-n-valeric acid) + water at 298.15K	Smith and Smith[29]
	(Serine, threonine, proline, hydroxyproline) + water at 298.15K	Smith and Smith[30]
	(Glycylglycine, alanylglycine, glycylalanine, alanylalanine, triglycine) + water at 298.15K	Smith and Smith[35]
Isopiestic	(Serine, arginine.HCl) + water at 298.15K	Hutchens, Figlio, Granito[31]
Isopiestic	(Glycine, glycylglycine, α-amino-n-butyric acid, valine, lactamide, raffinose) + water at 298.15K	Ellerton, Reinfelds, Mulcahy, Dunlop[32]
Freezing point	Glycine + water at 273.15K	Scatchard and Prentiss[36]
Freezing point	(Glutamic acid, aspartic acid) + water at 273.15K	Hoskins, Randall, Schmidt[37]
Direct static vapour pressure	Benzene + diphenyl at 303.15 to 353.15K	Baxendale, Enustun, Stern[38]
Differential and direct static vapour pressure	Polyglycols + methanol at 243.15K to 301.15K	Lakhanpal and Conway[39]
Differential static vapour pressure	Glucose + water at 298.15K to 338.15K	Taylor and Rowlinson[40]

which the total vapour pressure above the solution is measured or in a differential manner where the vapour pressure of the solution is compared with that of the pure solvent and only the vapour pressure difference is measured. The relative merits of these two alternative methods are discussed in Section II.A1(v).

The accuracy of the method depends on the manometer design and the method of measuring the pressure difference. The differential static method used in this work, utilising a mercury U-tube manometer and a cathetometer to measure the height differences, was capable of measuring the vapour pressures of solutions with an accuracy better than 7 Pa thus giving the activity coefficients of the solute in the solution to about 2%.

Examples of the different methods used to determine activities are tabulated in Table II.1.

II.A1(v) Choice of method

In determining the activities of amino acid-water solutions it was decided to use the static vapour pressure method in favour of the isopiestic comparison method and the freezing point depression method.

It was considered that the vapour pressure method would be less time-consuming than the isopiestic method in view of the long equilibration times, especially in more dilute solutions, necessary for the latter. Also, it was hoped that the vapour pressures of solutions of concentrations less than 0.1 molal would be able to be measured accurately with a sensitive magnifying manometer capable of resolving pressure differences of 0.2 - 0.3 Pascals.

The vapour pressure method was preferred to the freezing point depression method in view of the difficulty in the latter technique of determining the concentration of the amino acid solutions at the freezing point, and the concern that some solute might be frozen in the ice. The

method is also restricted to a single low temperature.

For the measurement of vapour pressures of amino acid-water solutions the differential static method has advantages over the direct static method. These can be appreciated by considering the percentage error in the activity of water caused by errors in the vapour pressure measurements.

According to Equation I.20 the activity of water in an amino acid solution can be approximated by,

$$a = p/p^{\circ} \qquad \text{(II.1)}$$

where p is the vapour pressure of the solution and p° is the saturated vapour pressure of the water, both at the same temperature.

If the differential method is used, Equation II.1 can be written as,

$$a = 1 - \Delta p/p^{\circ} \qquad \text{(II.2)}$$

where Δp is the difference in vapour pressure between the solvent and the solution, given by,

$$\Delta p = p^{\circ} - p$$

The maximum percentage error, α_a, in the activity a, caused by errors in the direct vapour pressure measurement is given by,

$$\alpha_a = 100\, \delta a/a$$
$$= 100(\delta p/p + \delta p^{\circ}/p^{\circ}) \qquad \text{(II.3)}$$

where δp and δp° can be considered as the errors in p and p° respectively and δa, the error in a.

The percentage error, α_a', for the differential method however, is found from Equation II.2 to be,

$$\alpha_a' = 100\, \delta a/a$$
$$= 100 \left[\delta \Delta p/p + \left(\delta p^{\circ}/p^{\circ}\right)\left(\Delta p/p\right)\right] \qquad \text{(II.4)}$$

where $\delta \Delta p$ can be considered to be the error in Δp.

If all the vapour pressure measurements, p, p° and Δp are made with about the same actual error (not percentage error) it can be seen from Equation II.3 and II.4 that the error in the activity of water, a, is less for the differential method than for the direct method whenever Δp is less than p, which is the case for all the aqueous amino acid solutions.

Another advantage in using the differential method when Δp is less than p, is that fluctuations in the temperature of the thermostat, and the effect of degassing of the apparatus, will cause smaller errors in Δp than in p.

It was therefore decided to use the differential static method of measuring the vapour pressures of the amino acid-water solutions.

II.A2 Vapour Pressure Apparatus

II.A2(i) General construction

A diagram of the principal components of the vapour pressure apparatus is given in Figure II.1. The apparatus was constructed mainly from Pyrex glass and firmly supported on an aluminium rod frame attached to a concrete wall. Those sections of the apparatus which were directly involved in vapour pressure measurements were constructed from 2mm capillary to reduce the volume of the dead space.

Tap T_1 which isolated the vacuum pumping system from the remainder of the apparatus was an L-shaped high vacuum stopcock greased with Apiezon N. Taps T_2 to T_{14} were either Springham Viton A diaphragm valves or Hoke 4613N4M valves. These latter valves were incorporated into the glass system with graded glass to metal seals. T_{15} was a valve connecting the two arms of the differential magnifying manometer, P, and is discussed in detail later in the description of the manometer.

The solvent and the solution were contained in vessels A and B respectively, both of which were capable of being stirred with Teflon-

encased metal bars turned by means of magnetic stirrers C and D. The demountable solution vessel was attached to the system using a Kontes O ring-sealed high vacuum joint. This joint was found to be completely reliable in maintaining a vacuum throughout the period of use.

The entire vapour pressure apparatus was housed in a room in which the temperature was maintained constant to $\pm$ 0.5K. Room temperature was set at a value of about 5K above the temperature of measurement to avoid condensation of water vapour in the system. Both the magnifying manometer, P, and the U-tube manometer, M, were lagged with cotton wool to reduce the effect of temperature fluctuations produced locally in the room. The temperature of the mercury in the manometers was measured with mercury thermometers whose lagging times were increased to be approximately as long as those of the manometers by immersing the bulbs in mercury-filled tubes (surrounded with cotton wool) of the same diameter as the manometer.

II.A2(ii) Vacuum pumping system and vacuum gauges

The apparatus was capable of being evacuated to a pressure less than 5×10^{-6} Torr with an Edwards ISC 50B single stage rotary backing pump, F, in combination with a Philips oil diffusion pump, H. A liquid air trap, I, was located between the oil diffusion pump and the remainder of the apparatus to prevent oil vapour from entering the vapour pressure system and also to prevent water vapour from entering the pump. A water-cooled jacket, G, prevented oil from the diffusion pump from entering the rotary backing pump.

The system pressure was measured with an Edwards Pirani gauge head (model G6B), J, in the range 3 to 10^{-3} Torr and with an Edwards Ionization gauge head (model 1G6G), K, below 10^{-4} Torr. Both were protected from volatile liquids by liquid air traps.

II.A2(iii) Thermostat (E)

This consisted of a 35cm x 35cm x 30cm copper tank lined with polystyrene and wood and covered with a sectioned polystyrene lid. The thermostat was supported on a scissor jack to permit convenient access to the solution and solvent vessels.

The water in the thermostat was stirred at 1100rpm with a centrally positioned 10cm diameter four-bladed paddle. The pitch of the blades was arranged so that the water was driven down in the middle and up at the sides of the tank. Cooling was provided by a Colora TK64 portable refrigeration coil and the permanent background heater was a Variac-controlled 1 kW immersion heater. The cooling coil and the immersion heater were located together away from the solution and solvent vessels. Intermittent heating was provided by a blackened 60 watt light bulb controlled through a relay by a mercury-toluene regulator. The temperature, measured with a 2801 A Hewlett-Packard Quartz thermometer, registered a long-term fluctuation of $\pm$ 0.002K. Prior to use the thermometer was checked against the ice point and the appropriate offset corrections were made.

II.A2(iv) U-Tube manometer (M)

This manometer was constructed from adjacent pieces of 2.5cm precision bore tubing. The average cross-sectional areas of the tubes, determined by measuring the weight of mercury discharged for a measured change in the mercury level in the tubes, was 4.9096 $\pm$ 0.0065cm^2. This cross-sectional area was required for subsequent measurements of the volumes of various parts of the apparatus. Care was taken in the assembly of the manometer to ensure that it was mounted in a vertical position.

Filling of the manometer was accomplished by operation of tap T_{12} which connected the manometer to a mercury reservoir. Use of this tap also permitted measurements of the height of the mercury columns

Figure II.2 Differential magnifying manometer.

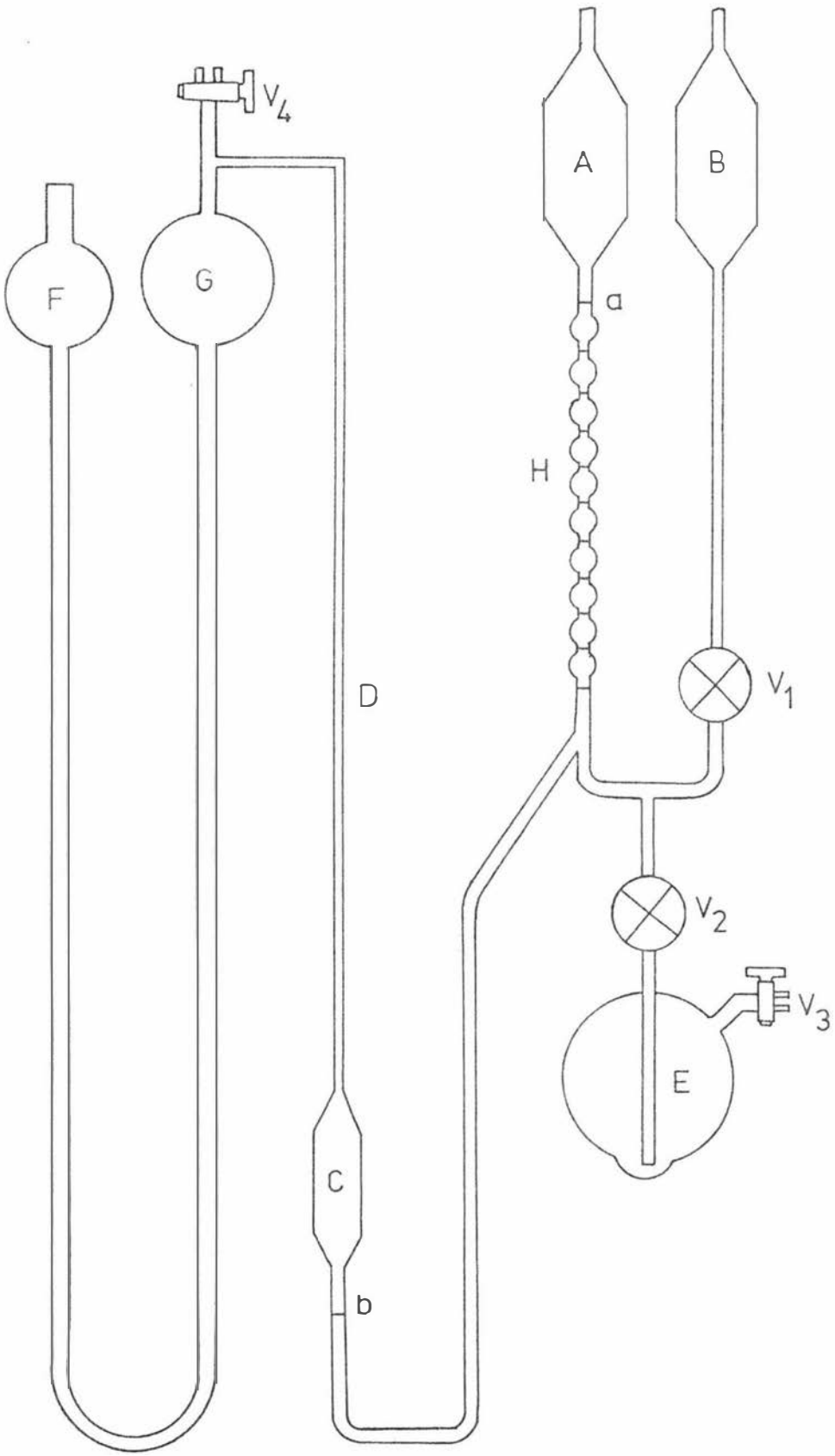

to be made with rising menisci thus facilitating reproducible menisci shapes.

The heights of the mercury columns were measured using a 1 m cathetometer (Precision Tool and Instrument Company) located about 50cm from the manometer, on a firm concrete support to prevent any movement of the instrument relative to the manometer because of movements of the observer. The cathetometer was also positioned such that no refocussing of the telescope was required between measuring the heights of the mercury columns in each arm of the manometer. Prior to each measurement it was ensured that the telescope was level. To assist in the precise determination of the mercury meniscus a 20 watt clear-white fluorescent light was placed behind the manometer and the light was directed using a sliding shield lowered to within 0.25mm of the mercury surface.

II.A2(v) Differential magnifying manometer (P)

This differential magnifying manometer is similar to those used by Puddington[41], Sirianni and Puddington[42], Lakhanpal and Conway[39] and Kershaw[43]. A more detailed diagram of the manometer is given in Figure II.2.

Construction

Arms A and B of the manometer were constructed from adjacent sections of 2.7cm precision bore tubing, and the indicator capillary D was a 60cm length of 0.1cm precision bore tubing. All other capillary used in the construction of the manometer was 0.3cm internal bore. The flow of the mercury between arms A and B was controlled by valve V_1, and the filling of the manometer from the mercury reservoir, E, was controlled by the valve V_2 and the two-way valve V_3. The small bulbs H below arm A were used to extend the measuring range of the manometer; the volume of each bulb was approximately equivalent to 40cm of capillary D. The marks between the bulbs enabled the equivalent length of capillary D corresponding to each bulb to be determined exactly. Bulb C attached to the

lower end of capillary D had a volume approximately half that of arm A. The two-way valve V_4 and the flask, F, were used to adjust the height of the mercury in the indicator capillary D.

To ensure that there was no movement of arms A and B relative to one another or to valve V_1, all were held rigidly by being set in plaster of paris.

Operation of the magnifying manometer

The operation of this manometer depends on the precise measurement of the volume of mercury that flows from arm A to arm B when they are subjected to a pressure difference across them. This was accomplished by measuring the decrease in the volume of mercury on the left hand side of valve V_1 using the following procedure.

With the manometer filled with a suitable volume of mercury, valve V_2 was securely closed. Equal pressures were then applied to arms A and B with V_1 open and the mercury level below bulb C adjusted to reference mark b. All adjustments to reference marks were observed through the cathetometer telescope. V_1 was closed and the mercury drawn up into bulb C and capillary D until the level below arm A had dropped to reference mark a. After careful setting of the mercury level to this reference mark, the height of the mercury in the indicator capillary D was measured with the cathetometer. This constituted the zero reading of the instrument. Sufficient mercury was used in filling the manometer so that the zero reading was near the top of the capillary. The mercury was lowered again to reference mark b, and V_1 opened in readiness for the next determination.

Now, with V_1 closed a pressure difference was applied to the arms of the manometer; the greater pressure (solvent vapour pressure) was exerted on arm A. V_1 was opened and after equilibration the mercury level below C was again adjusted to mark b. Then with V_1 closed the

mercury was drawn up into capillary D and the new height determined as for the zero reading.

The difference between the zero reading and this new height represents the volume of mercury that has been transferred from arm A to arm B on applying the pressure difference. If it so happened that this pressure difference was of such a magnitude that the mercury from arm A did not come up into capillary D then one or more of the small bulbs H was emptied until the height could be measured in the indicator capillary. The equivalent height in the capillary corresponding to the bulbs used was added to the zero reading for determining the pressure difference.

Calculation of pressure difference

To calculate the pressure difference the change in height of the mercury level in capillary D is combined with the magnification factor M of the manometer. This factor depends on the relative cross-sectional areas of arm A and capillary D and is given by $M = \frac{1}{2}(A_1/A_2)$; where A_1 is the cross-sectional area of arm A and A_2 is the cross-sectional area of capillary D. For this particular manometer the cross-sectional areas A_1 and A_2 (determined before assembly by measuring the weight of mercury discharged for a measured change in the mercury level in the tubes) were $5.931 \pm 0.012 cm^2$ and $0.008061 \pm 0.000033 cm^2$ respectively, giving a magnification factor of 367.9 ± 0.8.

Tests and modifications on manometer

In many series of zero readings the values obtained were reproducible to within $\pm$ 1.0cm in capillary D. Given that the same reproducibility was obtained when a pressure difference was applied, then the minimum expected error in the calculated vapour pressure was $\pm$ 0.0054cm. This precision was far worse than that obtained by Puddington and by Kershaw who were able to determine vapour pressures with an error of $\pm$ 0.0004cm, corresponding to a reproducibility of $\pm$ 0.1cm for readings in capillary D.

It was considered that since fluctuations in the manometer temperature were less than 0.1K they were not sufficient to produce the lack of precision in the zero readings. (From the volume of mercury in the expansion arm of the manometer the expected variation of the height of mercury in capillary D with temperature was determined to be 0.4cm K^{-1}.)

Many repetitions of the zero reading were carried out with valve V_1 closed and the reproducibility was better than $\pm$ 0.025cm indicating that the magnification operation wasfunctioning well. In order to check that the mercury levels in arms A and B were coming to equilibrium before V_1 was closed their heights were measured after the lower mercury level had been set to reference mark b. Within the limits of measurement ($\pm$ 0.002cm) no height difference was observed. Similarly no change in the levels could be detected after V_1 had been closed.

From the above considerations it seemed clear that the most likely source of the zero reading inconsistency was the valve V_1. V_1 was required to close without producing a volume change (or at least with a consistent volume change in one direction) and to hold against a possible leak from the atmosphere.

Much of the vapour pressure work for three years was concerned with making and testing modifications to the manometer principally through incorporating a variety of valves V_1. A summary is given below of some of the main modifications made to the manometer.

Following Kershaw, the first valve used was a greaseless Exelo tap. This consisted of two flat ground-glass plates held together by a stainless steel rod and spring clip and operated by turning one of the sections. To decrease the likelihood of leaking from the atmosphere the whole valve was submerged in a mercury seal. This valve was found to be difficult to turn and at times even jammed tightly. On inspection small chips could be seen in the glass around the centre spindle and some

scoring of the plate surface was also evident. In an attempt to remove the surface aberrations, the two plates were optically faced before reassembly. The valve then performed better mechanically but the reproducibility of the zero readings was little better than ± 1.0cm.

Puddington[41] and Sirianni and Puddington[42] used a 4mm Pyrex glass stopcock lubricated with a film of dried 'aquadag' and a very thin film of heavy lithium stearate grease. In line with this several glass stopcocks were tried. For example zero readings were made using a 2mm hollow key high vacuum stopcock, a 4mm hollow key high vacuum stopcock, and also a 3mm solid key high vacuum stopcock. All the stopcocks used were greased either with Apiezon N or Apiezon T hydrocarbon grease. Again the precision obtained for pressure readings was no better than before. No doubt the problem was accentuated with the transfer of minute amounts of grease to the glass and mercury surfaces in the manometer with continued operation of these stopcocks. As a result of this it was often necessary to completely dismantle and thoroughly clear the manometer and clean the mercury before a new valve could be inserted and tested.

In view of the need to exclude grease from the system, several stainless steel valves were used. Each valve was fitted into the manometer with graded glass to metal seals. The first stainless steel valve used was a 3mm bore Whitey Ball valve designed for use in fluid control situations. The valve however was not highly rated for vacuum applications. Initial precision using this valve was very encouraging (± 0.16 - 0.3cm), but with longer use the performance gradually deteriorated and air was admitted to the manometer through the valve. In an attempt to stop the valve leaking it was enclosed in a mercury seal but it was then discovered that some of the components of the valve were attacked by mercury.

It was decided next to use a stainless steel needle valve, and

a Whitey needle valve suitable for vacuum work was fitted into the manometer. Unfortunately the only valve available had a very small orifice and this necessitated long equilibration times for the mercury levels after a pressure difference had been applied. Care also had to be taken in filling the manometer as flow was very restricted through the needle valve. The long term reproducibility obtained with this valve was marginally better than the performance of the glass stopcocks, but though there was no tendency to leak this valve did not produce as good a precision as was first obtained with the ball valve.

Examples of some of the different valves used in the differential magnifying manometer are given in Table II.2 along with the standard deviations of sets of zero readings (heights in capillary D, Figure II.2) made with each valve. The figures in brackets are the number of individual readings made in any one set.

Apart from the early performance of the stainless steel ball valve the reproducibility of the vapour pressure measurements using the magnification manometer was less than that consistently obtainable using the ordinary U-tube manometer. In view of this disappointing experience extending over three years it was decided to make a series of vapour pressure measurements on L-serine-water solutions using the U-tube manometer. (At this time we reflected wryly on the comments at the end of the paper by Hutchens, Figlio and Granito[31] which were partly responsible for our decision to attempt to improve on their work by using a magnifying manometer. Their words were,

> "More precise values of isopiestic ratios could be obtained through a better knowledge of the molalities of standard solutions. This can readily be achieved through more precise weighing of solutes. That we did not do so reflects our early disenchantment with the method, from which we did not recover in time to improve our procedure.")

TABLE II.2

Examples of Some of the Valves Used in the Magnifying Manometer with the Corresponding Zero Reading Reproducibility

Valve	Standard deviation of zero reading (Height in mm in capillary D, Figure II.2)			Remarks
Exelo greaseless tap (1)	9.86(14);	10.97(12);	9.41(15)	Continually jamming
Exelo greaseless tap (2)	9.42(13);	8.96(16);	12.07(16)	Optically ground faces
2mm high vacuum stopcock (hollow key)	7.13(11);	12.30(11)		Greased with Apiezon T and N
4mm high vacuum stopcock (hollow key)	8.10(14);	8.61(9);	11.30(12)	Greased with Apiezon T and N
3mm high vacuum stopcock (solid key)	8.06(17);	10.53(12)		Greased with Apiezon T and N
2mm non-vacuum stopcock	7.65(13);	5.53(15)		Key hand-lapped in, greased with Apiezon T; continually leaked
Whitey 3mm stainless steel ball valve	1.63(10);	2.88(14)		Leaking from atmosphere into manometer
Whitey SS-2 stainless steel needle valve	9.01(8);	10.11(10);	10.11(9)	

II.A3 Vapour Space Volume of the Vapour Pressure Apparatus

To determine the exact concentration of the amino acid solution in the solution vessel for a particular vapour pressure measurement it was necessary to correct for the amount of water in the vapour space above the solution.

With cells A and B attached and empty (see Figure II.3), the entire system was evacuated. Dry nitrogen was then admitted to cell B through tap T_3, with tap T_5, T_6 and T_7 closed, until a pressure of about 8cm Hg was indicated on the manometer.

The initial distance h_1, between the mercury level in the left-hand arm of the U-tube manometer and a reference mark R, was measured. The pressure of the nitrogen p_1, at the temperature of the manometer T_1, was also determined. Mercury was then admitted from the reservoir and the distance h_2, between the new mercury level and the reference mark was measured, together with the corresponding manometer temperature T_2 and nitrogen pressure p_2.

The volume of the vapour space (including cell B) to the reference mark R, assuming nitrogen to be a perfect gas at room temperature, can be calculated from the equation,

$$V = \frac{A\left(\frac{p_1 h_1}{T_1} - \frac{p_2 h_2}{T_2}\right)}{\frac{p_2}{T_2} - \frac{p_1}{T_1}} \qquad \text{(II.5)}$$

where A is the average cross-sectional area of the arm of the U-tube manometer.

For each solution in cell B, the volume of the liquid was subtracted from the volume of the vapour space and the volume from the reference mark to the mercury level in the solution arm of the manometer was added on to give the appropriate vapour space volume for each measurement.

II.A4 Sample Preparation

II.A4(i) Materials

The amino acid L-Serine was supplied by the Sigma Chemical Company as Sigma grade (99% +). This was recrystallized twice from distilled water with about 60% recovery in each case. Following recrystallization, the amino acid was dried in a vacuum dessicator over P_2O_5 at room temperature for at least seventy-two hours. A nitrogen analysis of the sample gave 13.57% N compared with a theoretical nitrogen content for L-Serine of 13.33%.

The water for preparation of the L-Serine solutions and for the measurements of vapour pressure of pure water was prepared with reference to the method of Barber[44]. Laboratory tap-water was refluxed for 6 to 8 hours with alkaline potassium permanganate and then twice distilled, the middle fraction being retained in each case.

II.A4(ii) Weighing of the amino acid

The recrystallized and dried amino acid was weighed into a glass weighing boat from where it was transferred to the solution vessel E, Figure II.4, through the side loading arm. The loading arm was then sealed and the vessel attached to the sample preparation line by a Kontes O ring-sealed vacuum joint. The vessel was then evacuated for several hours until the sample showed no tendency to outgas.

The true mass, m_i of the amino acid in the solution vessel was calculated from the observed masses using buoyancy corrections according to the formula,

$$m_i = m_i' (1 - \rho_a/\rho_w) + V_i \rho_a \qquad \text{(II.6)}$$

where m_i' is the observed mass of the amino acid, V_i is the volume of air it displaced and ρ_a and ρ_w are the densities of air and of the material of the balance 'weights' at room temperature ($\rho_w = 8.4 g\ cm^{-3}$).

All weighings were made to 0.00005g and buoyancy corrections

Figure II.4 Degassing apparatus.

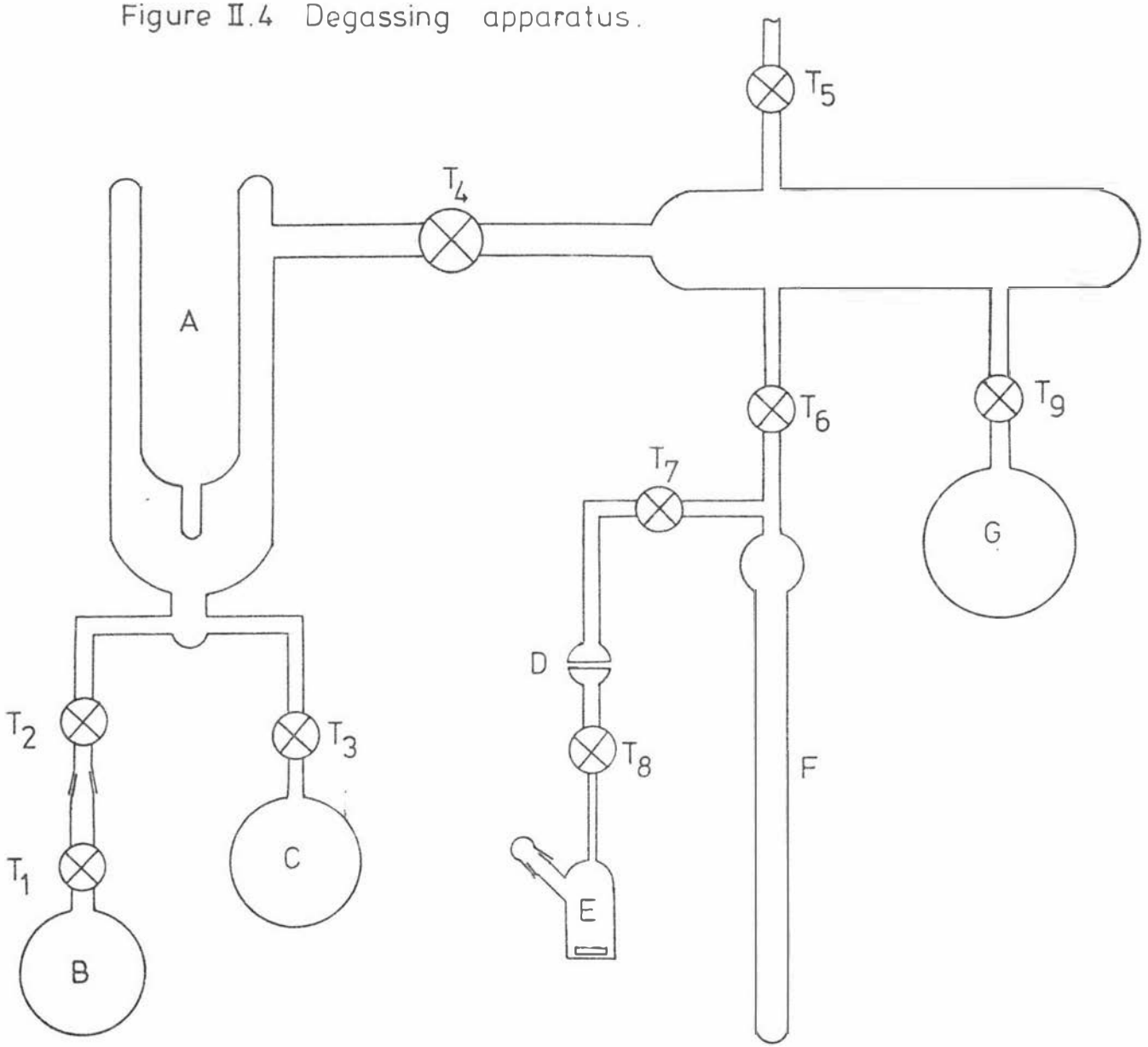

produced changes of less than 0.01% in the observed weight.

II.A4(iii) Degassing of water

The water was degassed using the vacuum sublimation method described by Bell[45]. A diagram of the apparatus is given in Figure II.4. A sample of water distilled from alkaline permanganate was boiled before being placed in flask B, attached to the system, and frozen by means of a mixture of acetone and dry ice. When the sample had been frozen, the whole apparatus was evacuated until the pressure was less than 10^{-4} Torr. The cold finger A, was then filled with a slurry of acetone and dry ice and the refrigerant around the sample was removed allowing it to warm and sublime. The water vapour slowly solidified on to the cold glass surface of the cold finger. On completion of the vacuum sublimation, taps T_2 and T_4 were closed and the water on the cold finger transferred to flask C. The vacuum sublimation was then repeated on the same sample before transferring it to the storage flask G.

Water degassed in the above manner was distilled directly into the solvent vessel in the vapour pressure apparatus to be used as the reference solvent, and was also used for the preparation of the amino acid solutions.

II.A4(iv) Addition of water to the amino acid

Degassed water from the storage flask G in the Figure II.4 was vacuum distilled into the calibrated delivery tube F. This delivery tube was constructed from 1.0cm precision bore tubing and had an average cross-sectional area of $0.50535 \pm 0.0009 cm^2$ (determined by weighing the mercury discharged for a measured height change in the mercury in the tube).

With taps T_6 and T_7 closed, the water (frozen from the distillation) was thawed and its level in the tube measured relative to a reference mark at a given temperature. When measuring the height of the column of water with the cathetometer, the tube F was surrounded by a

vertically-mounted water jacket maintained at a constant temperature (± 0.1K) below the room temperature.

A slurry of acetone and dry ice was then placed around the solution vessel E and on opening taps T_7 and T_8, water distilled into the solution vessel. After the required amount had been transferred, taps T_7 and T_8 were closed and the height of the water in the delivery tube determined as before.

To calculate the amount of water added to the amino acid each reading h(t') of the water level in the tube F was corrected to a common reference temperature t using the equation

$$h(t) = h(t') + \frac{V_w \alpha (t - t')}{A} + \frac{V_g M(p' - p)}{\rho ART} \qquad (II.7)$$

where V_w is the volume of water in the delivery tube F, α is the coefficient of thermal expansion of water, A is the cross-sectional area of the tube, V_g is the volume of the vapour space above the water in the tube, M is the molecular weight of water and p' and p are the vapour pressures of water at t' and t respectively. This equation accounts for the effect of a temperature change on the density of water ρ and on the amount of water in the vapour phase above the liquid water.

The mass of water m, added to the solution cell was then calculated from the equation,

$$m = \rho A(h_a - h_b) - MpA(h_a - h_b)/RT \qquad (II.8)$$

where h_a and h_b are the corrected liquid water levels from Equation II.7 before and after delivery respectively. The last term accounts for the change in volume of the vapour phase on making the addition to the solution cell.

The error in the measured height was ± 0.01cm, in the cross-sectional area of the tube ± 0.05% and in the density of the water ± 0.0003g cm^{-3}. This meant that the mass of water added to the amino acid could be determined with an accuracy of better than 0.4%.

Figure II.5 Vapour pressure apparatus

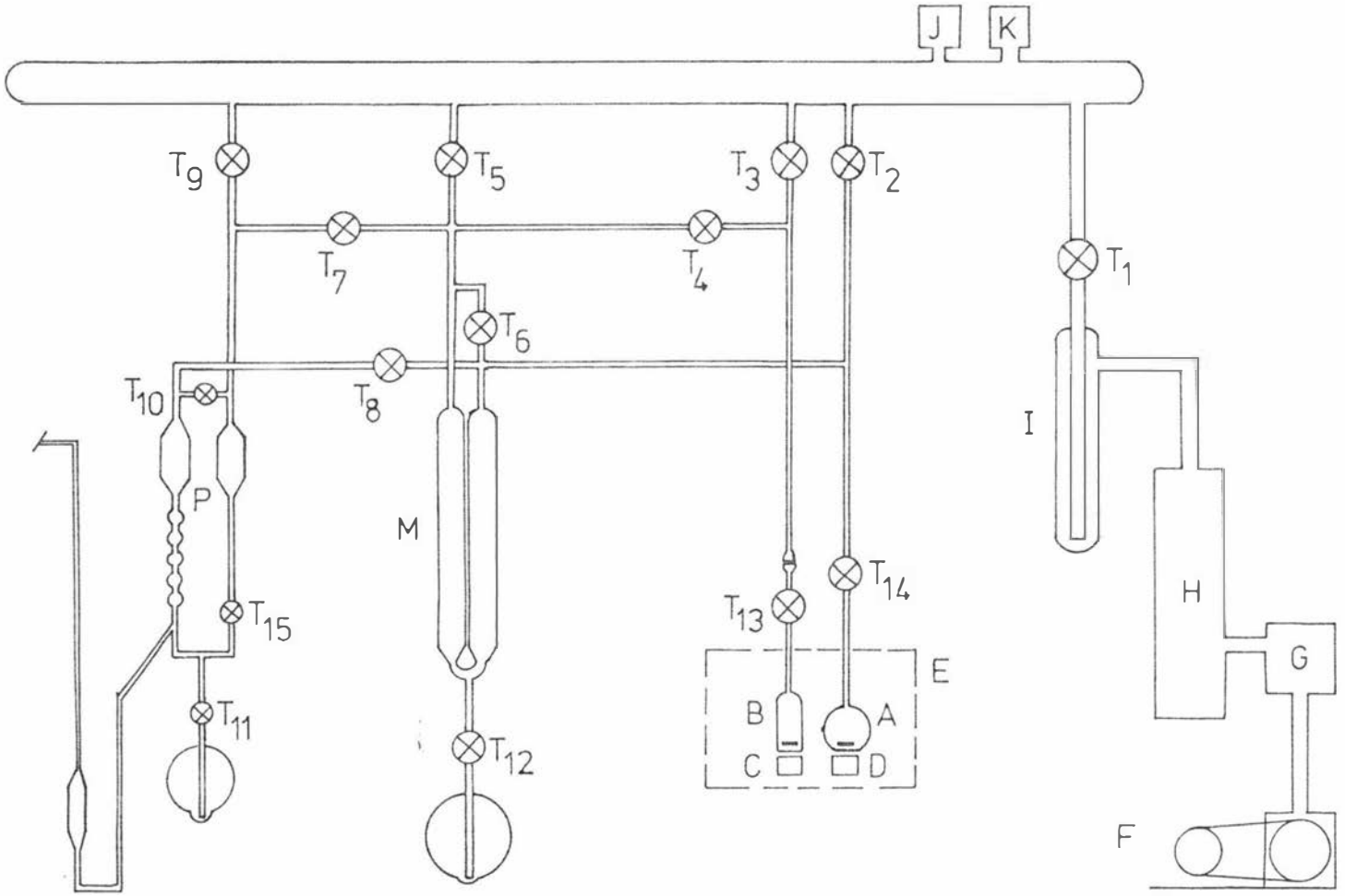

Following the addition of the water to the amino acid, the solution cell was removed from the sample preparation line and attached to the vapour pressure apparatus at B in Figure II.5.

II.A4(v) Amount of water in the vapour phase

In determining the exact concentration of the amino acid solution corresponding to a particular pressure difference it was necessary to correct each concentration for the amount of water in the vapour phase. Since the volumes of the various vapour spaces in the vapour pressure apparatus were known the amount of water in the vapour phase, m_v, could be calculated from the equation

$$m_v = Mp\left(\frac{V_r}{RT_r + B_r p} + \frac{V_t}{RT_t + B_t p}\right) \qquad (II.9)$$

where M is the molecular weight of water, p is the solution vapour pressure, V_r and B_r are the volume and second virial coefficient of water vapour at room temperature T_r; and V_t and B_t are the volume and second virial coefficient of water vapour at the thermostat temperature T_t. The amount of water in the solution was then obtained by subtracting this amount from the amount of water initially added to the solution vessel.

II.A5 Vapour Pressure Measurements

II.A5(i) Procedure of measurement

The steps involved in making a vapour pressure measurement can be summarized as follows (with reference to Figure II.5):

a) With vessel A empty and taps T_3 and T_4 closed (also T_7, T_8 and T_9 to the magnifying manometer) the entire system was evacuated through T_2 and T_5. There was no detectable difference between the mercury levels in the U-tube manometer.

b) For the measurement of the vapour pressure of pure water, a sample of degassed water was vacuum distilled into vessel A. The water was

frozen with a slurry of acetone and dry ice and pumped on before the taps T_2 and T_6 were closed and the thermostat raised into position.

c) After 4 to 5 hours, when liquid-vapour equilibrium had been attained, the vapour pressure of the pure water was measured on the U-tube manometer with one arm under vacuum.

d) Next, a solution vessel containing a prepared solution of L-Serine and water was attached to the system at B and the section of the line between taps T_3, T_4 and T_{13} evacuated. T_3 and T_5 were closed and T_4 and T_{13} were opened and the thermostat again raised into position. Again, when equilibrium had been attained the vapour pressure difference between the solvent and the solution was measured on the U-tube manometer.

II.A5(ii) Analysis of measurements

The pressure of a gaseous system is related to the height of the column of mercury it supports against vacuum in a manometer, by the equation

$$p/\mathrm{Pa} = \left[\rho(t)/\mathrm{kg\ m^{-3}}\right](\mathrm{g/m\ s^{-2}})\left[h(t)/\mathrm{m}\right] \qquad (II.10)$$

where p is the pressure in Pascals ($N\ m^{-2}$), $\rho(t)$ and h(t) are the density of the mercury and the height of the mercury column respectively at the Celsius temperature t at which the observation is made, and g is the local value of the acceleration of free fall (determined by the Physics Department to be $9.804 m\ s^{-2}$).

The height of the mercury column was measured using a catheto-meter with a brass scale adjusted to be correct at 20°C. For an observation at temperature t the true height of the column h(t) is given by,

$$h(t)/\mathrm{m} = \left[h'(t)/\mathrm{m}\right]\left\{1 + (\alpha\ K)\left[(t'/^{\circ}C) - 20\right]\right\} \qquad (II.11)$$

where h'(t)/m is the observed height of the column in metres, t' is the Celsius temperature at which the measurement was made and α is the linear coefficient of expansion of the brass scale ($\alpha = 1.84 \times 10^{-5}\ K^{-1}$)[46].

Figure II.6 Hydrostatic pressures in vapour pressure apparatus.

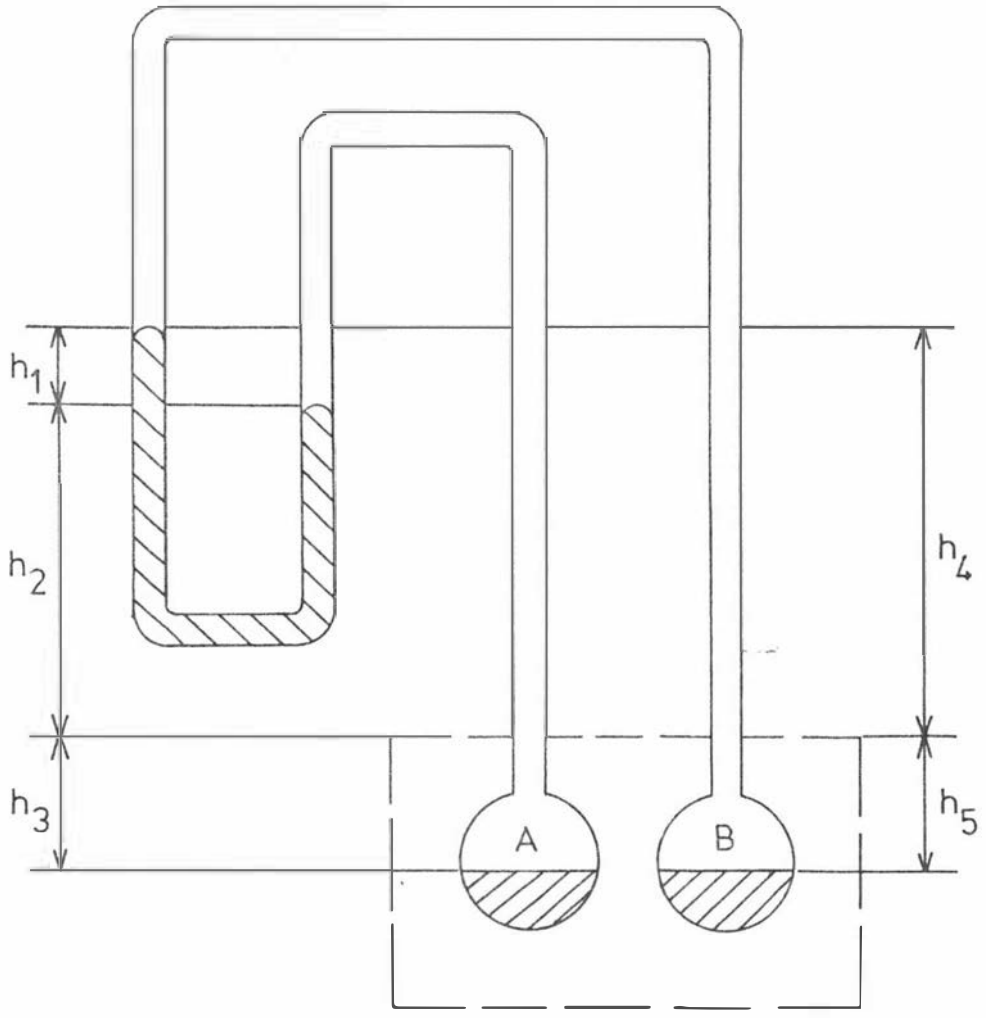

The International Practical Temperature Scale of 1968 (IPTS - 68)[47] gives the variation of the density of mercury with temperature as

$$\rho(t)/\text{kg m}^{-3} = \left[\rho(20^\circ\text{C})/\text{kg m}^{-3}\right]\left[1 + (\beta\ \text{K})\left\{(t/^\circ\text{C}) - 20\right\}\right]^{-1} \quad \text{(II.12)}$$

where $\rho(t)$ is the density of mercury at the Celsius temperature t of the measurement, β is the coefficient of cubical expansion of mercury ($\beta = 1.818 \times 10^{-4}\ \text{K}^{-1}$)[46] and $\rho(20^\circ\text{C})$ is the density of mercury at 20°C given by the IPTS - 68 as $13.54587 \times 10^3\ \text{kg m}^{-3}$.

With reference to Figure II.6 it is clear that to determine the difference in the vapour pressures at the surfaces of the liquids in the two cells A and B, account must be taken of the indicated hydrostatic pressures. The difference in the vapour pressures is then given by,

$$p_A - p_B = \rho_1 g h_1 + \rho_2 g h_2 + \rho_3 g h_3 - \rho_4 g h_4 - \rho_5 g h_5 \quad \text{(II.13)}$$

where the h_i's are the heights indicated in Figure II.6, ρ_1 is the density of mercury in the manometer at room temperature, ρ_2 and ρ_3 are the densities of the vapour above the liquid in cell A at room temperature and the thermostat temperature respectively, and ρ_4 and ρ_5 are the densities of vapour above the liquid in cell B at room temperature and the thermostat temperature respectively.

For this study, the last four terms in Equation II.13 are negligible, so that the expression for the vapour pressure difference at the surfaces of the liquids reduces to,

$$p_A - p_B = \rho_1 g h_1$$

as in Equation II.10.

II.B ENTHALPY OF DILUTION MEASUREMENTS

II.B1 Calorimeters Used for Enthalpy of Dilution Measurements

II.B1(i) Lange calorimeter

An adiabatic differential calorimeter described by Lange and Robinson[48] consisted of a 2 litre unsilvered Dewar flask, divided into two similar calorimeters by a partition containing a multi-junction thermel. This thermel, connected through a potentiometer to a galvanometer, permitted differential measurements to be made to 1×10^{-6}°C or better. Each calorimeter contained a stirrer, a small metal pipette and heating elements. The contents of the pipette could be mixed with the surrounding liquid by raising a ground-metal stopper by hand. Head liberated by a dilution in one calorimeter was balanced by quantitative electrical heating in the other, and heat absorbed by dilution was balanced by heating in the same calorimeter. The Dewar flask containing the calorimeters was supported in a constant temperature water bath. Adiabatic conditions were maintained by automatic adjustment of the temperature of the thermostat relative to the calorimeter.

Calorimeters of this basic design were used to measure the enthalpies of dilution of several aqueous solutions of amino acids and these are summarised in Table II.3.

Gucker, Pickard and Planck[77] have described a similar apparatus consisting of two 1 litre tantalum calorimeters suspended from the lid of a water-tight submarine jacket immersed in a thermostatted water bath. The difference in temperature between the calorimeters was measured to 1×10^{-6}°C with a multi-junction copper-constantan thermel connected to a galvanometer. With this design, thermal conduction between the calorimeters was reduced to a small fraction of that in Lange's apparatus by using fewer junctions in the thermel and having a small air gap between the calorimeters. Also complicated lifting devices were used to open the

dilution pipettes to ensure uniform mixing and reproducible heat effects in contrast to manually operated pipettes.

Examples of the use of this calorimeter are also given in Table II.3

II.B1(ii) Heat conduction batch calorimeter

In this type of calorimeter, heat evolved (or absorbed) in the reaction vessel is conducted out to (or from) a comparatively large surrounding heat sink through a thermopile. The heat flux is then proportional to the voltage-time integral i.e. the area under the voltage-time curve. Most microcalorimeters of this type have a reaction and reference vessel with their respective thermopiles being connected in opposition to give a differential signal with the intention of excluding external thermal effects.

An example of this type of calorimeter is one constructed by Wadsö[50] (commercially available as an LKB 10700 Batch microcalorimeter). The reaction vessels are rectangular cans of glass or metal which are partially divided into two compartments (one larger than the other) with a heater for electrical calibrations located in the partition. The reaction cells are positioned between thermocouple plates; with each pair of plates connected in series constituting a thermopile. These thermopiles are connected in opposition to one another to give a differential signal. The aluminium heat sink surrounding the two calorimeter units is insulated by polystyrene foam and enclosed in a steel cylinder. This whole calorimeter block is suspended in a thermostatted air bath. The reactants contained in each of the reaction vessel compartments and in contact only through the vapour phase are mixed by rotation of the calorimeter assembly. Electrical calibration experiments have indicated an attainable precision of 0.05% for the measurement of comparatively large heat quantities and better than 1% if 0.004J is evolved.

Examples of the use of this calorimeter are given in Table II.3.

II.B1(iii) Isothermal dilution calorimeter

Calorimeters of this type have been described by Savini[51] and Stokes[52]. In the latter model, the mixing vessel is made from silvered glass and is enclosed in a glass jacket filled with argon gas. The jacket is maintained at constant temperature in a water thermostat. The mixing vessel contains a stirrer, a heater and a thermistor. Initially the vessel is filled, half with mercury and the remainder with degassed component one. Stepwise addition of the second component from a piston burette progressively displaces the mercury. Electrical heating is used to match heat absorption from the mixing reaction or conversely if the mixing is exothermic steady thermoelectric cooling is employed to maintain isothermal conditions.

The conditions of the experiment correspond closely to the definition of the partial molar enthalpy of the injected component, provided the injections are limited to about $1cm^3$ so that they produce mole fraction changes $\leqslant 0.05$. The precision of such partial molar enthalpies is given as perhaps 0.3%.

Examples of the use of this calorimeter are given in Table II.3.

II.B1(iv) Steady state differential flow microcalorimeters

In a flow microcalorimeter, the two thermostatted reactant liquids are pumped into a mixing chamber where they are allowed to mix thoroughly and any temperature change during the mixing is followed. The system can be made adiabatic or isothermal depending on the type of thermal detection used. For isothermal operation the heat evolved (or absorbed) in the reaction cell is transferred to (or from) a heat sink. The magnitude of the heat flux is often determined using a thermopile located on the heat transfer path. Flow microcalorimeters designed by Monk[53] and Stoesser[54] use this principle of operation. The adiabatic condition is achieved when the flow cell and the temperature sensitive elements are thermally insulated from the surroundings; the steady state ΔT is then

TABLE II.3

Some Examples of Enthalpy of Dilution Measurements

Calorimeter	System	Reference
Lange	(α-amino-n-valeric acid, valine, norleucine, ε-aminocaproic acid) + water at 25°C	Mason, Offutt, Robinson[56]
Lange	(α-amino-i-butyric acid, α-amino-n-butyric acid, β-amino-n-butyric acid, γ-amino butyric acid) + water at 25°C	Mason and Robinson[57]
Lange	(α-, β-alanine) + water at 25°C	Benesi, Mason, Robinson[58]
Lange	glycine + water at 25°C	Wallace, Offutt, Robinson[59]
Gucker	(glycine, glycolamide) + water at 25°C sucrose + water at 20° and 30°C	Gucker, Pickard, Ford[49], Gucker, Pickard, Planck[77]
LKB Batch	boric acid + water between 10° and 50°C	Ward and Millero[60]
LKB Batch	tetrabutylammonium butyrate + water between 10° and 50°C	Levine and Lindenbaum[61]
Isothermal dilution	urea + (water, methanol, ethanol, formamide, N,N-dimethylformamide, dimethyl sulphoxide)	Hamilton and Stokes[62]
Flow	(sodium chloride, tetramethyl-ammonium bromide, n-tetrabutyl-ammonium bromide) + water at 25°C	Fortier, Leduc, Picker, Desnoyers[63]

the ΔT of mixing. Picker, Jolicoeur and Desnoyers[55] have described a flow microcalorimeter which is capable of being operated either isothermally of adiabatically. The reactant liquids are pumped into the mixing chamber either by peristaltic or quasi-pulseless pumps. The resultant heat flux is transferred to another liquid through a counter-current heat exchanger; with changes in the temperature of the heat exchanger liquid being measured relative to a twin heat exchanger serving as a reference. The whole reaction system is contained in an evacuated, thermally shielded vessel located in a constant temperature water bath. Temperature measurements are made with thermistors and the sensitivity of an improved version of the calorimeter is given as 1×10^{-6}°C. An overall precision of 0.5% is obtainable for the enthalpy of mixing.

Examples of the use of this calorimeter for enthalpy of dilution measurements are given in Table II.3.

II.B1(v) Choice of the calorimetric method

The choice of a calorimetric system to measure the enthalpies of dilution was largely determined by the fact that the author had access to an LKB 10700-1 flow microcalorimeter and an LKB 10700-2 batch microcalorimeter.

In an initial series of experiments both calorimeters were used to measure some enthalpies of dilution of aqueous solutions of sucrose. As a result, the experimental precision of the two instruments was compared and also the agreement of the results (given in Table II.4) with those of Gucker, Pickard and Planck[77]. The results obtained using the flow system were significantly better than those from the batch system.

The use of the flow microcalorimeter was also favoured from a consideration of the following comparison of the two systems. Flow reaction calorimetry is much less time-consuming than batch calorimetry as the equilibration time required prior to the mixing of the reactants

TABLE II.4

Integral Enthalpies of Dilution of Aqueous Sucrose Solutions by Batch and Flow Microcalorimeters

Calorimeter	m_i/mol kg^{-1}	m_f/mol kg^{-1}	ΔH_{ID}/Jmol^{-1} (measured)	ΔH_{ID}/Jmol^{-1} (calculated from Gucker)[77]
Batch	0.2082	0.0679	80.7	77.9
	0.2082	0.0687	79.2	77.4
	0.2082	0.0683	83.7	77.6
	0.2082	0.0682	84.6	77.7
Flow	0.7127	0.3569	190.9	189.2
	0.5239	0.2627	142.8	141.1
	0.5239	0.2627	142.6	141.1
	0.4926	0.2470	133.7	132.9
	0.4926	0.2470	133.9	132.9

is largely omitted, with the liquids being thermally equilibrated through a series of heat exchangers on their way to the mixing cell. With batch procedures the method chosen for the mixing of the reactants is critical, especially so in microcalorimetric experiments where mixing procedures can easily cause large irreproducible heat effects when only minute heat quantities are evolved or absorbed in the reaction itself. The method of mixing used in the LKB batch system (Section II.B1(ii)) does tend to be susceptible to possible complications in dilution reactions due to the relatively large gas phase present in the open compartment mixing cells. Distillation may occur during the equilibration time with consequent changes in energy and in reactant composition (though generally this would not be significant for aqueous solutions). The comparatively large gas phase also makes the batch system unsuitable for measurements on processes where there is a large change in the gas phase composition such as that which accompanies the mixing of volatile compounds, though for experiments with aqueous solutions near room temperature the change in the gas phase composition will be very small and usually insignificant. However, even for aqueous solutions care needs to be exercised in dilution experiments where one of the mixing compartments contains pure water. Surface adsorption effects would tend to be much more significant in the batch system with the consequent introduction of serious systematic errors; this can be neglected however, in a liquid flow system where the liquid flow is continued until all possible surface reactions have occurred.

Provided that care is taken to ensure that mixing of the reactants is complete (especially with more concentrated solutions) the flow method would appear to be ideally suited to mixing and dilution experiments. Fortier, Leduc, Picker and Desnoyers[63] have described a general procedure for precise measurements of enthalpies of dilution with a flow microcalorimeter.

Figure II.7 Calorimeter

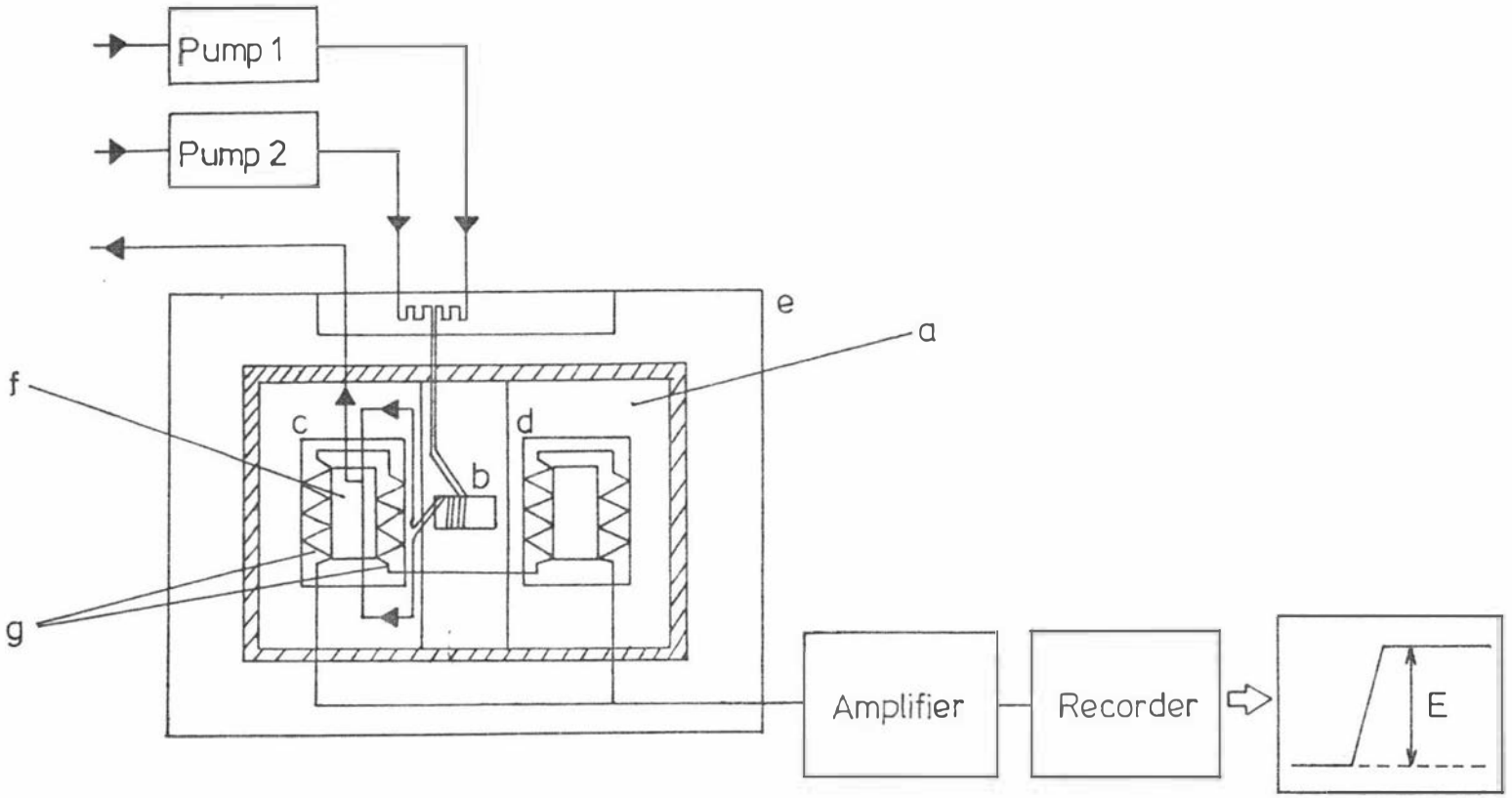

II.B2 The Calorimeter

The calorimetric system used in this work was the LKB 10700-1 flow microcalorimetry system. It was operated in a room thermostatted to 298.1 ± 0.5K.

A schematic diagram showing the arrangement of the principal components of the system is given in Figure II.7. The main heat sink a, constructed from aluminium, encloses a centrally located heat exchange unit b, and two calorimetric units c and d. The heat sink is surrounded by polystyrene foam insulation and is contained in a stainless steel vessel all of which is supported in an air bath e, thermostatted to 0.01K. The two calorimetric units are comprised of a reaction vessel f, two thermocouples g, and a primary heat sink. The reaction vessel which has the external shape of a square plate is positioned between the thermocouples which are in turn in direct contact with the two aluminium blocks of the primary heat sink on either side. The two thermocouples for each unit are connected in series whereas the two thermopiles thus formed are connected in opposition to give a differential signal. One of the calorimetric units contains a flow-through cell, generally for slow processes which are often initiated outside the calorimeter and the other contains a mixing cell for fast reactions. This mixing cell consists of a T-junction of gold tubing (where the two incoming liquid streams are initially mixed) joined to a channel system which is milled from a flat silver plate and covered with a lid. Those surfaces in contact with the calorimetric liquid are gold plated. A gold tube, on which is wound a 50 ohm calibration heater, carries the liquid flow from the T-piece to the channel where a series of constrictions are located in the mixing zone to ensure that the mixing of the reactants is complete. The total volume of this mixing cell is about 0.7cm^3.

The liquids are pumped through the calorimetric system by means of two LKB Perpex peristaltic pumps (model no. 10200). Silicone rubber

tubing (1.1mm diameter) is used to carry the liquids through the pumps and Teflon tubing (1.0mm diameter) is used to connect the pumps to the heat exchange units, flow cells and collection vessels. The pump flow rates can be varied by use of interchangeable gear-boxes.

The differential voltage from the thermopiles in the two calorimetric units is amplified by a Keithley 150B Microvolt Ammeter and this signal is recorded as a deflection by a Servogor RE 512 chart recorder.

II.B3 Sample Preparation

II.B3(i) Materials

The sucrose used was "Aristar" grade (99%+) supplied by British Drug Houses and was used directly without further purification. The glycine "Univar" grade (99%+) was supplied by Ajax Chemicals Australia; L-alanine (99%) and L-arginine (98% ex nitrogen assay) were supplied by British Drug Houses; L-serine and L-valine, Sigma grade (99%+) were supplied by the Sigma Chemical Company and L-cysteine (98% ex nitrogen assay) was supplied by Riedel-de Haen.

Each of the amino acids except L-cysteine was twice recrystallised from distilled water (Section II.A4(i)) before being dried in a vacuum dessicator over P_2O_5 at room temperature for at least 72 hours. Due to the susceptibility of aqueous solutions of L-cysteine to undergo oxidation by atmospheric oxygen[64], the sample was dried in a vacuum dessicator over P_2O_5 as above and used without further purification. It was noted from the literature[73] that L-arginine can recrystallise from aqueous solution as the monohydrate; therefore to test for this possibility, a sample was titrated with standard hydrochloric acid. The molecular weight thus determined was within 0.05% of the anhydrous molecular weight.

Samples of each of the amino acids before recrystallisation and after were used to prepare solutions of the same concentration which were then diluted in a similar manner with water. The two samples were found

to be indistinguishable within the limits of precision of the calorimetric technique.

Nitrogen analyses on each of the amino acids (and sulphur for L-cysteine) yielded the following results:

Amino Acid	Analysis %	Theoretical %
Glycine	18.51	18.64
L-Alanine	15.59	15.71
L-Arginine	31.82	32.15
L-Cysteine	11.65 S(26.29)	11.56 S(26.46)
L-Serine	13.41	13.32
L-Valine	11.84	11.96

The water was purified by refluxing laboratory tap water with alkaline permanganate for 6-8 hours before twice distilling it, the middle fraction being retained in each case. Prior to use the water was thoroughly boiled to remove CO_2 and sealed against the atmosphere while being cooled. The conductivity of the water was less than 1.0×10^{-6} ohm^{-1} cm^{-1}.

II.B3(ii) Preparation of solutions

The solutions were prepared by weighing a suitable quantity of recently degassed water into a known mass of amino acid in a small flask. All weighings and preparation of solutions were done in the same temperature-controlled room as the calorimeter system.

Care was taken in the preparation and handling of L-cysteine solutions to avoid oxidising conditions because of their susceptibility to oxidation[64]. Enthalpies of dilution of some L-cysteine solutions were measured at various times over several hours as a check on the possible occurrence of oxidation. No variation in the enthalpies of dilution was detected over a period of two hours. Since all L-cysteine solutions were diluted within thirty minutes of preparation it was assumed that effects due to oxidation of the solution could be neglected.

II.B4 Enthalpy of Dilution Measurements

II.B4(i) Procedure of measurement

With the calorimetric system at 298.15K, a steady base line (about 0.1% depending on the sensitivity scale of the amplifier) was obtained on the chart recorder, with water passing through both pumps into the mixing cell. When this base line was established, the pump for flowing the solution was momentarily stopped while the inlet tube was transferred from the water reservoir to a source of freshly prepared amino acid solution. The steady state heat effect from the dilution reaction was normally attained in fifteen to twenty minutes and allowed to continue for ten minutes before the solution pump was again stopped and the inlet tube returned to the water reservoir for the establishment of the "after" base line.

After the water-to-water base line was again established, a known current was passed through the mixing cell calibration heater for a preset period of time (1000 seconds). The current was chosen so that the steady state heat effect was of a similar magnitude to that obtained for the dilution reaction. Duplicates were performed for both reaction and calibration experiments with even further repetitions being made if base lines before and after showed undue drift.

The flow rates of the water (f_o), and the solution (f), could be varied within fixed ratios using the interchangeable gear boxes. The available gear box ratios of 3 : 250 and 3 : 125 gave flow rates of approximately 0.24 ml min^{-1} and 0.48 ml min^{-1} respectively. Dilution ratios of $f_o/f \approx 1$, $f_o/f \approx 2$ and $f_o/f \approx 0.5$ were used. The possibility of incomplete mixing at higher concentrations was tested for by varying the overall flow rate ($f_o + f$) while keeping the ratio f_o/f constant. The measured heats in every case, were found to be proportional to the overall flow rate, so mixing was assumed to be complete. The pump flow

rates were determined by weighing samples of water delivered for a known time, both before and after a complete dilution experiment. The variation in flow rate was less than 0.1%.

II.B4(ii) Analysis of measurements

The molalities of the solutions prior to dilution, m_i (mol kg^{-1}), were calculated, with corrections being made for buoyancy. From these, the corresponding molarity, c_i (mol l^{-1}) of each solution was calculated using known or measured densities (Section II.C).

The solution at the initial concentration, c_i, was introduced into the calorimeter mixing cell at a flow rate f(ml s^{-1}) and the water at a flow rate f_o(ml s^{-1}). The final solution concentration, c_f, after dilution was then given by,

$$c_f/\text{mol } l^{-1} = c_i \left[1 + f_o/f + (c_i/1000)(\phi_v^f - \phi_v^i)\right]^{-1} \qquad \text{(II.14)}^{63}$$

where ϕ_v^i and ϕ_v^f are the initial and final apparent molal volumes of the amino acid respectively. The last term in Equation II.14 which is a correction for the volume of mixing was negligible in this study.

From the final concentration of the amino acid solution, c_f, the corresponding molality m_f(mol kg^{-1}) was calculated.

The heat flux during a calibration experiment W_c, determined from the calibration current I, and the resistance of the calibration heater R, was given by,

$$W_c/\text{J s}^{-1} = I^2 R$$

From the corresponding recorder deflection during a calibration experiment E_c, the calibration constant ε could be determined,

$$\varepsilon/\text{watt division}^{-1} = W_c/E_c$$

Combining this with the dilution reaction deflection, E, the heat flux of the reaction, W, can be obtained

$$W/\text{J s}^{-1} = \varepsilon.E.$$

Figure II.8 A typical recorder trace for a dilution experiment

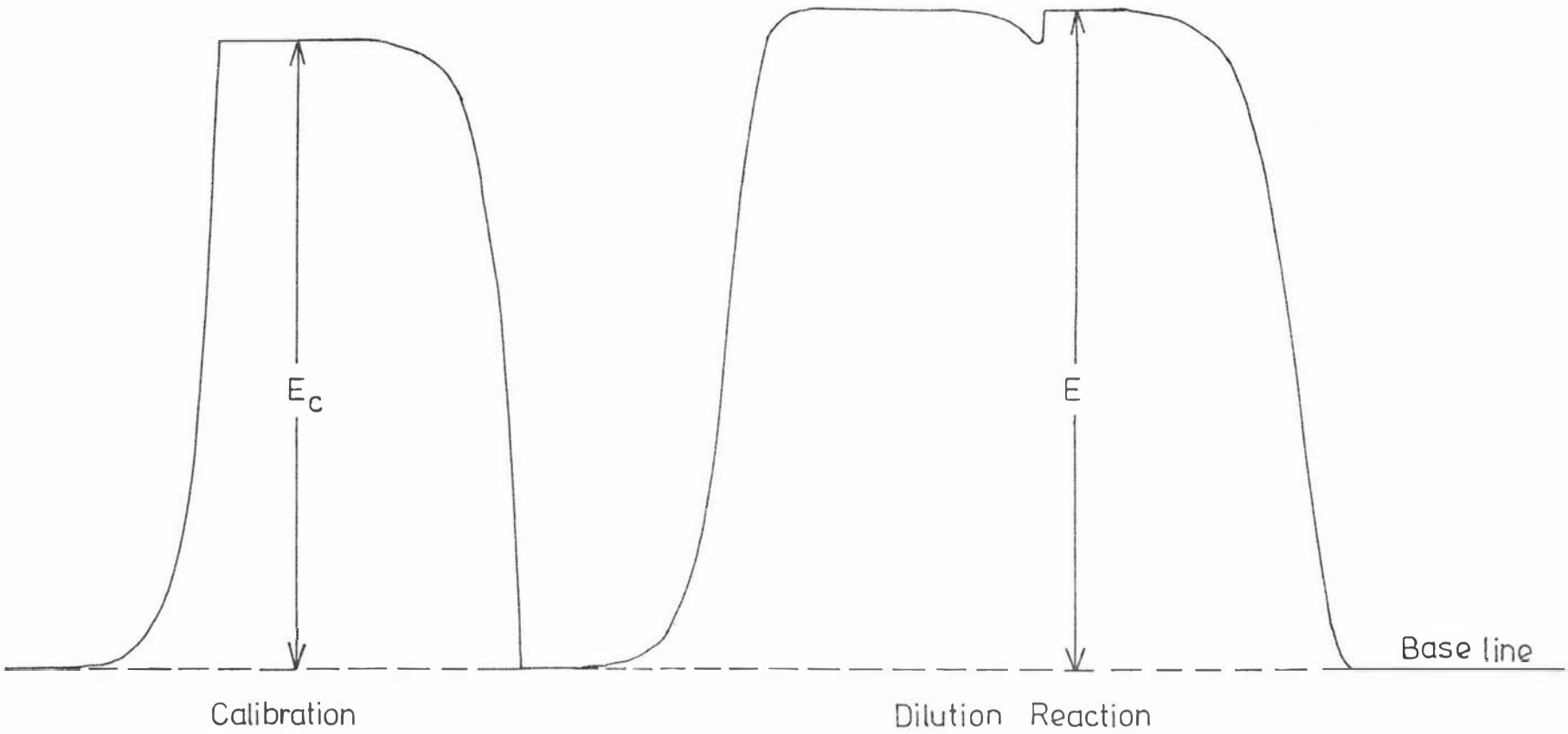

A typical recorder trace for a dilution experiment is shown in Figure II.8.

The integral enthalpy of dilution ΔH_{ID}, was given by,

$$\Delta H_{ID}/J\ mol^{-1} = 1000W/c_i f \qquad (II.15)$$

The results of the dilution experiments for each amino acid solution given in terms of ΔH_{ID}, m_i and m_f are tabulated in Section III.B. The calculations of the relative apparent molal enthalpy, ϕ_L, and the relative partial molal enthalpy, $\bar{L}_2$, are given in Section IV.B.

II.C DENSITIES OF AQUEOUS AMINO ACID SOLUTIONS AT 298.15K

Densities of the aqueous amino acid solutions were required in the analysis of the integral enthalpies of dilution (see Section II.E4) to calculate the molarities (mol l^{-1}) of the solutions from the prepared molalities (mol kg^{-1}).

II.C1 Experimental Procedure

The densities were determined by weighing bottle-type pycnometers of known volume containing aqueous solutions of the amino acids.

The pycnometers had an approximate capacity of 25cm^3 and were closed with ground glass stoppers. Before being used they were cleaned with chromic acid, thoroughly rinsed with water, A.R. acetone and A.R. ether and dried with pumping in a vacuum dessicator at room temperature. After each measurement only cold water, acetone and ether were used to clear the pycnometers.

After being weighed and filled with an amino acid solution, the pycnometers were suspended up to a point high on the neck of the bottle, in a water bath thermostatted to 298.15 $\pm$ 0.005K. The pycnometers remained in the bath for two hours before being removed, wiped dry and placed in a dessicator. They were weighed one hour after removal from the bath.

The volume of each pycnometer was first determined by following the above procedure using distilled water.

II.C2 Calculation of Densities of Aqueous Amino Acid Solutions

The densities, ρ_t, of the amino acid solutions were calculated using the equation,

$$\rho_t = \left\{ w_2\left(1 - \rho_2/\rho_w\right) - w_1 \left[\frac{\left(1 - \rho_1/\rho_w\right)\left(1 - \rho_2/\rho_g\right)}{1 - \rho_1/\rho_g} \right] \right\} / V$$

where w_2 and w_1 are the weights of the filled and empty pycnometers

respectively, V is the total volume of the liquid ρ_2 and ρ_1 are the densities of air during the weighing of the full and empty pycnometers, ρ_g is the density of glass and ρ_w is the density of the material of the weights in the balance.

The densities have been determined with an accuracy of 0.08%. The results of the density determinations for L-Alanine, L-Arginine, L-Cysteine, L-Serine and L-Valine at 298.15K are given in Table II.5.

TABLE II.5

Densities of Aqueous Amino Acid Solutions at 298.15K

m/mol kg^{-1}	ρ/g cm^{-3}	m/mol kg^{-1}	ρ/g cm^{-3}	m/mol kg^{-1}	ρ/g cm^{-3}	m/mol kg^{-1}	ρ/g cm^{-3}	m/mol kg^{-1}	ρ/g cm^{-3}
L-Alanine		L-Arginine		L-Serine		L-Valine		L-Cysteine	
1.8123	1.0422	0.8608	1.4022	3.6536	1.1239	0.4899	1.0092	1.4066	1.0561
1.4147	1.0332	0.7054	1.0332	3.2186	1.1080	0.4013	1.0072	1.1923	1.0480
1.0066	1.0227	0.6040	1.0227	2.8061	1.0969	0.2975	1.0046	1.0147	1.0418
0.7058	1.0160	0.5036	1.0160	2.1989	1.0791	0.2514	1.0037	0.8100	1.0328
0.4001	1.0083	0.4021	1.0083	1.7980	1.0661	0.1915	1.0022	0.6064	1.0224
0.3945	1.0082	0.3007	1.0082	1.2037	1.0453	0.1532	1.0011		
0.2005	1.0026	0.1986	1.0026	0.7930	1.0302				
				0.2977	1.0098				

CHAPTER III

EXPERIMENTAL RESULTS

III.A VAPOUR PRESSURE MEASUREMENTS

III.A1 Vapour Pressure Measurements of Pure Water at 288.15K, 293.15K and 298.15K

The results of the vapour pressure measurements of pure water at 288.15K, 293.15K and 298.15K are given in Table III.1, and are compared there with values from the literature.

III.A2 Vapour Pressure Measurements of L-Serine-Water Solutions at 288.15K and 298.15K

The results of the vapour pressure measurements of L-Serine-Water solutions at 288.15K and 298.15K are given in Table III.2 and represented graphically in Figure III.1.

In Table III.2, m refers to the molality of the L-Serine solution which has been determined from the observed mass of the amino acid (corrected for buoyancy) and the total amount of water added to it using Equation II.8. The mass of water added to the amino acid has also been corrected for the amount present in the vapour phase for each vapour pressure measurement (Equation II.9). The difference in vapour pressures between the pure water and the amino acid solution, Δ p, has been determined from the manometer readings (Section II.A5).

TABLE III.1

Comparison of Correlated Values for the Vapour Pressure of Pure Water[67]

T/K	p/Pa	Reference
288.15	1708.7 ± 9.3	This work
	1704.8	Osborne, Stimson and Ginnings[65]
	1705.1	Wexler and Greenspan[66]
	1705.3	Besley and Bottomley[67]
	1703.4	Osborne and Meyers[68]
	1706.6	Douslin[69]
293.15	2340.0 ± 9.5	This work
	2337.9	Osborne, Stimson and Ginnings[65]
	2338.3	Wexler and Greenspan[66]
	2338.7	Besley and Bottomley[67]
	2335.8	Oxborne and Meyers[68]
	2339.5	Douslin[69]
298.15	3171.3 ± 10.1	This work
	3167.9	Osborne, Stimson and Ginnings[65]
	3168.7	Wexler and Greenspan[66]
	3168.9	Besley and Bottomley[67]
	3165.2	Osborne and Meyers[68]
	3168.6	Stimson[70]

TABLE III.2

Vapour Pressures of L-Serine + H_2O at 288.15K

m/mol kg^{-1}	Δp/Pa
0.3410	8.0
1.0563	27.9
1.4924	35.8
1.9967	45.1
3.1129	71.6

Vapour Pressures of L-Serine + H_2O at 298.15K

m/mol kg^{-1}	Δp/Pa
0.3410	17.2
1.0563	53.0
1.4924	72.9
1.9967	94.2
3.1136	139.2

Figure III.1 Experimental vapour pressures of L-Serine-water solutions.

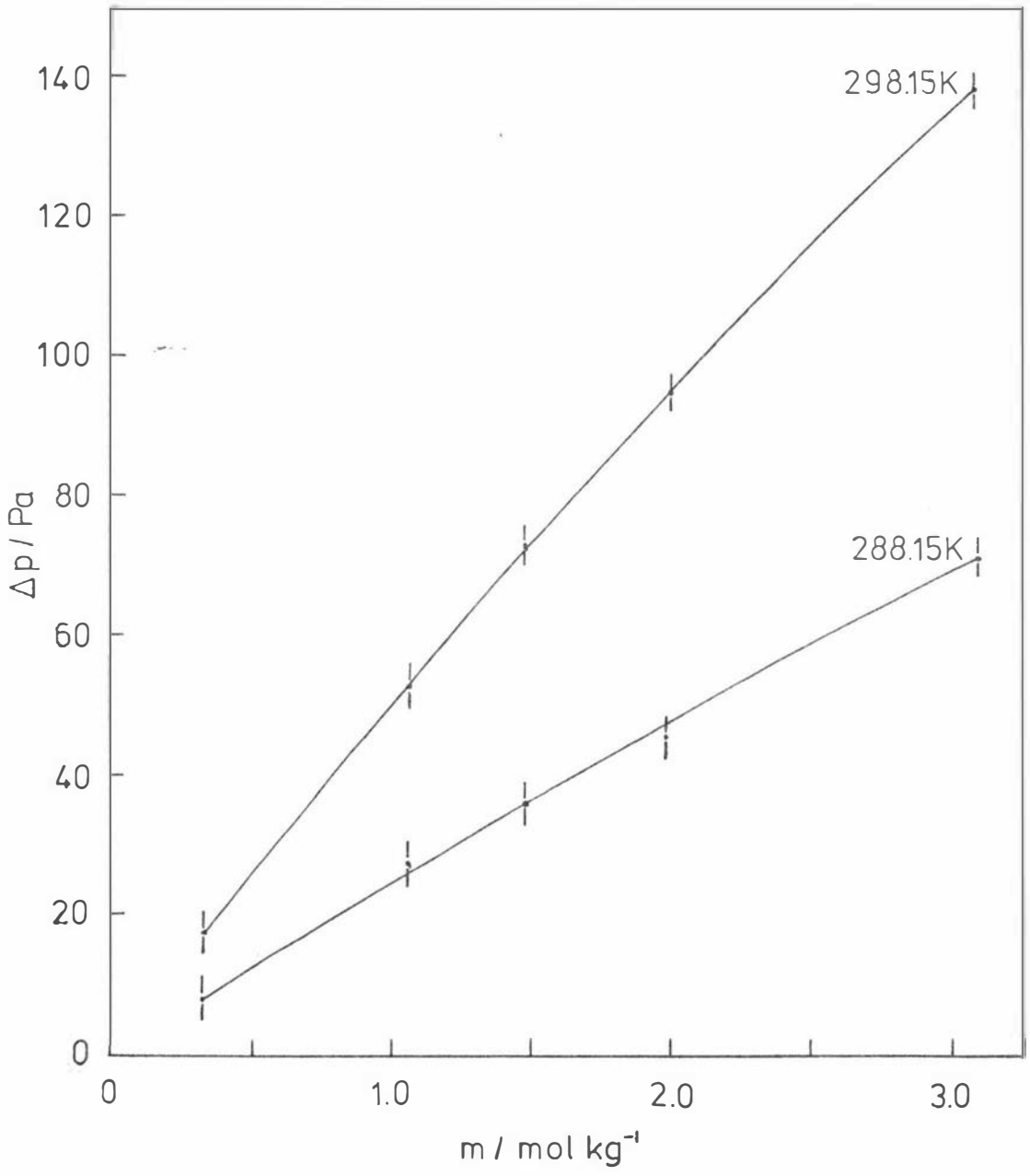

III.B ENTHALPY OF DILUTION MEASUREMENTS

III.B1 Integral Enthalpies of Dilution of Aqueous Amino Acid Solutions at 298.15K

The integral enthalpies of dilution of aqueous solutions of the amino acids, L-alanine, L-arginine, L-cysteine, glycine, L-serine and L-valine were measured at 298.15K over various concentration ranges appropriate to the solubility of the amino acid concerned.

The results are given in Tables III.3 to III.8 where m_i is the initial concentration of the amino acid solution in mol kg^{-1}, m_f is the final concentration of the solution after dilution in mol kg^{-1} and ΔH_{ID} is the integral enthalpy of dilution in J mol^{-1} as determined from Equation II.15.

TABLE III.3

Integral Enthalpies of Dilution of L-Alanine in Water at 298.15K

m_i/mol kg^{-1}	m_f/mol kg^{-1}	ΔH_{ID}/J mol^{-1}
1.8019	0.8563	-203.5
1.8019	0.5604	-269.5
1.6980	0.8903	-193.0
1.6980	0.5303	-253.2
1.4014	0.6720	-158.7
1.4014	0.4416	-208.1
1.1693	0.5741	-135.0
1.1693	0.3777	-174.9
0.9185	0.4471	-103.4
0.9185	0.2951	-136.7
0.8253	0.4022	-91.1
0.8253	0.2663	-121.4
0.5985	0.2939	-66.5
0.5985	0.1932	-88.3

TABLE III.4

Integral Enthalpies of Dilution of L-Arginine in Water at 298.15K

m_i/mol kg^{-1}	m_f/mol kg^{-1}	ΔH_{ID}/J mol^{-1}
0.8654	0.4102	468.7
0.8654	0.2689	647.9
0.7054	0.3369	407.3
0.7054	0.2212	573.6
0.6040	0.2906	364.7
0.6040	0.1911	511.4
0.4970	0.2410	322.6
0.4970	0.1586	440.9
0.4021	0.1962	270.7
0.4021	0.1294	373.6
0.2935	0.1442	214.6
0.2518	0.1239	187.9

TABLE III.5

Integral Enthalpies of Dilution of L-Cysteine in Water at 298.15K

m_i/mol kg^{-1}	m_f/mol kg^{-1}	ΔH_{ID}/J mol^{-1}
1.4458	0.6862	45.5
1.4302	0.6791	45.8
1.3179	0.6282	43.0
1.2209	0.5839	43.0
1.1064	0.5305	40.1
1.0872	0.5218	38.9
1.0020	0.4829	37.5
0.9886	0.4767	37.2
0.9082	0.4364	34.9
0.9067	0.4376	34.9
0.8036	0.3894	33.4
0.8017	0.3885	32.9
0.7027	0.3415	29.9
0.7009	0.3406	29.7

TABLE III.6

Integral Enthalpies of Dilution of Glycine in Water at 298.15K

m_i/mol kg^{-1}	m_f/mol kg^{-1}	ΔH_{ID}/J mol^{-1}
2.9971	1.4044	343.7
2.5078	1.1902	314.5
2.0046	0.9621	277.9
1.4942	0.7217	231.1
0.9974	0.4897	172.2
0.7917	0.3902	146.0
0.3929	0.1954	79.0

TABLE III.7

Integral Enthalpies of Dilution of L-Serine in Water at 298.15K

m_i/mol kg^{-1}	m_f/mol kg^{-1}	ΔH_{ID}/J mol^{-1}
3.8317	1.7044	583.3
3.0292	1.3788	527.5
3.0292	0.8927	735.2
2.0104	0.9482	434.8
1.8084	0.8541	411.6
1.8084	0.5592	573.7
1.6801	0.7986	393.2
1.0127	0.4912	279.4
1.0127	0.3237	386.3
0.7716	0.3774	227.8
0.7716	0.5114	146.1
0.7716	0.2480	312.9
0.5862	0.3879	118.2
0.5862	0.2876	181.7
0.5862	0.1919	244.9
0.3829	0.1900	124.1
0.3829	0.1258	170.4

TABLE III.8

Integral Enthalpies of Dilution of L-Valine in Water at 298.15K

m_i/mol kg^{-1}	m_f/mol kg^{-1}	ΔH_{ID}/J mol^{-1}
0.4899	0.1586	-282.4
0.4758	0.2323	-209.3
0.4013	0.1971	-175.4
0.3937	0.1284	-229.7
0.3506	0.1725	-153.7
0.3506	0.1148	-202.0
0.2947	0.1457	-127.7
0.2947	0.0967	-169.0
0.2474	0.1227	-107.5
0.1958	0.0972	-84.8
0.1955	0.0971	-84.5
0.1532	0.0763	-66.9

CHAPTER IV

ANALYSIS OF RESULTS

IV.A ANALYSIS OF VAPOUR PRESSURE MEASUREMENTS OF L-SERINE-WATER SOLUTIONS

IV.A1 Determination of Activity Coefficients, γ, for L-Serine-Water Solutions at 288.15K and 298.15K

The activity of the water a_1, in each L-Serine solution was calculated from the vapour pressure measurements according to Equation I.21. This enabled the calculation of the activity coefficient of the water γ_1, from,

$$\gamma_1 = a_1/x_1 \qquad \text{(IV.1)}$$

where x_1 is the mole fraction of the water in the L-Serine solution.

The activity coefficient of the L-Serine in solution, γ_2, could then be obtained from the integrated form of the Gibbs-Duhem equation for a two component solution (see Equation I.24),

$$\log \gamma_2' = -\int_{x_2 = 0}^{x_2 = x_2'} (x_1/x_2)\, d \log \gamma_1 \qquad \text{(IV.2)}$$

where γ_2' is the value of γ_2 at the particular mole fraction of the solute which is the upper limit of the integration.

The semi-empirical graphical procedure of Lakhanpal and Conway[22] was used to integrate Equation IV.2 and thus obtain values for the activity coefficient of L-Serine in solution. The method consists in plotting the values of x_1/x_2 against log γ_1 and determining the area under the curve between the limits indicated in Equation IV.2.

The graph of the function x_1/x_2 against log γ_1 is shown in Figure IV.1 for L-Serine in water at 298.15K, the experimental data for which was obtained as outlined in Section II.A. Since the curve of x_1/x_2 against log γ_1 is asymptotic to the axis of the ordinate x_1/x_2, it has to be extrapolated to an infinite value of x_1/x_2 in order to obtain the total area under the curve. The accurate assessment of the integral by measurement of the area under the extrapolated curve presents a practical

Figure IV.1 Mole fraction ratio x_1 / x_2 vs. $\log \gamma_1$ for L-Serine-water solutions.

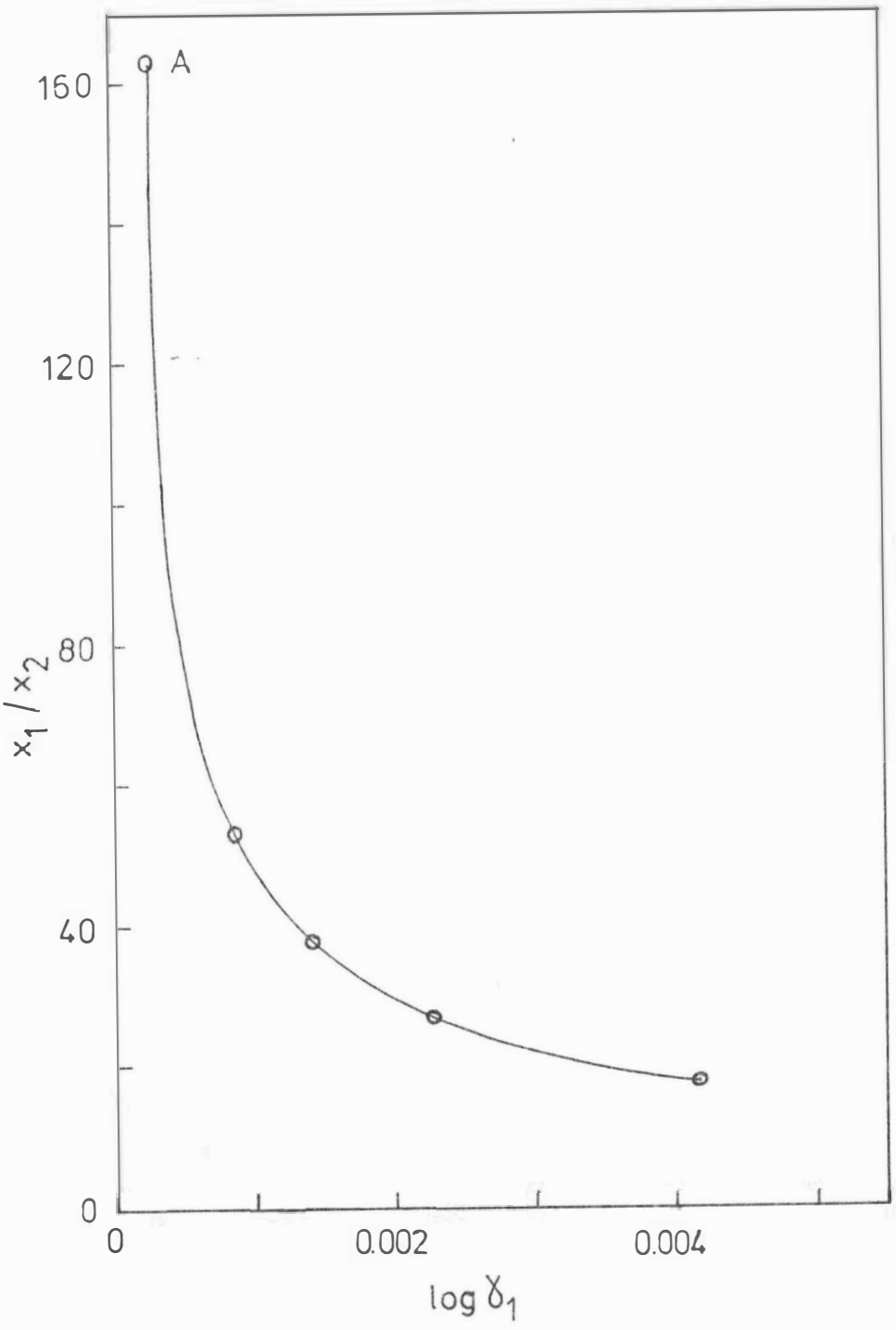

Figure IV.2 Mole fraction ratio x_2/x_1 vs. $\log \gamma_2$ for L-Serine-water solutions

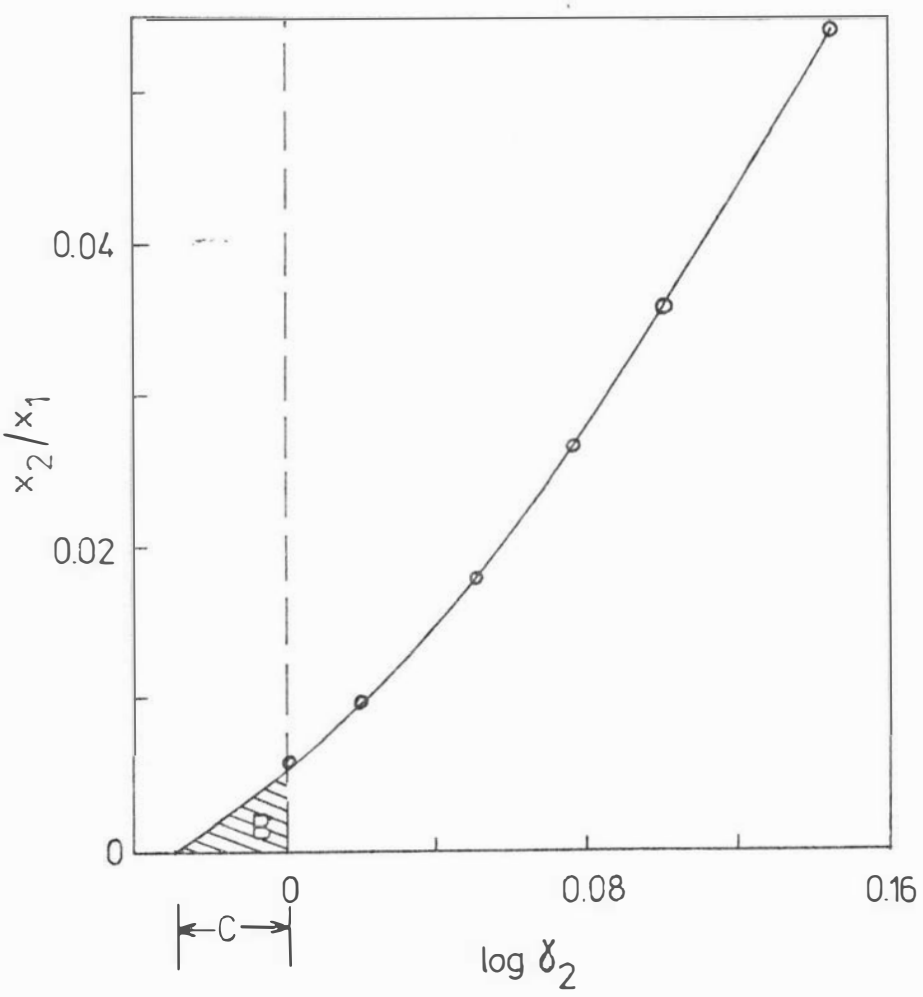

difficulty particularly in the asymptotic region of the curve. In view of this, Lakhanpal and Conway considered the area under the curve from a point A in the asymptotic region to an infinite value of x_1/x_2 to be equal to an unknown constant C, so that the total integral up to any point on the curve is equal to C plus the area under the curve from the point A to that point. If C is to a first approximation set equal to zero then values for log γ_2 can be obtained. The values of x_2/x_1 can then be plotted against the apparent values of log γ_2 as shown in Figure IV.2. It is found that the value of log γ_2 corresponding to the value of x_1/x_2 at the point A in Figure IV.1 is zero so that the curve in Figure IV.2 does not pass through the origin. If the curve in Figure IV.2 is smoothly extended back to the horizontal axis, the point at which the curve meets the axis should be the actual origin. Hence all the first approximation values of log γ_2 must be increased by the constant C, equal to the shift of the origin along the horizontal axis. The extrapolation is also assisted by the fact that the area B under the curve in Figure IV.2 must be equal to log γ_1 at the point A in Figure IV.1 and this is known experimentally.

The activity coefficients γ_2, of L-Serine in aqueous solutions of different concentrations at 288.15K and 298.15K determined by the above method are given in Tables IV.1 and IV.2. The concentrations of the L-Serine solutions, m are expressed on the molality scale.

IV.A2 Comparison of Values for Activity Coefficients with those Obtained by the Isopiestic Method

The activity coefficients for L-Serine in water at 298.15K are compared with those obtained by Hutchens, Figlio and Granito[31], and Smith and Smith[30] using the isopiestic method in Table IV.3.

TABLE IV.1

Activity Coefficients, γ_2, of L-Serine in Water at 288.15K

m/mol kg^{-1}	γ_2
0.4000	0.808
0.5000	0.804
0.7000	0.793
1.0000	0.754
1.5000	0.669
2.0000	0.605
2.5000	0.579
3.0000	0.563

TABLE IV.2

Activity Coefficients, γ_2, of L-Serine in Water at 298.15K

m/mol kg^{-1}	γ_2
0.4000	0.884
0.5000	0.861
0.7000	0.834
1.0000	0.802
1.5000	0.757
2.0000	0.719
2.5000	0.682
3.0000	0.664

TABLE IV.3

Activity Coefficients of L-Serine-Water Solutions at 298.15K

by Vapour Pressure and Isopiestic Methods

$m/mol\ kg^{-1}$	γ_2 (Vapour pressure)	γ_2 (Isopiestic[31])	γ_2 (Isopiestic[30])
0.5000	0.861	0.887	0.907
0.7000	0.834	0.851	
1.0000	0.802	0.805	
1.5000	0.757	0.746	
2.0000	0.719	0.705	
2.5000	0.682	0.670	
3.0000	0.644	0.641	

IV.A3 Error Analysis for Activity Coefficient Determination

The errors arising from the determination of the activity coefficients of L-Serine from the vapour pressure measurements outlined in Section II.A can be considered as follows:

a) Errors from cathetometry. This was the major contributor to the error in the vapour pressure measurements. Errors could have come from incorrect vertical adjustment of the cathetometer, bends in the beam, error in the length of the scale, incorrect levelling of the telescope, random error in the scale, and error in reading the scale. A detailed analysis of these contributions to the error in a measurement has been given by Kershaw[43]. Applying such an analysis to the measurements in this study yielded the maximum expected error in a vapour pressure measurement of ± 9 Pa.

b) Errors from measurement of thermostat temperature. The temperature of the thermostat was measured with a Hewlett-Packard Quartz thermometer which had been set at the ice point (273.15K). Thus the expected accuracy in the temperature measurement of the thermostat would be no less than ± 0.01K. In the direct static vapour pressure measurements of pure water this would introduce an uncertainty of up to ± 1.5 Pa.

c) Errors in preparation of amino acid solutions. The amino acids were weighed to ± 0.0001g and the mass of water added could be determined to better than ± 0.4%. Thus the overall expected uncertainty in the mole fractions would be about ± 0.4%.

By combining the above experimental errors with those involved in the graphical procedure for integrating the Gibbs-Duhem equation we arrive at an expected precision for the activity coefficients in the range from 2 - 5%.

IV.B ANALYSIS OF INTEGRAL ENTHALPIES OF DILUTION OF AQUEOUS AMINO ACID SOLUTIONS

IV.B1 Determination of Relative Apparent Molal Enthalpies, ϕ_L, of Aqueous Amino Acid Solutions at 298.15K

The relative apparent molal enthalpy, ϕ_L, was given in Equation I.39 as a polynomial in the molality m i.e.

$$\phi_L = A_1 m + A_2 m^2 + A_3 m^3 + \ldots. \qquad (IV.3)$$

The experimental integral enthalpy of dilution, ΔH_{ID} was given in Equation I.34 as,

$$\Delta H_{ID} = A_1(m_f - m_i) + A_2(m_f^2 - m_i^2) + \ldots. \qquad (IV.4)$$

A least-squares computer programme incorporating a weighting factor to account for the variation of uncertainty in ΔH_{ID} with concentration and a test of the goodness of fit, was used to obtain the minimum number of adjustable coefficients, A_i, necessary to fit the experimental data, ΔH_{ID}, m_i and m_f to Equation IV.4.

The coefficients of the polynomial expressions for ϕ_L for each of the amino acids are given in Table IV.4 together with their estimated errors. The values of ϕ_L are shown graphically in Figure IV.3.

IV.B2 Determination of Relative Partial Molal Enthalpies, $\bar{L}_2$, of Aqueous Amino Acid Solutions at 298.15K

From Equation I.38, $L = n_2 \phi_L$ and when the molality scale is used this becomes $L = m \phi_L$. Using this equation together with Equation IV.3 above we obtain

$$L = A_1 m^2 + A_2 m^3 + A_3 m^4 + \ldots\ldots$$

Hence $\bar{L}_2 = (\partial L/\partial n_2)_{n_1 = 55.51} = \partial L/\partial m = 2A_1 m + 3A_2 m^2 + 4A_3 m^3 + \ldots.$

Also $\bar{L}_2 = (L - m\bar{L}_2)/55.51 = -(A_1 m^2 + 2A_2 m^3 + 3A_3 m^4 + \ldots.)/55.51$

Values of $\bar{L}_2$ are shown graphically in Figure IV.4.

TABLE IV.4

Relative Apparent Molal Enthalpies, ϕ_L, of Amino Acids in Water at 298.15K

Coefficients of the Expression, $\phi_L = A_1 m + A_2 m^2 + A_3 m^3 + \ldots$

Amino Acid	A_1	A_2	A_3	m_1/mol kg^{-1}
L-Alanine	217.0 ± 0.4	-	-	0.60 to 1.80
L-Arginine	-1764 ± 33	857 ± 81	-283 ± 58	0.25 to 0.86
L-Cysteine	-113 ± 7	34 ± 8	-5.6 ± 3	0.70 to 1.40
Glycine	-439 ± 5	74 ± 3	-6.8 ± 0.7	0.40 to 3.00
L-Serine	-720 ± 5	134 ± 3	-12.4 ± 0.5	0.38 to 3.80
L-Valine	858 ± 1	-	-	0.15 to 0.49

Figure IV.3 Relative apparent molal enthalpies of amino acids in water at 298.15K

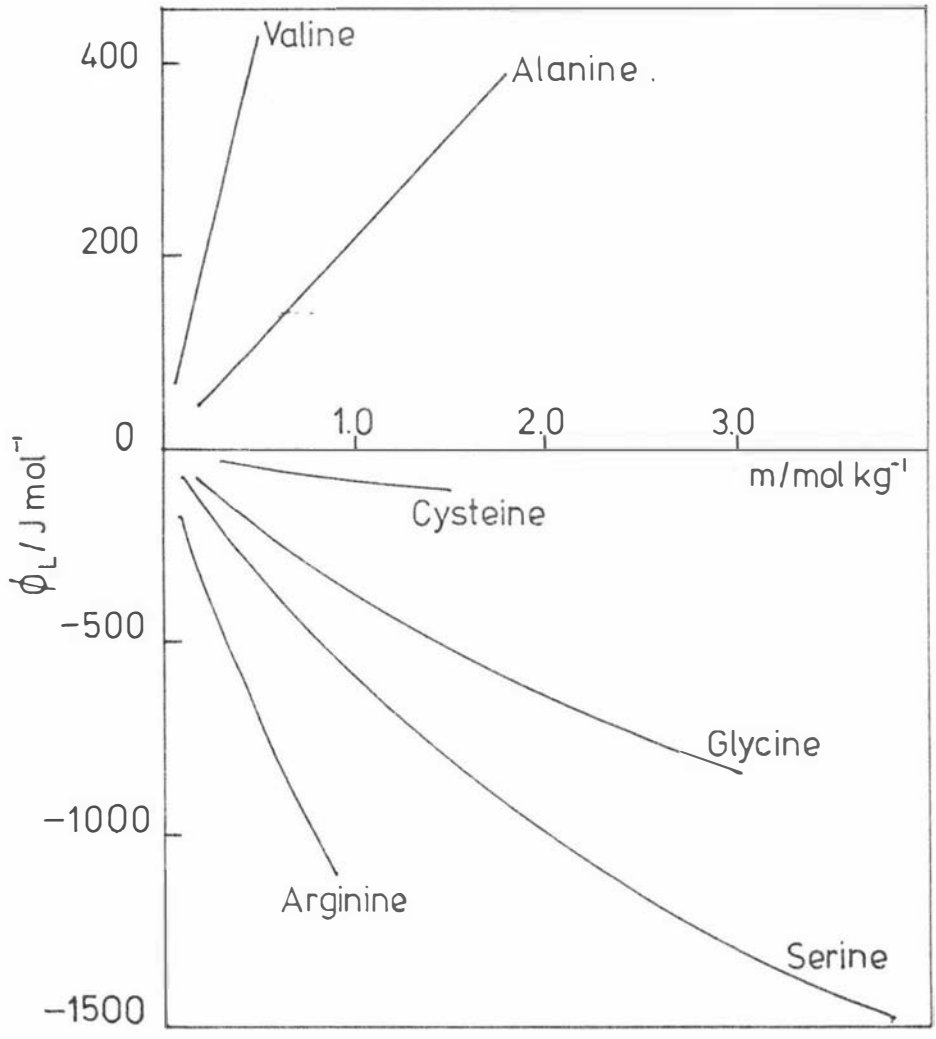

Figure Ⅳ.4 Relative partial molal enthalpies of amino acids in water at 298.15K.

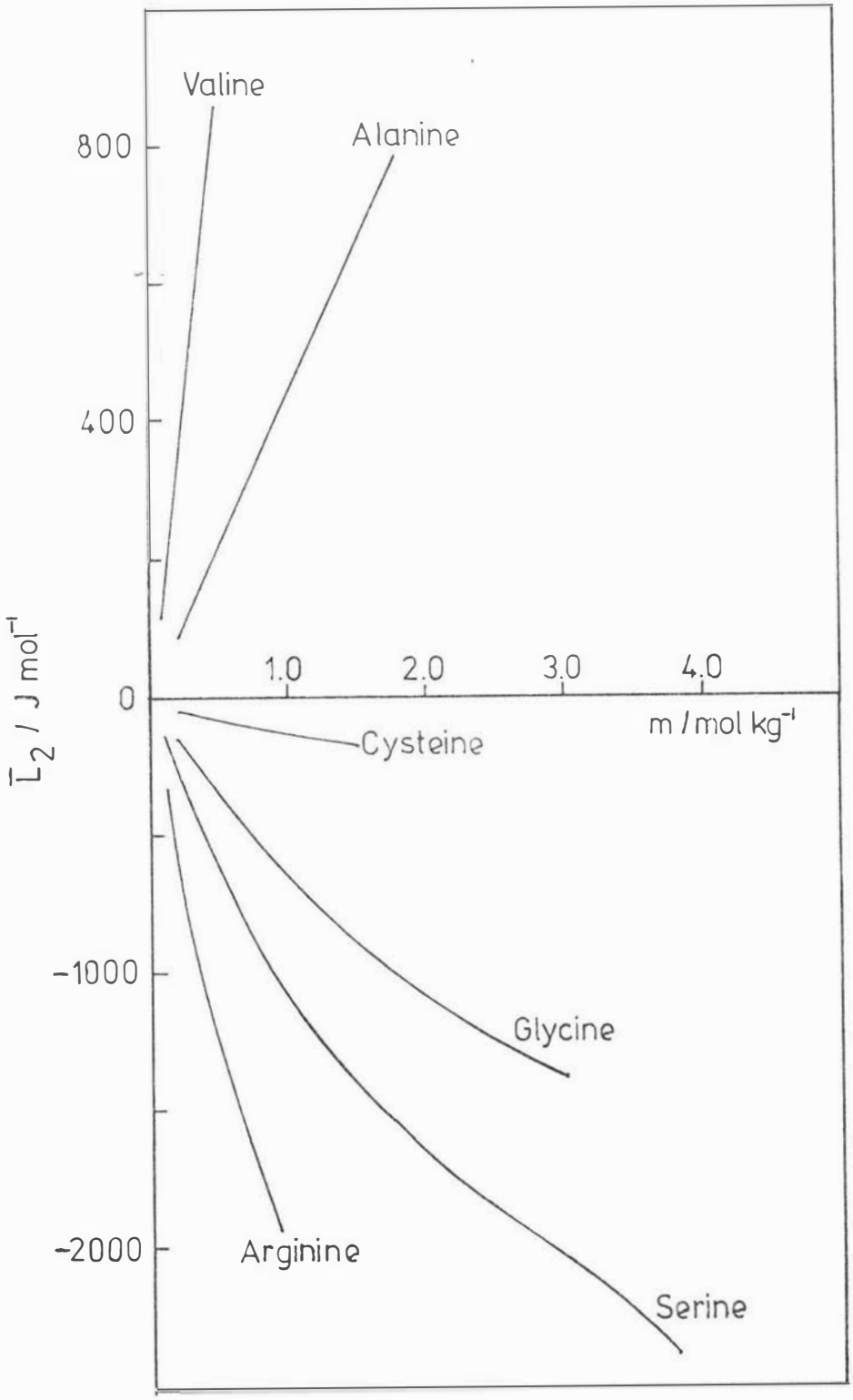

IV.B3 Comparison of Relative Apparent Molal Enthalpies, ϕ_L, with Literature Values

The values of ϕ_L for aqueous solutions of glycine were compared with those from the literature as a test of the calorimetric method used. However, on completion of the experimental work it was found that the values for ϕ_L of aqueous solutions of α-alanine and valine had also been determined previously. These values are also compared with those obtained in this study.

The expressions for ϕ_L for aqueous solutions of glycine, α-alanine and valine from different sources are given in Table IV.5. These different expressions for the ϕ_L's are compared graphically in Figures IV.5 to IV.7.

IV.B4 Error Analysis for Enthalpy of Dilution Measurements

The flow rates of the reactants, f and f_o, determined before and after a dilution experiment usually did not differ by more than 0.1%. This produced an uncertainty of at least 0.2% in c_f. The initial concentrations of the amino acid solutions, m_i were known to 0.1% whereas the final concentrations, m_f because of their dependence on c_i, f and f_o were known only to 0.5%.

W, the heat flux produced in the reaction cell, was determined (Section II.B4(ii)) from recorder deflections for both the dilution and calibration experiments. If the uncertainty in these was combined with that of 0.1% in the current supplied to the calibration heater the overall expected uncertainty in W was 0.6%. As a result, the uncertainty in ΔH_{ID} under the best conditions, was expected to be about 1%. This uncertainty in ΔH_{ID} is included in the estimated uncertainty in the parameters A_1, A_2 etc. in Table IV.4.

TABLE IV.5

Relative Apparent Molal Enthalpies, ϕ_L, of Aqueous Solutions of Glycine, Alanine and Valine

Amino Acid	ϕ_L/J mol^{-1}	m/mol kg^{-1}	Reference
Glycine	$-446.9m + 76.6m^2 - 7.1m^3$	0.005 - 3.0	Gucker, Pickard and Ford[49]
Glycine	$-439m + 74m^2 - 6.8m^3$	0.20 - 3.00	This study
Glycine	$-508.8m + 94.6m^2 - 10.0m^3$		Zittle and Schmidt[76]
Glycine	$\left[-484.9/(1 + 0.395m)\right] - 23.7m^2$	0.036 - 1.14	Sturtevant[75]
Glycine	$(1084e^{-20.6m} - 384.9)m + 36.4m^2$	0.0003 - 0.8	Wallace, Offutt and Robinson[59]
L-Alanine	$217.0m$	0.20 - 1.80	This study
α-Alanine	$199.2m - 2157.7m\ e^{-58.79m}$	0.001 - 1.3	Benesi, Mason and Robinson[58]
dl-Alanine	$236.4m$		Zittle and Schmidt[76]
L-Valine	$858m$	0.07 - 0.49	This study
Valine	$790.8m$	0.0007 - 0.64	Mason, Offutt and Robinson[56]

Figure IV.5 Relative apparent molal enthalpy of Glycine in water at 298.15 K : a comparison with literature.

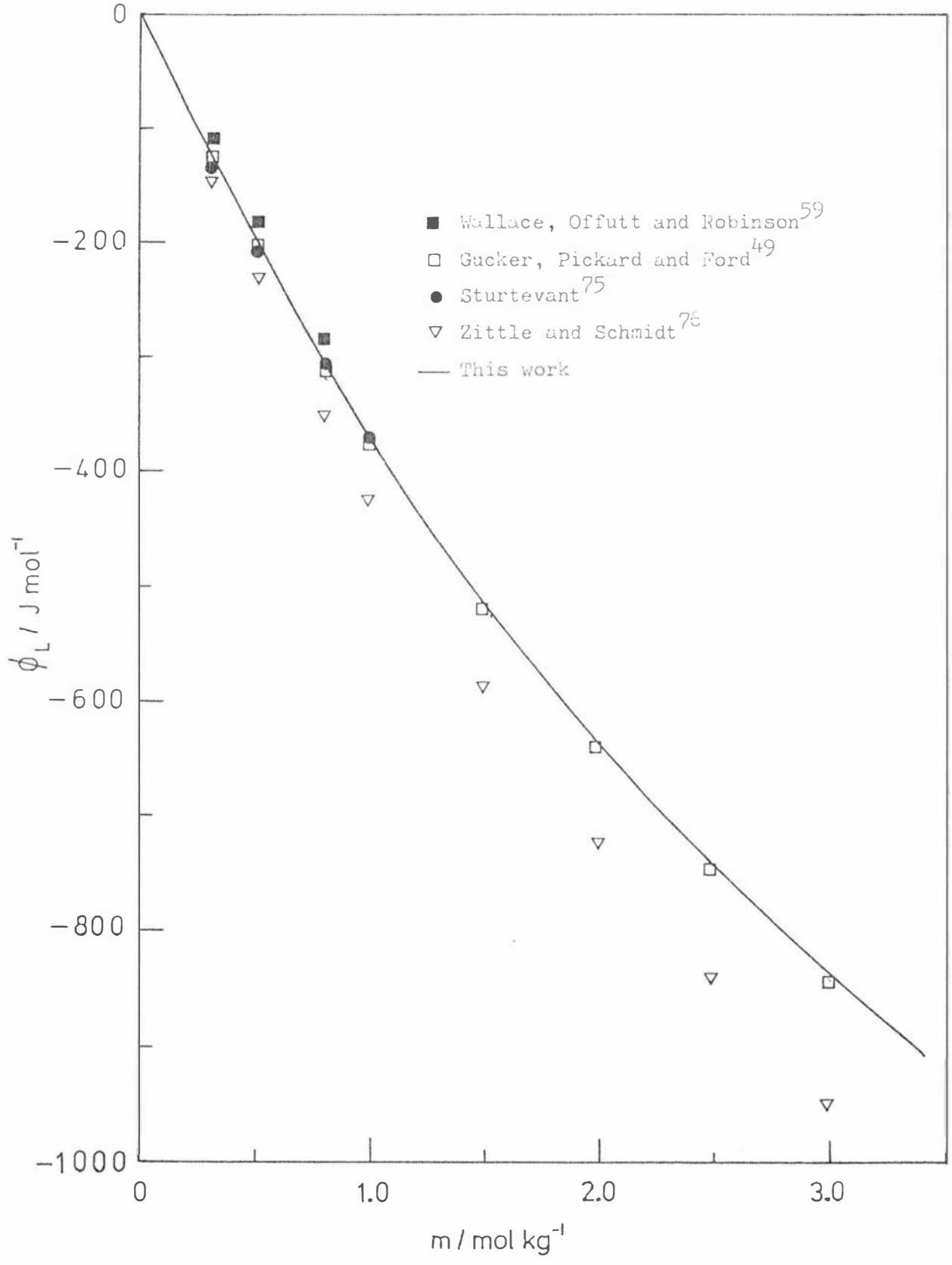

Figure IV.6 Relative apparent molal enthalpy of L-Alanine in water at 298.15K: a comparison with literature.

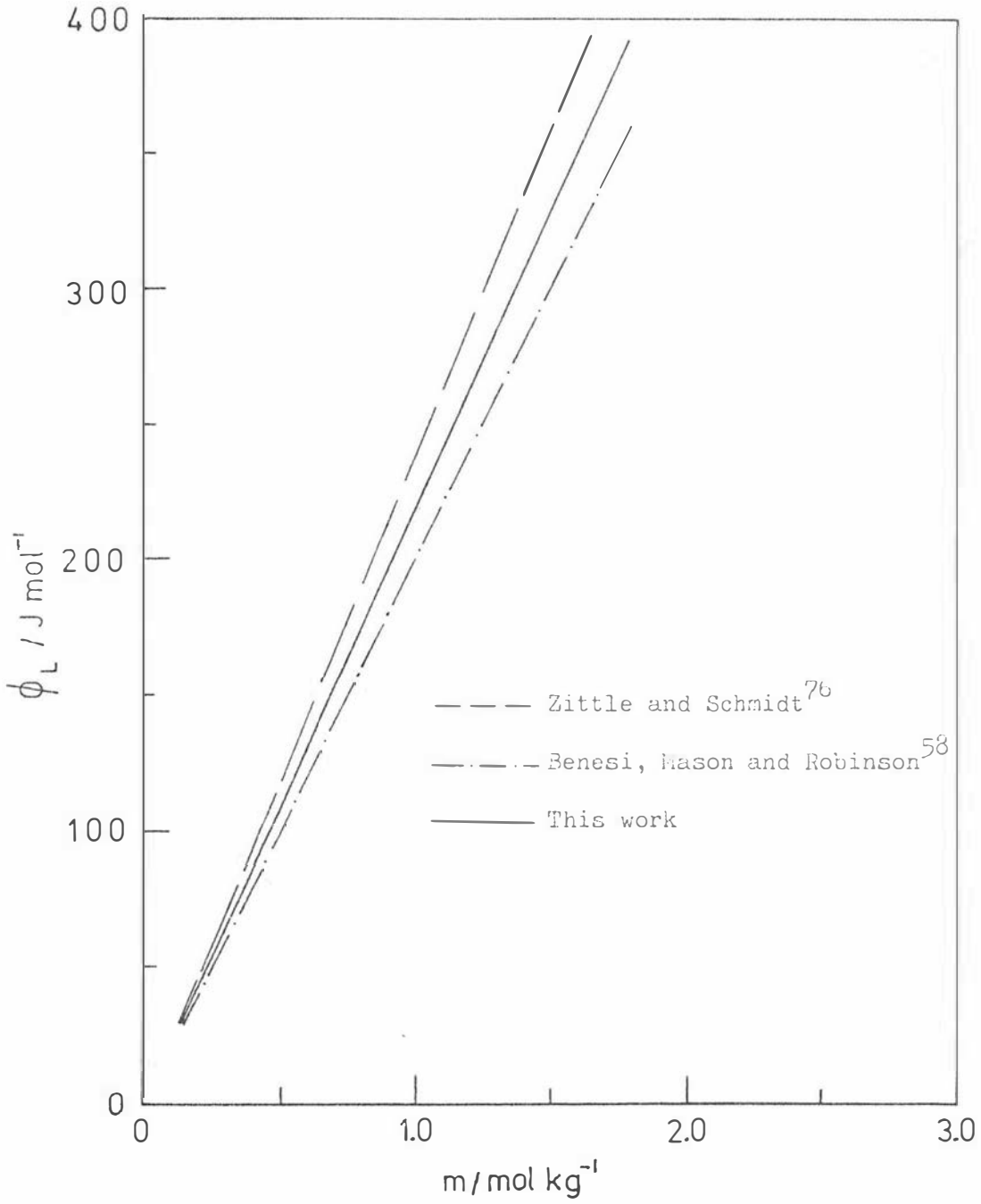

Figure IV.7 Relative apparent molal enthalpy of L-Valine in water at 298.15K: a comparison with literature.

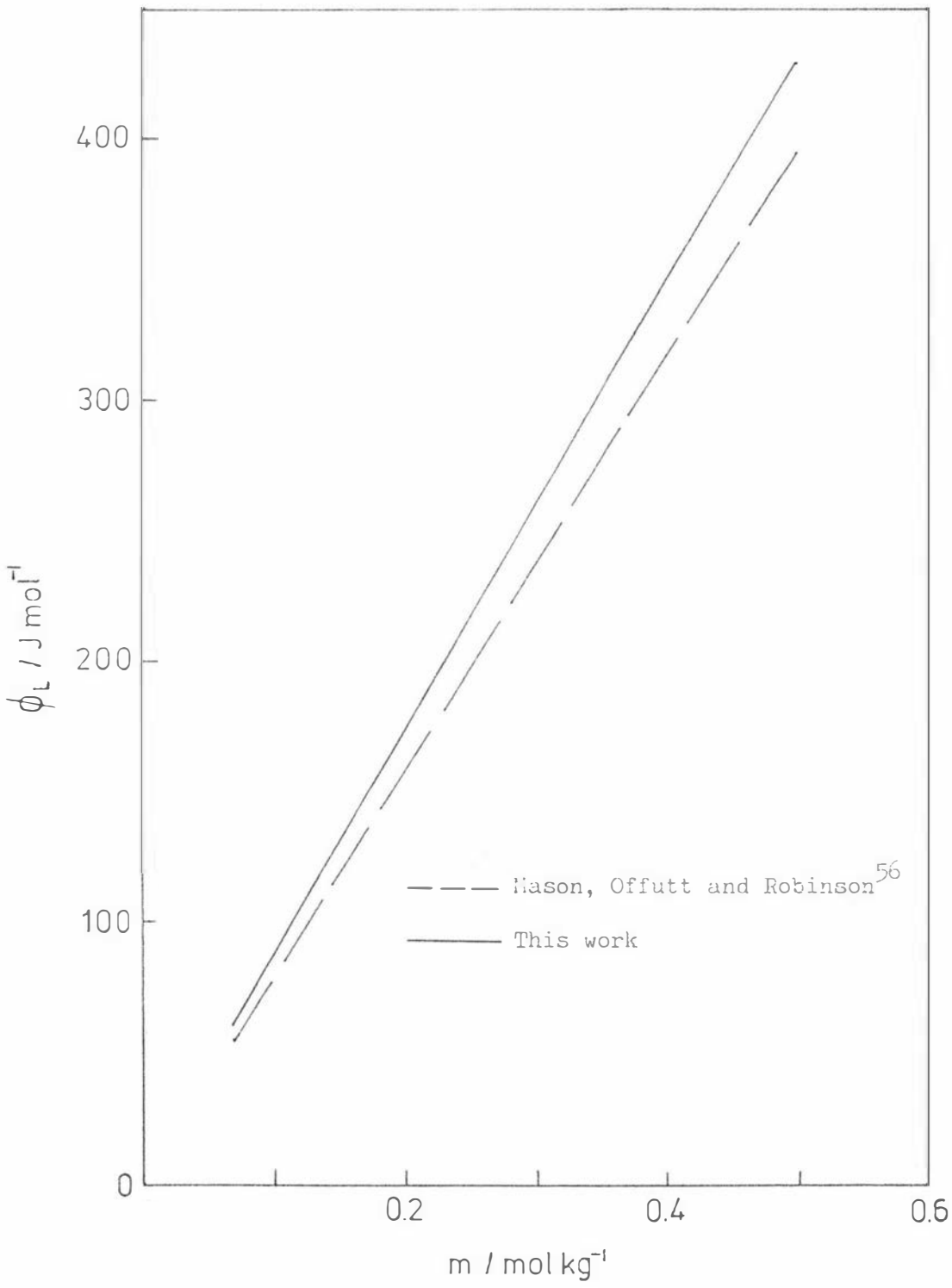

IV.C TEMPERATURE DEPENDENCE OF THE ACTIVITY COEFFICIENTS OF L-SERINE-WATER SOLUTIONS

The temperature dependence of the activity coefficient, γ_i, from Equation I.44 is given by,

$$\partial \ln \gamma_i / \partial T = - \bar{L}_i / RT^2 .$$

Integration of this expression between two temperatures T and T' (assuming $\bar{L}_i$ to be constant) gives,

$$\log(\gamma'/\gamma) = \bar{L}_i/R \left[{}^1/_{T'} - {}^1/_{T} \right]$$

From the values of $\bar{L}_2$ determined for L-serine-water solutions, the ratio of the activity coefficient at T' = 298.15K to that at T = 288.15K as a function of concentration (m/mol kg^{-1}) has been calculated. These ratios are given in Table IV.6 and compared with the same ratio as determined from vapour pressure measurements.

TABLE IV.6

Values of $\gamma_2(298.15K)/\gamma_2(288.15K)$ as Determined by Vapour Pressure Measurements and Enthalpy of Dilution Measurements

m/mol kg^{-1}	$\gamma_2(298.15K)/\gamma_2(288.15K)$ (vapour pressure)	$\gamma_2(298.15K)/\gamma_2(288.15K)$ (enthalpies of dilution)
0.4000	1.09	1.02
0.5000	1.07	1.02
0.7000	1.05	1.03
1.0000	1.06	1.04
1.5000	1.13	1.06
2.0000	1.19	1.06
2.5000	1.18	1.06
3.0000	1.18	1.07

IV.D ENTROPIES OF DILUTION

From Equation I.49 we can write the relative partial molal entropy of water in an aqueous amino acid solution as

$$(\bar{S}_1 - \bar{S}_1^{\circ})^* = \bar{L}_1/T - R\ln(a_1/x_1) \qquad (IV.5)$$

where the contribution solely from the mixing of the components has been subtracted.

Values of $(\bar{S}_1 - \bar{S}_1^{\circ})^*$ have been calculated for aqueous solutions of the amino acids L-serine, L-alanine, glycine and L-valine and these are listed in Table IV.7. The values of $\bar{L}_1$ were those from this thesis and the values of the activity, a_1, for L-alanine, glycine and L-valine were those from the work of Smith and Smith[26].

TABLE IV.7

Relative Partial Molal Entropies* of Water in Aqueous Amino Acid Solutions at 298.15K

m/mol kg^{-1}	$(\bar{S}_1 - \bar{S}_1^\circ)^*$	m/mol kg^{-1}	$(\bar{S}_1 - \bar{S}_1^\circ)^*$
Alanine		Serine	
0.2	-0.00037	0.2	0.0016
0.4	-0.00161	0.5	0.0052
0.6	-0.00372	1.0	0.0152
0.8	-0.00669	1.5	0.0269
1.0	-0.01049	2.0	0.0388
1.2	-0.01506	2.5	0.0520
1.4	-0.02049	3.0	0.0678
1.6	-0.02844	3.5	0.0925
1.8	-0.03639		
Valine		Glycine	
0.07	-0.00017	0.2	0.0010
0.09	-0.00034	0.5	0.0020
0.10	-0.00044	1.0	0.0095
0.20	-0.00157	1.5	0.0219
0.30	-0.00358	2.0	0.0290
0.40	-0.00628	2.5	0.0435
0.50	-0.00994	3.0	0.0608

* These values have been corrected for the mixing term (see Section I.B7).

CHAPTER V

DISCUSSION

Values have been obtained for the activity coefficients of L-serine in water, the relative apparent and relative partial molal enthalpies of L-alanine, L-arginine, L-cysteine, glycine, L-serine and L-valine in water and also the relative partial molal entropies of water in aqueous solutions of L-alanine, glycine, L-serine and L-valine.

At present there is no theoretical model to provide a quantitative explanation of the thermodynamic behaviour of these zwitterions in aqueous solution. Calculations that have been made from the point of view of pure electrostatic interactions from simplified models have not proved satisfactory. It is therefore intended in this discussion to attempt some purely qualitative correlations of the thermodynamic data available for amino acids in aqueous solution with the structures of these substances (see Figure V.1). The concepts used will be those first proposed by Frank and Evans[2] and later Frank and Wen[3] for solute-water interactions.

Enthalpies of Dilution

The relative apparent partial molal enthalpy, ϕ_L, and the relative partial molal enthalpy of the solute, $\bar{L}_2$, both provide information on the contribution of the solute to the total solution properties. ϕ_L however, is an approximation to the solute contribution in that it considers the solvent contribution as that of the pure solvent whereas $\bar{L}_2$ does not make this approximation. Both ϕ_L and $\bar{L}_2$ show similar trends with concentration for each of the amino acids studied (see Figures V.2 and V.3).

Glycine does not have a side chain and so can be considered to show the thermodynamic behaviour of the unsubstituted zwitterion in aqueous solution. An increasingly negative enthalpy contribution to the total enthalpy of the solution with increasing concentration, by glycine would suggest some disruption of water network structure by the zwitterion. This may be inferred from the following comments. If $\bar{L}_2$ becomes more negative with increasing concentration then by Gibbs-Duhem or Equation I.35

Figure V.1 The structures of some amino acids

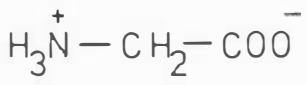

Glycine

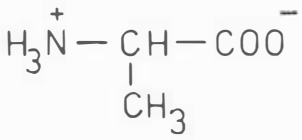

Alanine

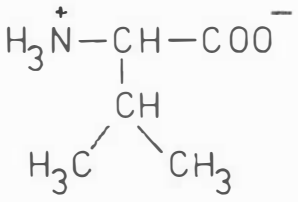

Valine

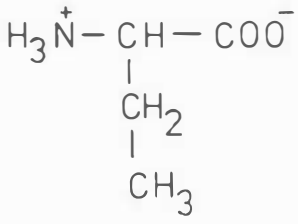

∝-Aminobutyric acid

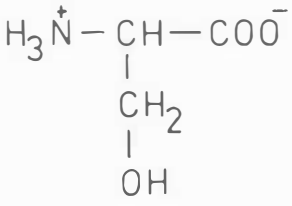

Serine

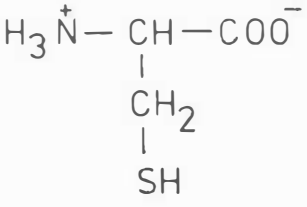

Cysteine

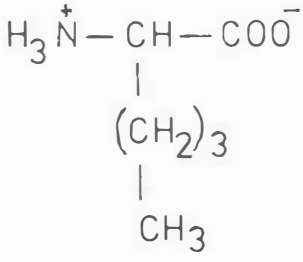

Norleucine

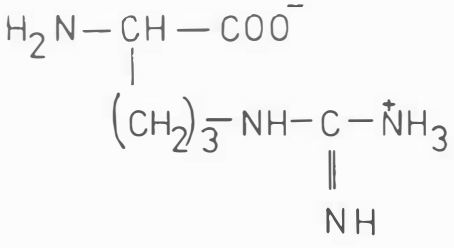

Arginine

Figure V.2 Relative apparent molal enthalpies of amino acids in water at 298.15K

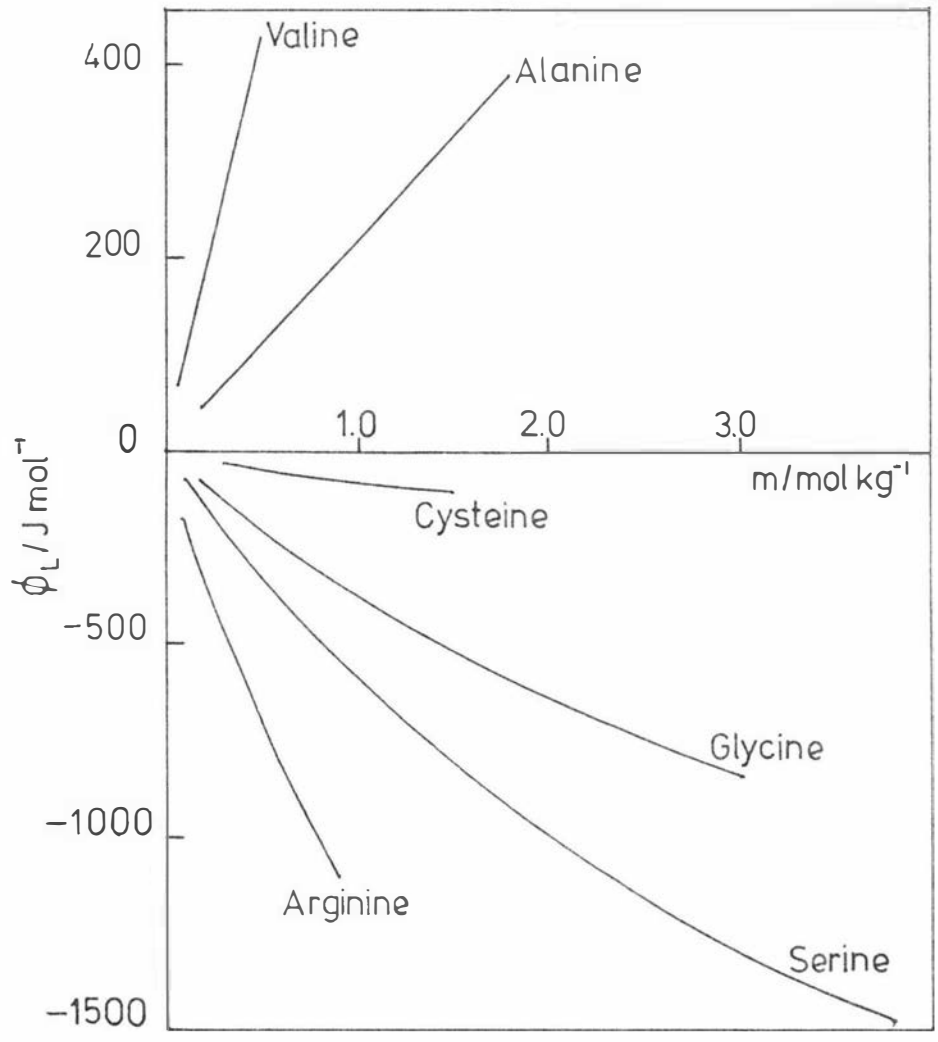

Figure V.3 Relative partial molal enthalpies of amino acids in water at 298.15K.

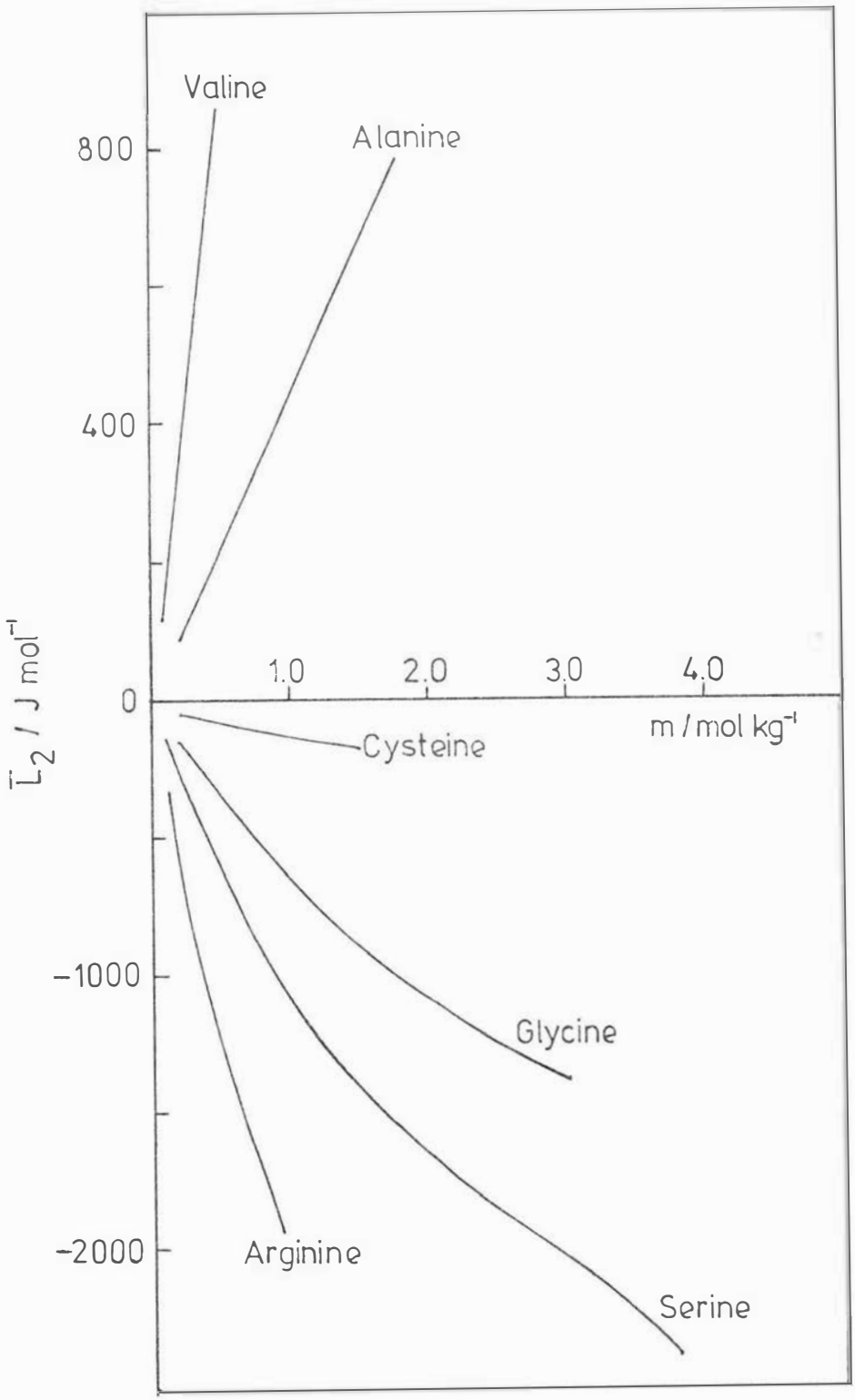

$\bar{L}_1$ becomes more positive. Thus if $\bar{L}_1$ increases to more positive values, the solvent enthalpy contribution increases similarly, therefore the solvent must absorb energy presumably by breaking or distorting bonds. There is some evidence in the literature[71,72] supporting the suggestion that glycine has a water structure-breaking effect. The more negative values of $\bar{L}_2$ for L-serine compared to glycine suggest that not only is L-serine structure-breaking but it is even more so than glycine. This could be attributed to the combined structure-breaking effects of the zwitterion portion and the polar OH group on water network structure. The $\bar{L}_2$ values for alanine are positive and increase with concentration. Therefore it can be argued in a converse manner to that for glycine and serine that $\bar{L}_1$ values for alanine decrease with concentration, presumably because of an increase in water network structure. Alanine can thus be considered as a structure-making solute in aqueous solution. The $\bar{L}_2$ values for L-valine (which has a larger aliphatic side chain than alanine) indicate a similar but greater structure-making effect than alanine. Such comments about these amino acids with solely hydrocarbon side chains are consistent with the proposals of Frank and Evans[2] that hydrocarbon solutes in aqueous solution cause an increase in the amount of network water at the expense of non-bonded water in the vicinity of the non-polar solute molecules. Similar trends to those of the $\bar{L}_2$ values for alanine and valine have been observed for other aliphatic amino acids e.g. α-aminobutyric acid and norleucine[56]. A comparison of the $\bar{L}_2$ values for each of the aliphatic amino acids at the same concentration reveals that the values are positive and increase to more positive values with increasing size of the hydrocarbon side chain. Therefore it would appear that the influence of the hydrocarbon portion on water structure dominates that of the zwitterion.

The substitution of a sulphydryl group (SH), for H in alanine to give cysteine results in values of ϕ_L and $\bar{L}_2$ that are more negative than those of alanine but not as negative as those for serine, which differs

structurally from alanine in that an OH group is substituted for the H in the side chain. The effect of cysteine on water network structure appears to be only very slightly structure-breaking. The fact that it is much less structure-breaking than serine may be rationalized by recognizing that sulphur is larger and less electronegative than oxygen therefore there would be less specific or directed interactions of a polar nature with water molecules. However, the CH_2SH side chain is still polar compared to the CH_3 for alanine so in relation to alanine there is a small net breaking of water network structure.

The ionic side chain of arginine is complex in structure and so without further information speculation as to its behaviour would be difficult and will not be attempted.

Entropies of Dilution

The relative partial molal entropy of water, $\bar{S}_1 - \bar{S}_1^\circ$, in an aqueous amino acid solution, is the entropy change for the transfer of one mole of water from a large amount of an infinitely dilute solution to a large amount of a solution of finite concentration. It was considered desirable to calculate the relative partial molal entropies of water since entropy is related to structural order and it seemed that the structural changes in the water due to the presence of amino acid solutes would be more clearly revealed in $\bar{S}_1 - \bar{S}_1^\circ$ values than in the activity coefficients and enthalpies of dilution from which they are derived. Using the concepts of Frank and Evans[2], positive values of $\bar{S}_1 - \bar{S}_1^\circ$ would indicate disruption or breaking of water network structure and negative values making or enhancement of water network structure.

It would appear from the results (Figure V.4) that for amino acids with aliphatic side chains, the non-polar hydrocarbon group is playing the dominant role in solute-water interactions giving rise to promotion of water network structure (evidenced by negative $\bar{S}_1 - \bar{S}_1^\circ$ values).

Figure V.4 Relative partial molal entropies of water in aqueous amino acid solutions at 298.15K.

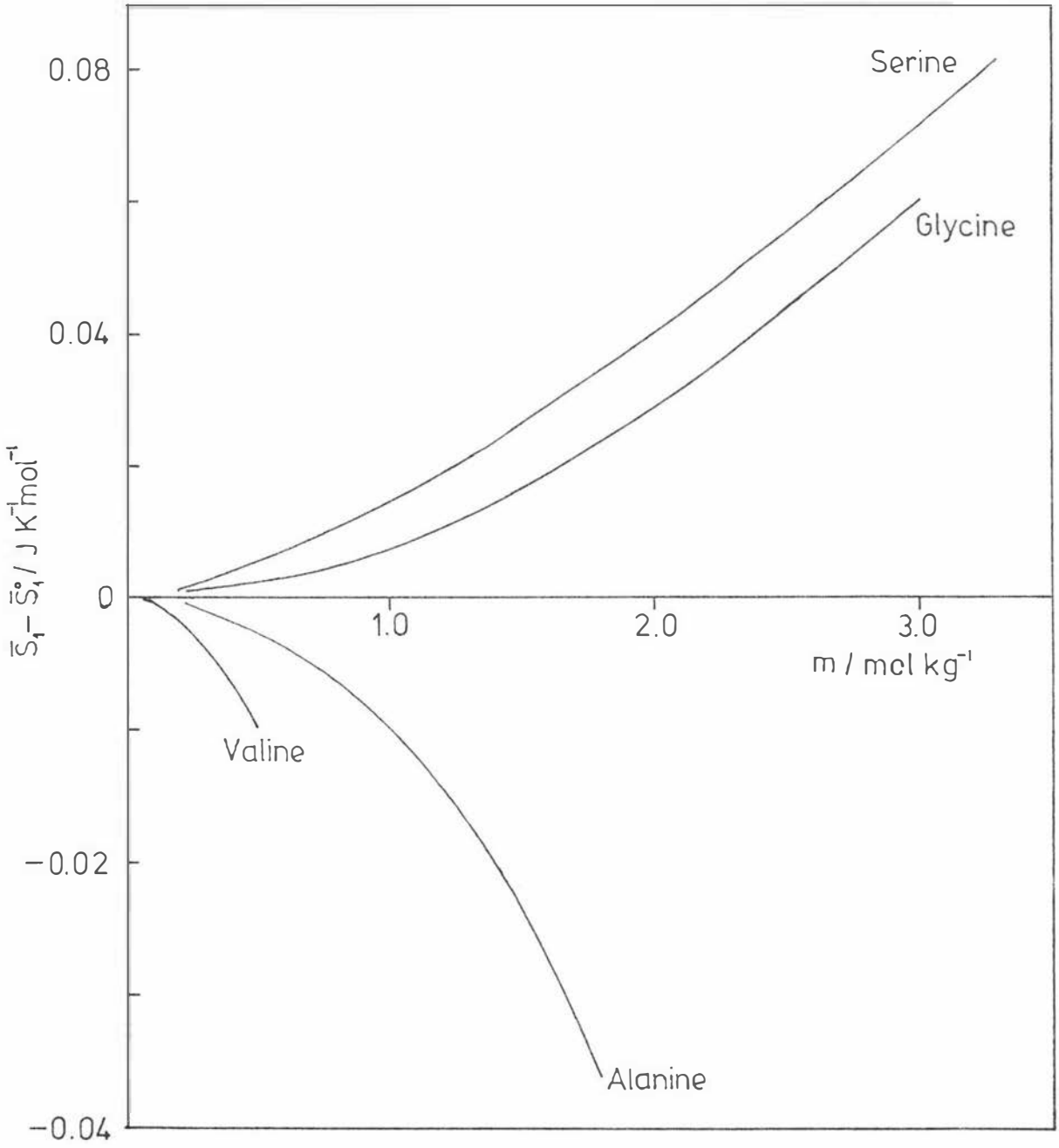

The order of values for $\bar{S}_1 - \bar{S}_1^{\circ}$, valine more negative than alanine, illustrates the effect of the increasing size of the hydrocarbon side chain toward greater structure promotion of water. Several other aliphatic amino acids also show this trend dependent on the size of the hydrocarbon portion e.g. see Mason[56] and Robinson[18]. The water network disrupting effects of glycine and serine are again apparent from the positive values for $\bar{S}_1 - \bar{S}_1^{\circ}$. Serine shows a greater structure-breaking effect than glycine again possibly due to the combination of the effect of the zwitterion and the polar OH group on water network structure.

Other Properties

Spink and Wadsö[7] have determined the partial molar heat capacities of amino acids in aqueous solution at infinite dilution at 298K. The values obtained are given in Table V.1. The aliphatic amino acids alanine, α-aminobutyric acid and valine demonstrate the structure-making influence of their non-polar groups in having large positive partial molar heat capacities. Serine shows a lowering of approximately 20 $J\ K^{-1}\ mol^{-1}$ from alanine with the substitution of the polar OH group in the side chain which is consistent with previous observations.

TABLE V.1

Partial Molar Heat Capacities of Amino Acids in Aqueous Solution at Infinite Dilution at 298K[7]

Amino Acid	$C_{p,2}^{\circ}$ / $J\ K^{-1}\ mol^{-1}$
Glycine	44
Alanine	146
α-Aminobutyric acid	226
Valine	307
Serine	125

Tsangaris and Martin[74] determined the viscosity B-coefficients and their temperature dependence (dB/dT) for several amino acids in water in the range 30° to 40°C. They commented that features of solute effects on solvent structure ought to be temperature dependent, with a positive dB/dT indicating a structure-breaking molecule, and a negative sign, a structure-making one. Thus glycine and serine were considered from their results to have structure-breaking effects on water in the range 30° to 40°C. These interpretations for glycine and serine would appear to be in qualitative agreement with those of the enthalpy and entropy of dilution results given in this thesis.

Conclusion

It would appear that the thermodynamic behaviour of the amino acids studied is governed by the size and structure of the side chain rather than by the charge distribution of the zwitterion (dipolar ion).

As to further work, activity coefficients are still required for aqueous solutions of cysteine and arginine and for others to lower concentrations. In general a more complete picture of the solute-water interaction of amino acids will continue to be provided from systematic determinations of such properties as activity coefficients, enthalpies and entropies of dilution, heat capacities, viscosities and partial molal volumes; especially of solutions of very low concentrations such that the extrapolations to infinite dilution can be made with good precision.

BIBLIOGRAPHY

1. Kauzmann, W.
Some Factors in the Interpretation of Protein Denaturation. Advances in Protein Chemistry 14: 1-63, 1959.

2. Frank, H.S. and Evans, M.W.
Free Volume and Entropy in Condensed Systems. III. Entropy in Binary Liquid Mixtures; Partial Molal Entropy in Dilute Solutions; Structure and Thermodynamics in Aqueous Electrolytes. Journal of Chemical Physics 13: 507-532, 1945.

3. Frank, H.S. and Wen, W-Y.
Structural Aspects of Ion-Solvent Interaction in Aqueous Solutions: A Suggested Picture of Water Structure. Discussions of the Faraday Society 24: 133-140, 1957.

4. Nozaki, Y. and Tanford, C.
The Solubility of Amino Acids and Three Glycine Peptides in Aqueous Ethanol and Dioxane Solutions. Journal of Biological Chemistry 246: 2211-2217, 1971.

5. Kresheck, G.C. and Benjamin, L.
Calorimetric Studies of the Hydrophobic Nature of Several Protein Constituents and Ovalbumin in Water and in Aqueous Urea. Journal of Physical Chemistry 68: 2476-2486, 1964.

6. Greenstein, J.P. and Winitz, M.
Chemistry of the Amino Acids. Volume 1: p. 547, John Wiley and Sons: New York, 1961.

7. Spink, C.H. and Wadsö, I.
The Partial Molar Heat Capacities of Some Amino Acids in Aqueous Solution. Journal of Chemical Thermodynamics 7: 561-572, 1975.

8. Pople, J.A.
Molecular Association in Liquids. II. Theory of the Structure of Water. Proceedings of the Royal Society A205: 163-178, 1951.

9. Bernal, J.D.
The Structure of Liquids. Proceedings of the Royal Society A280: 299-322, 1964.

10. Claussen, W.F.
Second Water Structure for Inert Gas Hydrates. Journal of Chemical Physics 19: 1425-1426, 1951.

11. Pauling, L. and Marsh, R.E.
Proceedings of the National Academy of Science (U.S.) 38: 112, 1952.

12. Rosseinsky, D.R.
Electrode Potentials and Hydration Energies. Theories and Correlations. Chemical Reviews 65: 467-490, 1965.

13. Fortier, J.-L., Leduc, P.-A., Desnoyers, J.E.
Thermodynamic Properties of Alkali Halides. II. Enthalpies of Dilution and Heat Capacities in Water at 25°C. Journal of Solution Chemistry 3: 323-349, 1974.

14. Nemethy, G. and Scheraga, H.A.
Structure of Water and Hydrophobic Bonding in Proteins. II. Model for the Thermodynamic Properties of Aqueous Solutions of Hydrocarbons. Journal of Chemical Physics 36: 3401-3417, 1962.

15. Alexander, D.M. and Hill, D.J.T.
The Heats of Solution of Alcohols in Water. Australian Journal of Chemistry 22: 347-356, 1969.

16. Sarma, T.S., Mohanty, R.K., Ahluwalia, J.C.
Heat Capacity Changes and Standard Partial Molal Heat Capacities of Aqueous Solutions of Some Tetraalkyl Ammonium Halides at 30°C and the Effect on Water Structure. Transactions of the Faraday Society 65: 2333-2338, 1969.

17. Lindenbaum, S.
Thermodynamics of Aqueous Solutions of Tetra-n-alkylammonium Halides. Enthalpy and Entropy of Dilution. Journal of Physical Chemistry 70: 814-820, 1966.

18. Robinson, A.L.
The Differential Entropy of Dilution in Aqueous Solutions of Amino Acids. Journal of Chemical Physics 14: 588-590, 1946.

19. Denbigh, K.
The Principles of Chemical Equilibrium. 3rd ed. University of Cambridge Press, 1971.

20. Lewis, G.N. and Randall, M.
Revised by Pitzer, K.S. and Brewer, L. Thermodynamics. 2nd ed. McGraw-Hill: New York, 1961.

21. Glasstone, S.
Thermodynamics for Chemists. Van Nostrand: New York, 1966.

22. Lakhanpal, M.L. and Conway, B.E.
A Method of Integration of the Gibbs-Duhem Equation when Activities of a Solute are Required from those of the Solvent. Canadian Journal of Chemistry 38: 199-203, 1960.

23. Sinclair, D.A.
A Simple Method for Accurate Determinations of Vapour Pressures of Solutions. Journal of Physical Chemistry 37: 495-504, 1933.

24. Bousfield, W.R. and Bousfield, C.E.
Vapour Pressure and Density of Sodium Chloride Solutions. Proceedings of the Royal Society (London) 103A: 429-443, 1923.

25. Robinson, R.A. and Sinclair, D.A.
The Activity Coefficients of the Alkali Chlorides and of Lithium Iodide in Aqueous Solution from Vapour Pressure Measurements. Journal of the American Chemical Society 56: 1830-1835, 1934.

26. Smith, E.R.B. and Smith, P.K.
The Activity of Glycine in Aqueous Solution at 25°. Journal of Biological Chemistry 117: 209-216, 1937.

27. Smith, E.R.B. and Smith, P.K.
Thermodynamic Properties of Solutions of Amino Acids and Related Substances. II. The Activity of Aliphatic Amino Acids in Aqueous Solution at 25°. Journal of Biological Chemistry 121: 607-613, 1937.

28. Richards, M.M.
The Effect of Glycine upon the Activity Coefficient of Glycine, Egg Albumin and Carboxyhemoglobin. Journal of Biological Chemistry 122: 727-743, 1938.

29. Smith, E.R.B. and Smith, P.K.
Thermodynamic Properties of Solutions of Amino Acids and Related Substances. IV. The Effect of Increasing Dipolar Distance on the Activities of Aliphatic Amino Acids in Aqueous Solution at 25°. Journal of Biological Chemistry 132: 47-56, 1940.

30. Smith, E.R.B. and Smith, P.K.
The Activities of Some Hydroxy- and N-Methylamino Acids and Proline in Aqueous Solutions at 25°. Journal of Biological Chemistry 132: 57-64, 1940.

31. Hutchens, J.O., Figlio, K.M., Granito, S.M.
An Isopiestic Comparison Method for Activities. The Activities of L-Serine and L-Arginine Hydrochloride. Journal of Biological Chemistry 238: 1419-1422, 1963.

32. Ellerton, H.D., Reinfelds, G., Mulcahy, D.E., Dunlop, P.J.
Activity, Density and Relative Viscosity Data for Several Amino Acids, Lactamide, and Raffinose in Aqueous Solution at 25°. Journal of Physical Chemistry 68: 398-402, 1964.

33. Gordon, A.R.
Isopiestic Measurements in Dilute Solutions; the System Potassium Chloride-Sodium Chloride at 25° at Concentrations from 0.03 to 0.10 molal. Journal of the American Chemical Society 65: 221-224, 1943.

34. Scatchard, G., Jones, P.T., Prentiss, S.S.
The Freezing Points of Aqueous Solutions. I. The Freezing Point Apparatus. Journal of the American Chemical Society 54: 2676-2690, 1932.

35. Smith, E.R.B. and Smith, P.K.
The Activities of some Peptides in Aqueous Solution at 25°. Journal of Biological Chemistry 135: 273-279, 1940.

36. Scatchard, G. and Prentiss, S.S.
Freezing Points of Aqueous Solutions. VII. Ethyl Alcohol, Glycine and Their Mixtures. Journal of the American Chemical Society 56: 1486-1492, 1934.

37. Hoskins, W.M., Randall, M. and Schmidt, C.L.A.
The Conductance and Activity Coefficients of Glutamic and Aspartic Acids and their Monosodium Salts. Journal of Biological Chemistry 88: 215-239, 1930.

38. Baxendale, J.H., Enustun, B.V. and Stern, J.
A Thermodynamic Investigation of the System: Benzene-Biphenyl. I. Experimental Method and the Vapour Pressure of Pure Benzene. Transactions of the Royal Society (London) A243: 169-176, 1951.

39. Lakhanpal, M.L. and Conway, B.E.
Studies on Polyoxypropylene glycols. Part 1: Vapour pressures and Heats of Mixing in the Systems: Polyglycols-Methanol. Journal of Polymer Science 46: 75-92, 1960.

40. Taylor, J.B. and Rowlinson, J.S.
The Thermodynamic Properties of Aqueous Solutions of Glucose. Transactions of the Faraday Society 51: 1183-1192, 1955.

41. Puddington, I.E.
A Sensitive Mercury Manometer. Review of Scientific Instruments 19: 577-579, 1948.

42. Sirianni, A.I. and Puddington, I.E.
The Determination of Molecular Weight. Canadian Journal of Chemistry 33: 755-762, 1955.

43. Kershaw, R.W.
The Thermodynamics of Polymer Solutions. Thesis, Ph.D., Otago University, 1965.

44. Barber, C.R., Handley, R. and Herington, E.F.G.
The Preparation and Use of Cells for the Realization of the Triple Point of Water. British Journal of Applied Physics 5: 41-44, 1954.

45. Bell, T.N., Cussler, E.L., Harris, K.R., Pepela, C.N. and Dunlop, P.J.
An Apparatus for Degassing Liquids. Journal of Physical Chemistry 72: 4693-4695, 1968.

46. Ambrose, D.
Vapour Pressures. p. 218-267. In McGlashan, M.L. ed. Chemical Thermodynamics. Chemical Society Specialist Periodical Report. Vol. 1. Chemical Society: London, 1973.

47. The International Practical Temperature Scale of 1968. Metrologia 5: 35-44, 1969.

48. Lange, E. and Robinson, A.L.
The Heats of Dilution of Strong Electrolytes. Chemical Reviews 9: 89-116, 1931.

49. Gucker, F.T., Pickard, H.B. and Ford, W.L.
The Heats of Dilution of Aqueous Solutions of Glycine and Glycolamide, and Other Thermodynamic Properties of Glycine at 25°. Journal of the American Chemical Society 62: 2698-2704, 1940.

50. Wadsö, I.
Design and Testing of a Micro Reaction Calorimeter. Acta Chemica Scandinavica 22: 927-937, 1968.

51. Savini, C.G., Winterhalter, D.R., Kovach, L.H. and Van Ness, H.C.
Endothermic Heats of Mixing by Isothermal Dilution Calorimetry. Journal of Chemical and Engineering Data 11: 40-43, 1966.

52. Stokes, R.H., Marsh, K.N. and Tomlins, R.P.
An Isothermal Displacement Calorimeter for Endothermic Enthalpies of Mixing. Journal of Chemical Thermodynamics 1: 211-221, 1969.

53. Monk, P. and Wadsö, I.
A Flow Micro Reaction Calorimeter. Acta Chemica Scandinavica 22: 1842-1852, 1968.

54. Stoesser, P.R. and Gill, S.J.
Precision Flow-Microcalorimeter. The Review of Scientific Instruments 38: 422-425, 1967.

55. Picker, P., Jolicoeur, C. and Desnoyers, J.E.
Steady State and Composition Scanning Differential Flow Microcalorimeters. Journal of Chemical Thermodynamics 1: 469-483, 1969.

56. Mason, L.S., Offutt, W.F. and Robinson, A.L.
The Heats of Dilution of Aqueous Solutions of Four Amino Acids at 25°. Journal of the American Chemical Society 71: 1463-1468, 1949.

57. Mason, L.S. and Robinson, A.L.
The Heats of Dilution of Aqueous Solutions of Four Amino Butyric Acids at 25°. Journal of the American Chemical Society 69: 889-893, 1947.

58. Benesi, H.A., Mason, L.S. and Robinson, A.L.
Heats of Dilution of Aqueous Solutions of α- and β-Alanine at 25°. Journal of the American Chemical Society 68: 1755-1759, 1946.

59. Wallace, W.E., Offutt, W.F. and Robinson, A.L.
The Heats of Dilution of Aqueous Solutions of Glycine at 25°. Journal of the American Chemical Society 65: 347-350, 1943.

60. Ward, G.K. and Millero, F.J.
The Enthalpies of Dilution of Aqueous Boric Acid Solutions at Several Temperatures. Journal of Chemical Thermodynamics 5: 591-594, 1973.

61. Levine, A.S. and Lindenbaum, S.
Enthalpy of Dilution and Heat Capacity of Aqueous Solutions of Tetrabutylammonium Butyrate as a Function of Temperature. Journal of Solution Chemistry 2: 445-455, 1973.

62. Hamilton, D. and Stokes, R.H.
Enthalpies of Dilution of Urea Solutions in Six Polar Solvents at Several Temperatures. Journal of Solution Chemistry 1: 223-235, 1972.

63. Fortier, J.-L., Leduc, P.-A., Picker, P. and Desnoyers, J.E.
Enthalpies of Dilution of Electrolyte Solutions by Flow Microcalorimetry. Journal of Solution Chemistry 2: 467-475, 1973.

64. Tarbell, D.S.
The Mechanism of Oxidation of Thiols to Disulphides. p. 97-102. In Kharasch, N. ed. Organic Sulphur Compounds. Pergamon: London, 1961.

65. Osborne, N.S., Stimson, H.F. and Ginnings, D.C.
Thermal Properties of Saturated Water Steam. Journal of Research of the National Bureau of Standards 23: 261-270, 1939.

66. Wexler, A. and Greenspan, L.
Vapour Pressure Equation for Water in the Range 0 to 100°C. Journal of Research of the National Bureau of Standards 75A: 213-230, 1971.

67. Besley, L. and Bottomley, G.A.
Vapour Pressure of Normal and Heavy Water from 273.15K to 298.15K. Journal of Chemical Thermodynamics 5: 397-410, 1973.

68. Osborne, N.S. and Meyers, C.H.
A Formula and Tables for the Pressure of Saturated Water Vapour in the Range 0 to 374°C. Journal of Research of the National Bureau of Standards 13: 1-20, 1934.

69. Douslin, D.R.
Vapour Pressure of Water from -2.5 to 20°C. Journal of Chemical Thermodynamics 3: 187-193, 1971.

70. Stimson, H.F.
Some Precise Measurements of the Vapour Pressure of Water in the Range from 25 to 100°C. Journal of Research of the National Bureau of Standards 73A: 493-496, 1969.

71. Kay, R.L. and Evans, D.F.
The Effect of Solvent Structure on the Mobility of Symmetrical Ions in Aqueous Solution. Journal of Physical Chemistry 70: 2325-2335, 1966.

72. Longsworth, L.G.
Diffusion Measurements at 25°C of Aqueous Solutions of Amino Acids, Peptides, and Sugars. Journal of the American Chemical Society 75: 5705-5709, 1953.

73. Amino Acids, Amines, Amides, Peptides and their Derivatives. p. 10. In Dawson, R.M.C. ed. Data for Biochemical Research. Clarendon Press: Oxford, 1969.

74. Tsangaris, M.J. and Martin, B.R.
Viscosities of Aqueous Solutions of Dipolar Ions. Archives of Biochemistry and Biophysics 112: 267-272, 1965.

75. Sturtevant, J.M.
Heats of Dilution of Aqueous Solutions of Glycine at 25°C. Journal of the American Chemical Society 62: 1879, 1940.

76. Zittle, C.A. and Schmidt, C.L.A.
Heats of Solution, Heats of Dilution, and Specific Heats of Aqueous Solutions of Certain Amino Acids. Journal of Biological Chemistry 108: 161-185, 1935.

77. Gucker, F.T.; Pickard, H.B.; Planck, R.W.
A new microcalorimeter: the Heats of Dilution of Aqueous Solutions of Sucrose at 20 and 30° and their Heat Capacities at 25°. Journal of the American Chemical Society 61: 459-470, 1939.